NASA CR 72987
PWA-4283

DEVELOPMENT OF MAINSHAFT SEALS FOR ADVANCED AIR BREATHING PROPULSION SYSTEMS
– PHASE III –

BY
V. P. POVINELLI AND A. H. McKIBBIN

Pratt & Whitney Aircraft DIVISION OF UNITED AIRCRAFT CORPORATION

FACILITY FORM 602
N71-38022 (ACCESSION NUMBER)
111 (PAGES)
CR-72987 (NASA CR OR TMX OR AD NUMBER)
(THRU)
1
(CODE)
15
(CATEGORY)

Prepared for
NATIONAL AERONAUTICS AND SPACE ADMINISTRATION
NASA Lewis Research Center
Contract NAS3-7609
L. P. Ludwig, Project Manager

1. Report No.	2. Government Accession No.	3. Recipient's Catalog No.
NASA CR-72987		

4. Title and Subtitle	5. Report Date
Development of Mainshaft Seals For Advanced Air Breathing Propulsion Systems Final Report – Phase III	25/July/71
	6. Performing Organization Code

7. Author(s)	8. Performing Organization Report No.
V. P. Povinelli A. H. McKibbin	PWA-4263
	10. Work Unit No.

9. Performing Organization Name and Address	11. Contract or Grant No.
Pratt & Whitney Aircraft Division of United Aircraft Corporation East Hartford, Conn.	NAS-3-7609
	13. Type of Report and Period Covered
12. Sponsoring Agency Name and Address	Contractor Report
National Aeronautics and Space Administration Washington, D. C. 20546	14. Sponsoring Agency Code

15. Supplementary Notes

Project Manager, Lawrence P. Ludwig, Fluid Systems Components Division, NASA Lewis Research Center, Cleveland, Ohio.

16. Abstract

Five self-acting gas-film face seals for advanced gas-turbine engines were analyzed and four were tested. All five seal designs incorporated shrouded Rayleigh step lift pads at the primary seal surfaces to provide the gas-film lubrication. The wide pad and revised narrow pad seal were successfully operated at seal sliding speeds up to 500 ft/sec (17,300 rpm), pressure differentials up to 300 psi, and gas temperatures up to 1200°F. The air leakages for both seals were in good agreement with calculated values and were about 1/10 of leakages expected from labyrinth seals at comparable conditions. The operating range of the narrow pad seal was limited due to insufficient film thickness. The ceramic seal suffered damage due to chipping during testing.

17. Key Words (Suggested by Author(s))	18. Distribution Statement
Gas-film Seals Mainshaft Seals Rayleigh Step Pad Self-Acting Seals	Unclassified – Unlimited

19. Security Classif. (of this report)	20. Security Classif. (of this page)	21. No. of Pages	22. Price*
Unclassified	Unclassified	117	$3.00

* For sale by the National Technical Information Service, Springfield, Virginia 22151

PRECEDING PAGE BLANK NOT FILMED

FOREWORD

This report describes the work conducted during Phase III of contract NAS 3-7609 by the Pratt & Whitney Aircraft Division of United Aircraft Corporation, East Hartford, Connecticut. Phase III was initiated on 26 February 1970 and completed on 25 June 1971. The work was performed for the Lewis Research Center of the National Aeronautics and Space Administration. Mr. Lawrence P. Ludwig, Fluid System Components Division, NASA Lewis Research Center was the Project Manager. Mr. John E. Dilley, NASA Lewis Research Center was the Contracting Officer.

TABLE OF CONTENTS

		Page
FOREWORD		iii
LIST OF ILLUSTRATIONS		v
LIST OF TABLES		xiii
SUMMARY		1
I	INTRODUCTION	3
II.	CONCLUSIONS AND RECOMMENDATIONS	7
III.	DESIGN ANALYSIS	9
IV.	EXPERIMENTAL EVALUATION OF THE CERAMIC SEAL	37
V.	EXPERIMENTAL EVALUATION OF THE NARROW-PAD SEAL	55
VI.	EXPERIMENTAL EVALUATION OF THE WIDE-PAD SEAL	67
VII.	EXPERIMENTAL EVALUATION OF THE REVISED NARROW-PAD SEAL	85
VIII.	TEST EQUIPMENT	95
REFERENCES		99
DISTRIBUTION LIST		101

LIST OF ILLUSTRATIONS

Figure	Title	Page
1	Typical Positive-Contact Seal	3
2	Typical Multi-Labyrinth Seal	4
3	Typical Gas-Film Seal With Self-Acting Rayleigh Step Pads	5
4	Design Features of the Ceramic Seal	11
5	Design Features of the Narrow-Pad Seal	12
6	Design Features of the Wide-Pad Seal	13
7	Design Features of the Revised Narrow-Pad Seal	14
8	Design Features of the Recessed Seat Seal	15
9	Schematic Diagram of the Steady-State Forces Acting on the Nosepiece and Seal Seat. Forces Represented by the Cross-Hatched Regions of the Axial Pressure Profiles are Equal and Opposite, and Therefore Omitted from the Equation	18
10	Effect of Recess Depth and Number of Pads on Total Load Capacity	20
11	Relationship Between Total Hydrodynamic Pad Load Capacity and Ratio of Recess Length to Land Length	20
12	Load Capacity of the Rayleigh Pads in the Ceramic Seal at an Air Temperature of 150°F	21
13	Load Capacity of the Rayleigh Pads in the Ceramic Seal at an Air Temperature of 800°F	21
14	Load Capacity of the Rayleigh Pads in the Narrow-Pad Seal at an Air Temperature of 150°F	22
15	Load Capacity of the Rayleigh Pads in the Wide-Pad Seal at an Air Temperature of 150°F	23
16	Load Capacity of the Rayleigh Pads in the Wide-Pad Seal at an Air Temperature of 800°F	23

LIST OF ILLUSTRATIONS (Cont'd)

Figure	Title	Page
17	Load Capacity of the Rayleigh Pads in the Revised Narrow-Pad Seal at an Air Temperature of 150°F	24
18	Load Capacity of the Rayleigh Pads in the Revised Narrow-Pad Seal at an Air Temperature of 800°F	24
19	Load Capacity of the Rayleigh Pads in the Recessed Seat Seal at an Air Temperature of 150°F	25
20	Load Capacity of the Rayleigh Pads in the Recessed Seat Seal at an Air Temperature of 800°F	25
21	Seal Dam Load Capacity for the Ceramic Seal, Wide-Pad Seal, and the Revised Narrow-Pad Seal	26
22	Seal Dam Load Capacity for the Narrow-Pad Seal	27
23	Seal Dam Load Capacity for the Recessed Seat Seal	27
24	Typical Seal Force Balance Diagram	29
25	Calculated Primary Leakage and Film Thickness for the Ceramic Seal with Air at 150°F	30
26	Calculated Primary Leakage and Film Thickness for the Ceramic Seal with Air at 800°F	30
27	Calculated Primary Leakage and Film Thickness for the Narrow-Pad Seal with Ar at 150°F	31
28	Calculated Primary Leakage and Film Thickness for the Wide-Pad Seal with Air at 150°F	32
29	Calculated Primary Leakage and Film Thickness for the Wide-Pad Seal with Air at 800°F	32
30	Calculated Primary Leakage and Film Thickness for the Revised Narrow-Pad Seal with Air at 150°F	33
31	Calculated Primary Leakage and Film Thickness for the Revised Narrow-Pad Seal with Air at 800°F	33

LIST OF ILLUSTRATIONS (Cont'd)

Figure	Title	Page
32	Calculated Primary Leakage and Film Thickness for the Recessed Seat Seal with Air at 150°F	34
33	Calculated Primary Leakage and Film Thickness for the Recessed Seat Seal with Air at 800°F	34
34	Air Leakage Past the Secondary Seals	35
35	Estimated Air-Film Temperature as a Function of Seal Air Temperature	36
36	Completed Ceramic Nosepiece Ring Assembly with Close-Up of Ceramic Ring	38
37	Ceramic Nosepiece Seal Assembly Before Testing	38
38	Representative Profile Trace Taken Radially Across the Face of the Ceramic Nosepiece Before Testing in Build 1	39
39	Air Leakage Past Build 1 of the Ceramic Nosepiece Seal	40
40	Seal Seat After Build 1 Testing of the Ceramic Nosepiece Seal	41
41	Profile Trace Taken Radially Across the Face of the Seal Seat Showing Wear Track After 0.5 Hour of Build 1 Testing	42
42	Ceramic Nosepiece After Build 1 Testing	43
43	Close-Up of the Ceramic Nosepiece After Build 1 Testing	43
44	Air Leakage Past Build 2 of the Ceramic Nosepiece Seal	44
45	Air Leakage Past Build 3 of the Ceramic Seal	45
46	Air Leakage Past Build 4 of the Ceramic Nosepiece Seal	46
47	Calculated and Actual Air Leakage Past Build 3 of the Ceramic Seal at a Sliding Speed of 250 ft/sec with Ambient Air	47
48	Calculated and Actual Air Leakage Past Builds 3 and 4 of the Ceramic Seal at a Sliding Speed of 310 ft/sec with Ambient Air	48

LIST OF ILLUSTRATIONS (Cont'd)

Figure	Title	Page
49	Calculated and Actual Air Leakage Past Builds 3 and 4 of the Ceramic Seal at a Sliding Speed of 360 ft/sec with Ambient Air	48
50	Calculated and Actual Air Leakage Past Build 3 of the Ceramic Seal at a Sliding Speed of 410 ft/sec with Ambient Air	49
51	Air Leakage Past Build 5 of the Ceramic Nosepiece Seal	50
52	Ceramic Nosepiece After Build 5 Testing. Total Test Time 27.7 Hours	50
53	Close-Up of Ceramic Nosepiece After Build 5 Testing	50
54	Seal Seat After Tests on Build 5 of the Ceramic Nosepiece Seal	51
55	Profile Trace Taken Radially Across the Face of the Seal Seat Showing Ceramic Nosepiece Wear Track After 4.3 Hours of Build 5 Testing. Total Test Time on Seal 27.2 Hours	52
56	Representative Profile Trace Taken Radially Across the Face of the Ceramic Nosepiece After 4.3 Hours of Build 5 Testing. Total Time on Nosepiece 27.7 Hours	52
57	Profile Trace Taken Radially Across the Face of The Ceramic Nosepiece at a Rayleigh Pad Land After 4.3 Hours of Build 5 Testing. Total Time on Nosepiece 27.7 Hours	53
58	Nosepiece from the Narrow-Pad Seal Before Testing	56
59	Close-Up of the Nosepiece from the Narrow-Pad Seal Before Testing	56
60	Representative Profile Trace Taken Radially Across the Face of the Carbon Nosepiece from the Narrow-Pad Seal Before Build 1 Testing	57
61	Air Leakage Past Build 1 of the Narrow-Pad Seal	57
62	Calculated and Actual Air Leakage Past Build 1 of the Narrow-Pad Seal with Ambient Air	58
63	Air Leakage Past Build 2 of the Narrow-Pad Seal	59

LIST OF ILLUSTRATIONS (Cont'd)

Figure	Title	Page
64	Calculated and Actual Air Leakage Past Build 2 of the Narrow-Pad Seal with Ambient Air	59
65	Air Leakage Past Build 3 of the Narrow-Pad Seal	60
66	Calculated and Actual Air Leakage Past Build 3 of the Narrow-Pad Seal with Ambient Air	61
67	Representative Profile Trace Taken Radially Across the Face of the Carbon Nosepiece from the Narrow-Pad Seal After 5.9 Hours of Build 3 Testing. Total Time on Nosepiece 14.5 Hours	61
68	Air Leakage Past Build 3 of the Narrow-Pad Seal	62
69	Calculated and Actual Air Leakage Past Build 3-1 of the Narrow-Pad Seal at a Sliding Speed of 310 ft/sec with Ambient Air	63
70	Calculated and Actual Air Leakage Past Build 3-1 of the Narrow-Pad Seal at a Sliding Speed of 360 ft/sec with Ambient Air	63
71	Representative Profile Trace Taken Radially Across the Face of the Carbon Nosepiece from the Narrow-Pad Seal After First 5.0 Hours of Build 3-1 Endurance Testing. Total Time on Nosepiece 29.9 Hours	64
72	Close-Up View of the Carbon Nosepiece from Build 3-1 of the Narrow-Pad Seal. Total Time on Nosepiece 70.2 Hours	65
73	Representative Profile Trace Taken Radially Across the Face of the Carbon Nosepiece from the Narrow-Pad Seal After 55.7 Hours of Build 3-1 Testing. Total Time on Nosepiece 70.2 Hours	65
74	Profile Trace Taken Radially Across the Face of the Carbon Nosepiece from the Narrow-Pad Seal at a Rayleigh Pad Land After 55.7 Hours of Build 3-1 Testing. Total Time on Nosepiece 70.2 Hours	66
75	Air Leakage Past Build 1 of the Wide-Pad Seal	70
76	Dimensions of the Carbon Piston Ring Used in Build 2 of the Wide-Pad Seal	71
77	Asbestos Insulation and Thermocouples Added Near the Piston Ring in the Wide-Pad Seal	72

LIST OF ILLUSTRATIONS (Cont'd)

Figure	Title	Page
78	Air Leakage and Temperature Data from Build 2 of the Wide-Pad Seal	73
79	Representative Profile Trace Across the Carbon Piston Ring from Build 3 of the Wide-Pad Seal Before Testing	74
80	Representative Profile Trace Across the Carbon Piston Ring from Build 3 of the Wide-Pad Seal After 2.5 Hours of Testing	74
81	Revised Piston-Ring Support to Prevent Thermal Coning	75
82	Representative Profile Trace Across the Carbon Piston Ring from Build 4 of the Wide-Pad Seal After 14.7 Hours of Testing	76
83	Representative Profile Trace Taken Radially Across the Nosepiece of the Build 5 Wide-Pad Seal Before Testing	76
84	Representative Profile Trace Taken Radially Across the Nosepiece of the Build 5 Wide-Pad Seal After 49.0 Hours of Testing. Same Location as Figure 83.	77
85	Representative Profile Trace Across the Carbon Piston Ring from Build 5 of the Wide-Pad Seal. Total Time on Piston Ring 75.3 Hours	77
86	Representative Profile Trace Taken Radially Across the Nosepiece of the Build 6 Wide-Pad Seal. Total Time on Nosepiece: 70.3 Hours	78
87	Profile Trace Across a Point of Maximum Wear on the Carbon Piston Ring from Build 6 of the Wide-Pad Seal. Total Time on Piston Ring (Build 3 and Build 6): 27.3 Hours	79
88	Representative Profile Trace Taken Radially Across the Nosepiece of the Build 7 Wide-Pad Seal. Total Time on Nosepiece: 103.8 Hours	79
89	Representative Profile Trace Across the Carbon Piston Ring from Build 7 of the Wide-Pad Seal. Total Time on Piston Ring: 23.25 Hours	80
90	Nosepiece from the Wide-Pad Seal After Build 7 Testing	80
91	Close-Up of the Nosepiece from the Wide-Pad Seal After Build 7 Testing	80

LIST OF ILLUSTRATIONS (Cont'd)

Figure	Title	Page
92	Representative Profile Trace Across the High-Temperature Carbon Piston Ring from Build 8 of the Wide-Pad Seal After 20 Hours of Testing	81
93	Close-Up of the High-Temperature Carbon Piston Ring from Build 8 of the Wide-Pad Seal After 20 Hours of Testing	81
94	Representative Profile Trace Taken Radially Across the Nosepiece of the Build 9 Wide-Pad Seal. Total Time on Nosepiece: 128 Hours	82
95	Representative Profile Trace Across the TZM Piston Ring from Build 9 of the Wide-Pad Seal Before Testing	83
96	Representative Profile Trace Across the TZM Piston Ring from Build 9 of the Wide-Pad Seal After 24.25 Hours of Testing	83
97	Carbon Nosepiece of the Revised Narrow-Pad Seal Before Testing	85
98	Air Leakage Past Build 1 of the Revised Narrow-Pad Seal	87
99	Calculated and Actual Air Leakage Past Build 1 of the Revised Narrow-Pad Seal at a Sliding Speed of 300 ft/sec with Ambient Air	87
100	Calculated and Actual Air Leakage Past Build 1 of the Revised Narrow-Pad Seal at a Sliding Speed of 350 ft/sec with Ambient Air	88
101	Calculated and Actual Air Leakage Past Build 1 of the Revised Narrow-Pad Seal at a Sliding Speed of 400 ft/sec with Ambient Air	88
102	Calculated and Actual Air Leakage Past Build 1 of the Revised Narrow-Pad Seal at a Sliding Speed of 450 ft/sec with Ambient Air	89
103	Air Leakage Past Build 1 of the Revised Narrow-Pad Seal with Ambient Air. These Measurements Made After Elevated-Temperature Testing	90
104	Representative Profile Trace Taken Radially Across the Nosepiece of the Revised Narrow-Pad Seal Before Testing	91

LIST OF ILLUSTRATIONS (Cont'd)

Figure	Title	Page
105	Representative Profile Trace Taken Radially Across the Nosepiece of the Revised Narrow-Pad Seal After Testing	91
106	Carbon Nosepiece of the Revised Narrow-Pad Seal After Testing	92
107	Close-Up of the Carbon Nosepiece from the Revised Narrow-Pad Seal After Testing	92
108	Schematic Diagram of Seal Test Facility	95
109	Overall View of the Test Stand Showing Mainshaft Seal Rig, Gearbox, and Drive Engine	95
110	Rig Layout Showing Test Seal Location and Materials Used	96
111	Schematic Diagram of Pressure Check Fixture for the Seal	97
112	Schematic Diagram of Pressure Check Fixture for the Rig	98

LIST OF TABLES

Table	Title	Page
I	Seal Characteristics	17
II	Total Closing Forces	28
III	Ceramic Seal Test Summary	37
IV	Narrow-Pad Seal Test Summary	55
V	Wide-Pad Seal Test Summary	68

SUMMARY

During Phase III, five mainshaft face seal designs for advanced gas-turbine engines were analyzed and four were evaluated. All of the designs incorporated Rayleigh step lift geometry which used the relative motion between the primary seal faces to provide positive separation (gas-film lubrication) between the sealing surfaces. The five designs were designated the ceramic seal, the narrow-pad seal, the revised narrow-pad seal, the wide-pad seal, and the recessed seat seal. The ceramic seal used an aluminum oxide nosepiece, while the others used carbon nosepieces. The recessed seat seal had the Rayleigh pads machined into the seal seat, unlike the other designs which had the Rayleigh pads machined into the nosepieces.

The performance analyses of the five designs were based on the steady-state force balance between the opening and closing forces acting on the primary sealing surfaces. In general, the steady-state performance analyses were adequate for predicting seal leakages. When deviations from predicted leakage occurred, they were usually caused by erosion of the primary sealing surfaces or fretting wear of the secondary sealing surfaces.

The ceramic seal was operated for 27.7 hours at sliding speeds up to 410 ft/sec and pressure differentials up to 300 psi using unheated air. The primary sealing surfaces suffered damaging wear from intermittent contact during the tests.

The narrow-pad seal was tested for 70.2 hours with both heated (750°F) and unheated air. Sliding speeds up to 360 ft/sec and pressure differentials of 300 psi were attained. Testing of this seal indicated that the film thickness and stiffness were insufficient to allow for mechanical distortions, thermal distortions, and axial seal seat runout.

The wide-pad seal was tested for a total of 302.7 hours at air temperatures from 150 to 1200°F. The testing included successful operation at the maximum contract conditions of 500 ft/sec, 300 psi, and 1200°F air temperature. In general the actual leakage during the elevated-temperature tests was somewhat higher than the predicted leakage, but the overall operation of the seal was quite satisfactory.

The revised narrow-pad seal was successfully tested for 119.8 hours at speeds, pressures, and temperatures up to and including the maximum contract conditions. The seal's performance was generally good, but there was some deterioration in performance during operation at the elevated temperature conditions.

The recessed seat seal was not tested under this contract.

PRECEDING PAGE BLANK NOT FILMED

SECTION I
INTRODUCTION

Advanced air-breathing engines require the development of mainshaft seals capable of accommodating increasingly severe environments. The intent of Contract NAS3-7609 is to develop mainshaft seals capable of operating at higher pressures, temperatures, and surface speeds than are employed in current production engines. For Phase III, the upper extremes of these parameters were a pressure differential of 300 psi, a sealed gas temperature of 1200°F, and a seal sliding speed of 500 ft/sec.

Positive-contact mainshaft seals are commonly used in current engines. A typical seal of this type is shown in Figure 1. Despite significant advances in nosepiece materials, seal-seat hardface coatings and materials, lubrication technology, heat-transfer technology, and surface finishing, several attempts to significantly extend the operating range of the present positive-contact seal have demonstrated a limited growth potential. Current practice has been to use these seals at conditions not exceeding a pressure differential of 130 psi, a gas temperature of 800°F, and a sliding speed of 350 ft/sec. It is expected that advanced engines will operate at pressure differentials over 250 psi, gas temperatures over 1200°F, and sliding speeds over 400 ft/sec. Therefore, conventional positive-contact seals are entirely inadequate for these advanced conditions.

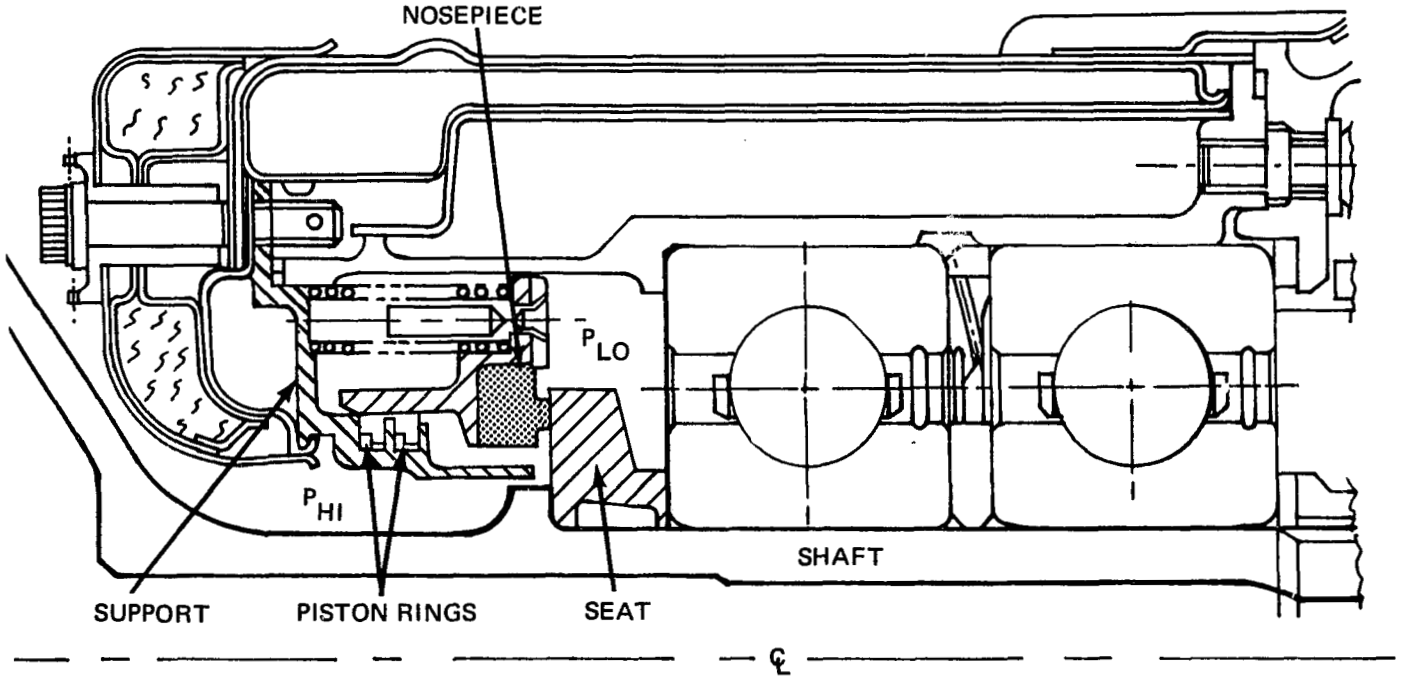

Figure 1 Typical Positive-Contact Seal

The most common alternative to the positive-contact seal is the labyrinth seal; however, once certain limitations on temperature and pressure differential are reached, the simple, lightweight labyrinth seals must give way to complicated multi-labyrinth designs similar to the one shown in Figure 2. These designs utilize high pressure air bleed-off and cold air pressurization schemes. The seal becomes heavy and bulky, and its high air leakage penalizes engine performance.

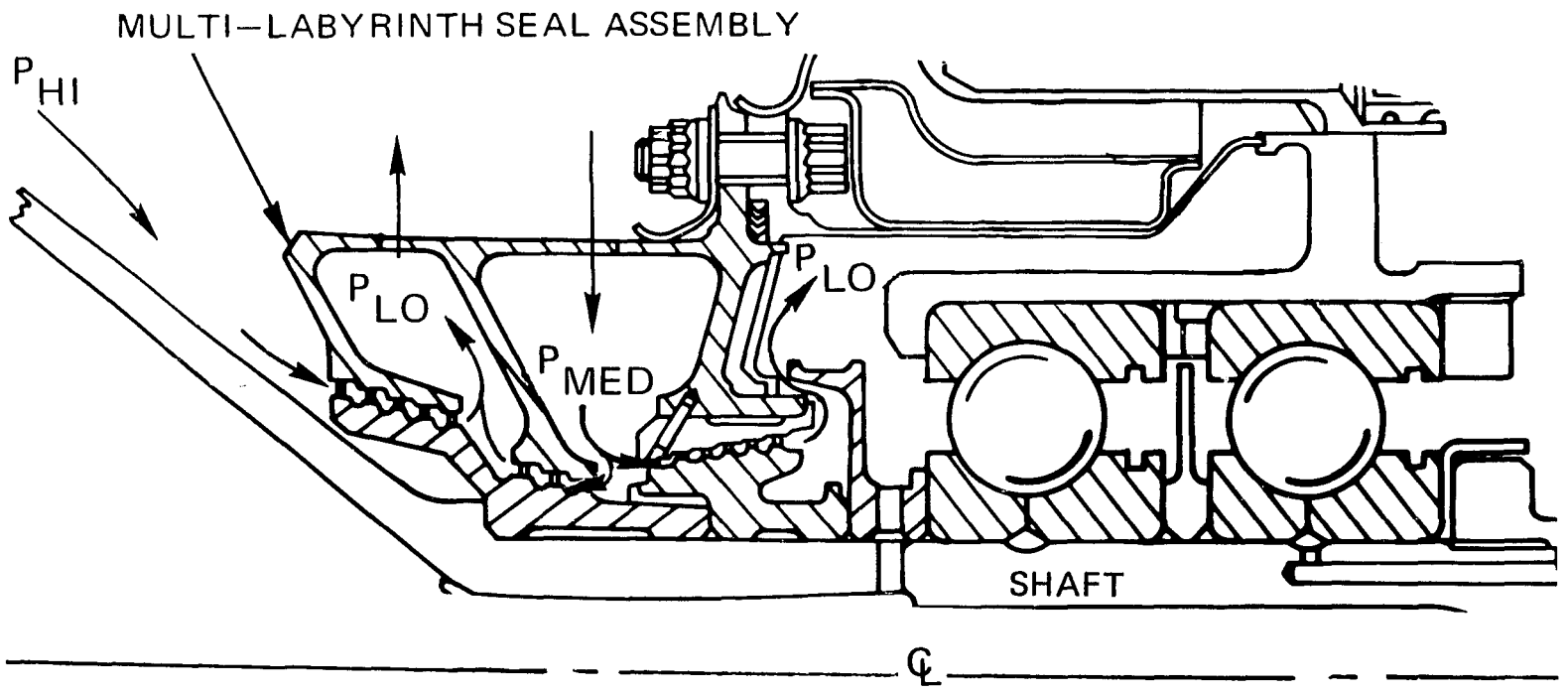

Figure 2 Typical Multi-Labyrinth Seal

A. PHASES I AND II

Development testing under Phase I of this contract indicated that film-lubricated face seals would not have the high wear rates of positive-contact seals under the harsh conditions of advanced engines, and could reduce air leakage to about one tenth of that experienced with multilabyrinth seals. Thus those seal designs in which positive separation of the sliding surfaces was obtained by externally pressurized and self acting means were candidates for advanced engine applications. Based on the results of Phase I, two seals using self-acting (gas) and hydrodynamic (oil) geometries were designed by NASA for testing in Phase II. In one face seal the sliding faces were separated by a gas film produced by shrouded Rayleigh step lift pads. The other face seal had oil-lubricated spiral grooves to maintain separation. Testing of the gas-film seal shown in Figure 3 demonstrated the feasibility of operation at gas temperatures up to 1200°F, pressure differentials from 50 to 250 psi, sliding speeds up to 450 ft/sec, and calculated gas-film thicknesses as low as 0.18 mil. The tests yielded excellent correlation with analytically predicted performance. A total of 911.4 hours of testing was accumulated. The testing included 320 hours at an air temperature of 1000°F, a pressure differential of 200 psi, and a sliding speed of 400 ft/sec. The average leakage for those 320 hours was 14 scfm, and the face wear was less than 0.1 mil. The performance of the gas film seal exceeded the capability of conventional contact seals and the air leakage was one tenth that of the calculated leakage for labyrinth seals at the same condition. In another phase of the testing, 40 starts and stops caused only insignificant wear of the Rayleigh pads, indicating that positive separation of the surfaces occurred at low speeds.

The oil-film seal testing indicated an inadequate seal force balance which precluded successful operation. The tests also identified the need for improved retention of the carbon nosepiece by the retaining ring, and identified the need for better dimensional stability in the nosepiece assembly.

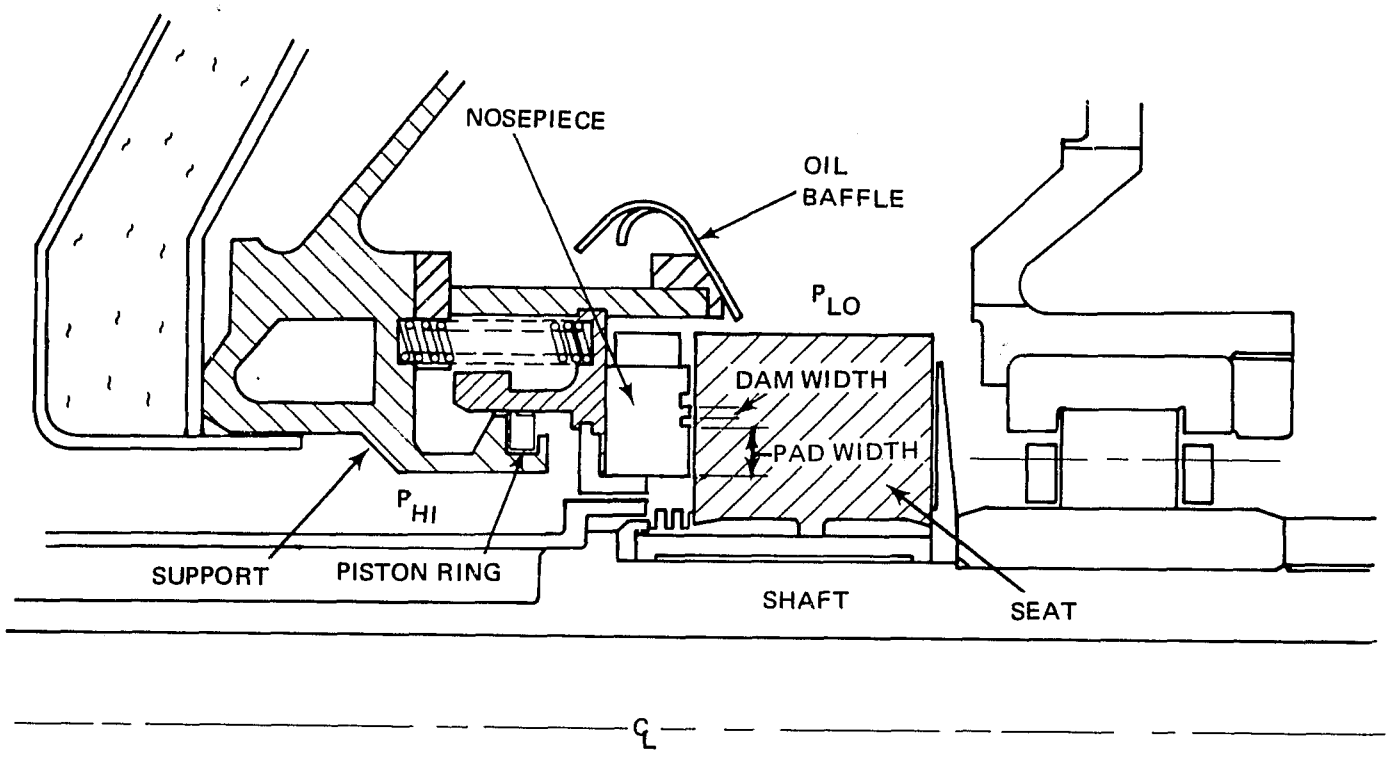

Figure 3 Typical Gas-Film Seal With Self-Acting Rayleigh Step Pads

B. PHASE III

During Phase III the development of self-acting gas-film seals was continued. Five designs were analyzed, all of the self-acting type having Rayleigh step shrouded pads to generate the self-acting lift force. These designs were named according to their distinguishing features as follows (refer to Figure 3):

- Ceramic Seal – Seal with Al_2O_3 nosepiece having the self-acting pads in the nosepiece
- Narrow-Pad Seal – Seal having self-acting pads with a radial width of 0.125 inch in a carbon nosepiece
- Wide-Pad Seal – Seal having self-acting pads with a radial width of 0.250 inch in a carbon nosepiece
- Revised Narrow-Pad Seal – Seal having self-acting pads with a radial width of 0.187 inch in a carbon nosepiece
- Recessed Seat Seal – Seal having self-acting pads in the rotating seat instead of the nosepiece

All designs except the recessed seat seal were experimentally evaluated. A total of 523.6 hours of testing was accumulated on the four designs evaluated. In general, low wear and acceptable leakage rates were obtained.

The objectives of the Phase III program were to:

- Determine the feasibility of operating self-acting seals at conditions beyond those reached in Phase II (Reference 3).
- Reveal design weaknesses by running endurance tests at extreme conditions.
- Evaluate variations of the self-acting gas-film seal design of Phase II (Reference 3) to optimize tolerance to thermal deformation and obtain improved oxidation resistance.

Under Task I of Phase III the contractor conducted a performance analysis of two seal designs furnished by NASA. These designs were the ceramic seal and the recessed-seat seal.

Under Task II the contractor conducted an experimental evaluation of the ceramic seal, the narrow-pad seal, the wide-pad seal, and the revised narrow-pad seal. The recessed-seat seal was not evaluated under Task II. NASA instead furnished the narrow-pad seal and a performance analysis for it. When the experimental evaluation of this design indicated shortcomings, the contractor designed and tested the revised narrow-pad seal. The wide-pad seal was tested when the experimental evaluation of the ceramic seal design indicated shortcomings.

The test rig used in Phase III simulated the roller bearing sump at the turbine location in an advanced gas-turbine engine. The test seal provided the separation between the high-pressure hot gas (turbine side) and the low-pressure mixture of oil and air (sump side). The test seals evaluated during this program had a maximum face diameter of 7.02 inches.

The rig was operated at seal sliding speeds up to 500 ft/sec (17,300 rpm), sealed gas temperatures up to 1200°F, and pressure differentials up to 300 psi. The maximum oil inlet temperature was 290°F.

SECTION II
CONCLUSIONS AND RECOMMENDATIONS

The testing conducted under Phase III of this contract has provided significant insight into the operational limits of gas-film face seals and the factors which affect them. Specific conclusions are listed below:

- The operational ranges of the wide pad and revised narrow pad seals extend beyond the objectives of the Phase III test program.
- Reduction of the mass of the seal nosepiece makes a small but significant improvement in the seal's tracking ability and hence in its leakage characteristics.
- Increasing the width of the Rayleigh pads increases the operational speed range of the seal.
- Increasing the width of the seal dam reduces its susceptibility to edge breakage.
- In the narrow-pad seal the film thickness variations induced by mechanical distortions, thermal distortions, and axial seal seat runout were greater than the mean film thickness, producing excessive contact and wear.
- Aluminum oxide proved to be an unsatisfactory material for the nosepiece, since contact with the seal seat during operation caused chipping.
- When air leakages were encountered which were significantly higher than calculated values, it was found that deterioration of the nosepiece sealing dam and the piston-ring sealing dam were the prime causes of the high leakage.
- Leakage past the piston-ring secondary seal accounts for a significant fraction of the total leakage past the seal.
- The support for the piston ring must be designed so that mechanical or thermal distortions of the support do not unseat the piston ring.

Based on experience gained during the Phase III test and analytical work, the contractor recommends that:

- An analytical model should be developed for gas-film face seals to predict the tracking ability of the nosepiece.
- Fabrication techniques employing composite or honeycomb materials should be explored in an effort to improve the seal's tracking ability by reducing the mass of the nosepiece and nosepiece carrier assembly.

- A recessed seat seal (self-acting geometry in the rotating seat) design using a nosepiece assembly and support structure similar to the configuration used in the other Phase III seals should be tested.

- Tests to establish the operational limits of the wide-pad and revised narrow-pad seal should be run.

- Nosepiece and piston-ring materials should be developed to improve seal durability at gas temperatures of 1200°F and above.

- Self-acting face seals of larger diameters should be developed for possible uses as turbine cooling gas seals and small-diameter compressor end seals.

SECTION III
DESIGN ANALYSIS

A Performance Analysis was done for five gas-film face seal designs during Phase III of this contract. The ceramic seal, the wide-pad seal, the revised narrow-pad seal and the recessed seal seat design were analyzed by Pratt & Whitney Aircraft, while the narrow-pad seal was analyzed by NASA. The designs and analyses of all five seals are discussed below.

A. GENERAL FEATURES OF ALL OF THE SEALS

All five of the seals analyzed under Phase III were self-acting gas-film face seals with piston-ring secondary seals. The designs, primary face configurations, and dimensions for the seals are shown in Figures 4 through 8.

Except for the recessed seat seal, the design features of the Phase III seals were the results of test and analytical experience gained during the first two phases of this contract. The recessed seat seal design was based on a seal developed under NASA contract NAS3-6267 (References 5 and 6). It also used some of the design features included in the other four designs.

Design features common to all five seals are listed below:

- The seal seats were center-pilot mounted, with keys connecting them to the shaft spacer. A machined bellows provided a static seal between the shaft and the seal seat to accommodate differential expansion of the parts and to mitigate seal deformation from clamping.

- Cooling oil was passed through the shaft spacer and then through the seat to reduce thermal gradients.

- Heat shields were used on both sides of the seal seat to minimize thermal gradients and seal-seat deformation.

- Rayleigh step lift pads were used at the interface between the nosepiece and seal seat to provide self-acting support for the nosepiece.

B. GENERAL FEATURES OF THE FOUR SEALS EVALUATED IN EXPERIMENTAL TESTS

Design features common to the ceramic seal, the narrow-pad seal, the wide-pad seal, and the revised narrow-pad seal are listed below:

- Shrouded Rayleigh-step lift pads were used on the face of the nosepiece for self-acting support.

- Some of the same parts were used in all four designs. In certain redesigns, the seal nosepiece and piston ring were made of different materials having significantly different physical properties. The nosepiece face dimensions were different for each design.

- The seat was made from a molybdenum alloy (TZM) material.
- Outward-pumping spiral grooves were used on the outer half of the face of the seal seat to keep oil from leaking inward to the bearing compartment.
- A static seal between the mating faces on the nosepiece and the carrier permitted radial movement of the nosepiece relative to the carrier, thereby reducing nosepiece distortion due to carrier displacement.
- A resilient piloting ring was used to minimize eccentricity between the sealing dam on the nosepiece and the secondary sealing diameter on the carrier.

The principal difference between the ceramic seal (Figure 4) and the narrow-pad seal, the wide-pad seal, and the revised narrow-pad seal is that the ceramic seal used a ceramic nosepiece, while the other three used a carbon nosepiece. Dimensional differences between the ceramic and carbon nosepieces were confined to the primary sealing surfaces. The ceramic seal was the only design analyzed under this contract which did not use a carbon nosepiece.

The narrow-pad seal (Figure 5) had self-acting Rayleigh pads 0.125 inch in radial width. In addition, the narrow-pad nosepiece had a 0.025-inch wide (radial) sealing dam.

The wide-pad seal (Figure 6) was the same as the narrow-pad seal except that the self-acting pads were 0.250 inch in radial width and the sealing dam was 0.050 inch in radial width.

The revised narrow-pad seal (Figure 7) had Rayleigh pads 0.188 inch in radial width, and its sealing dam was 0.050 inch wide.

C. RECESSED SEAT SEAL

The recessed seat seal design is shown in Figure 8. The feature that most distinguishes the design from the other four is that the self-acting geometry is machined into the face of the rotating seat. Other major differences from the other four designs are in the method of nosepiece retention and seat cooling design. Note that for this design the seat material is AISI 8740. A helical groove windback operating over the seat outside diameter was used to prevent oil from migrating back into the primary seal region. Carbon-graphite material was used for the primary ring (nosepiece) and secondary seal ring. Dimensions of the self-acting geometry are given in Figure 8. This geometry consists of feed grooves (0.125 inch deep) connected to the shallow recesses (0.0004 inch deep). The radial width of the carbon-graphite nosepiece is such that it overlaps these recesses to form a shrouded self-acting geometry.

A summary of key dimensions and operating characteristics for each of the five seals analyzed is presented in Table I. Despite the design differences between the recessed seat seal and the other four seals, the performance analyses of all five were very similar. The analyses of all five are discussed in the following section.

FOLDOUT FRAME 1

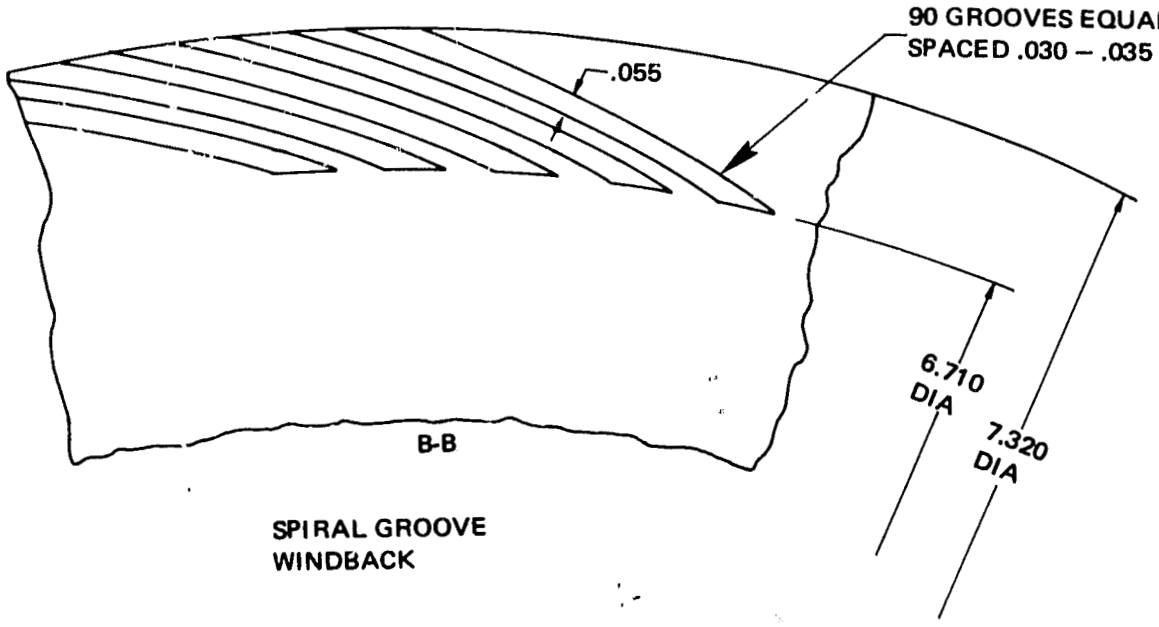

SPIRAL GROOVE
WINDBACK

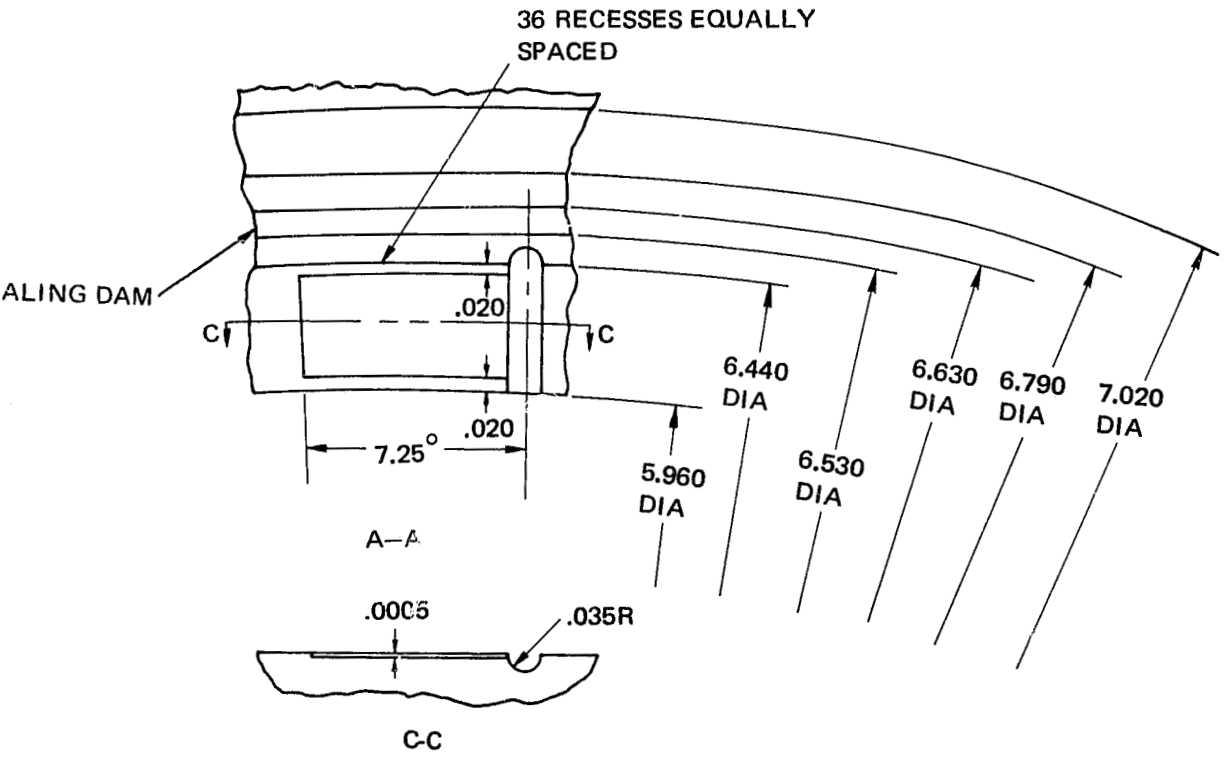

RAYLEIGH PAD AND
SEAL DAM DIMENSIONS

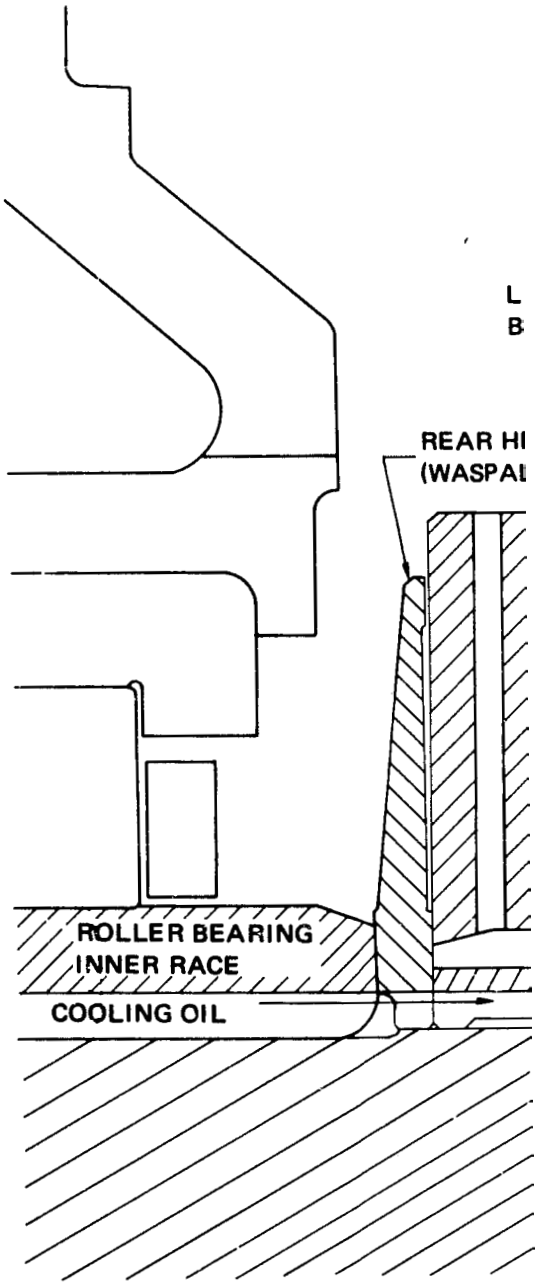

FOLDOUT FRAME 2

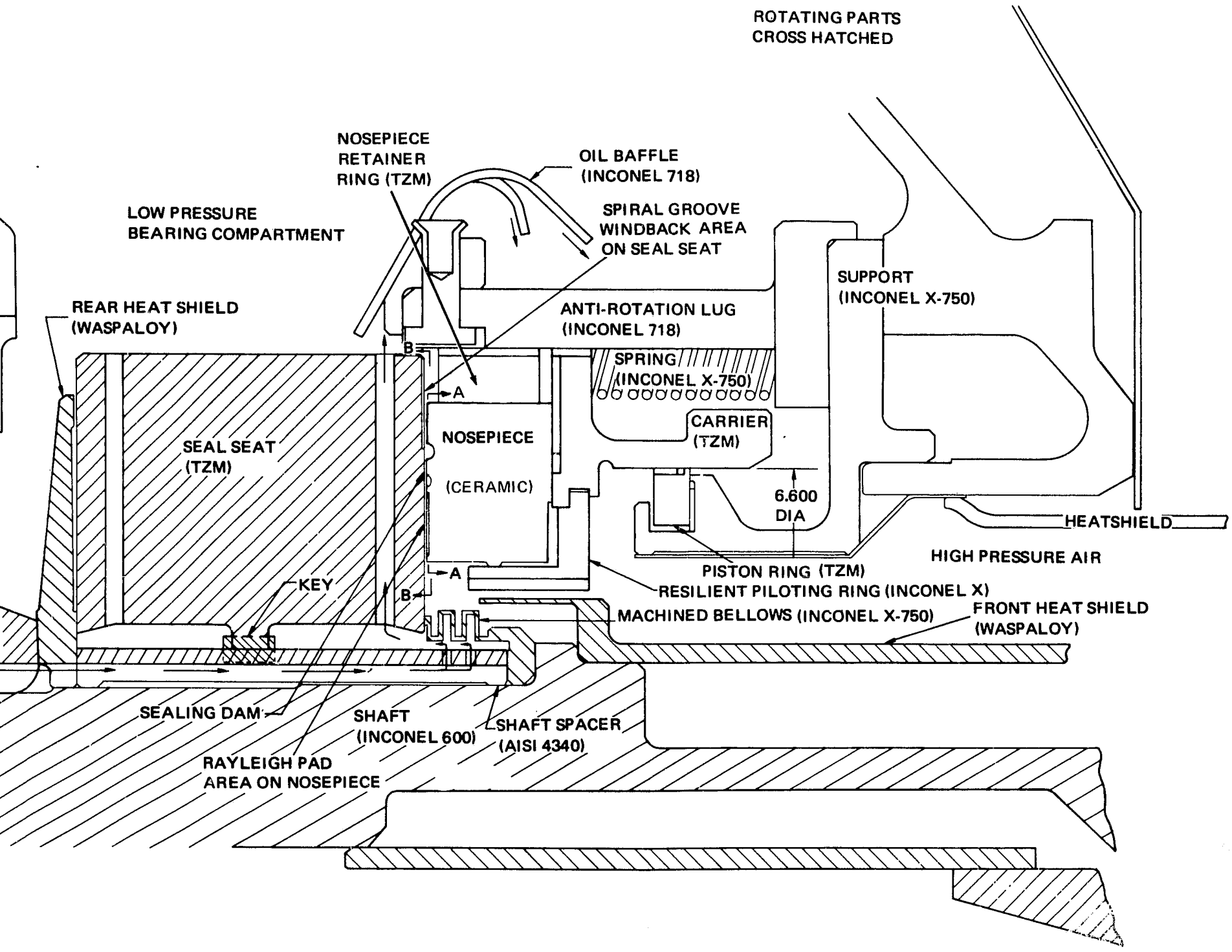

Figure 4 Design Features of the Ceramic Seal

FOLDOUT FRAME 1

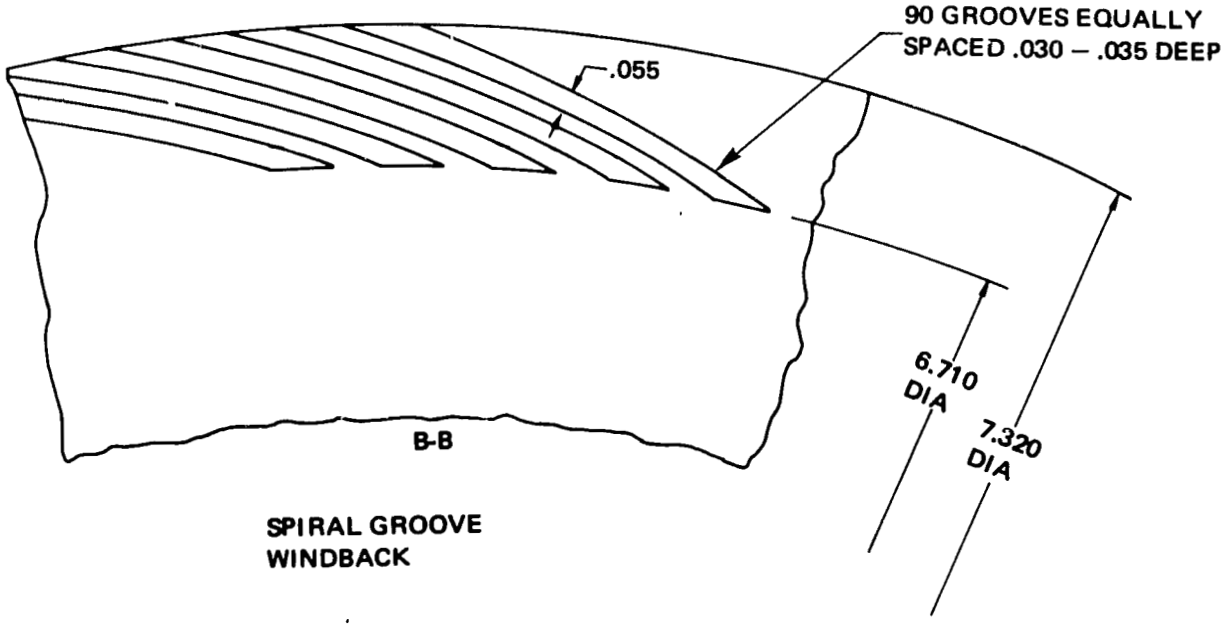

SPIRAL GROOVE
WINDBACK

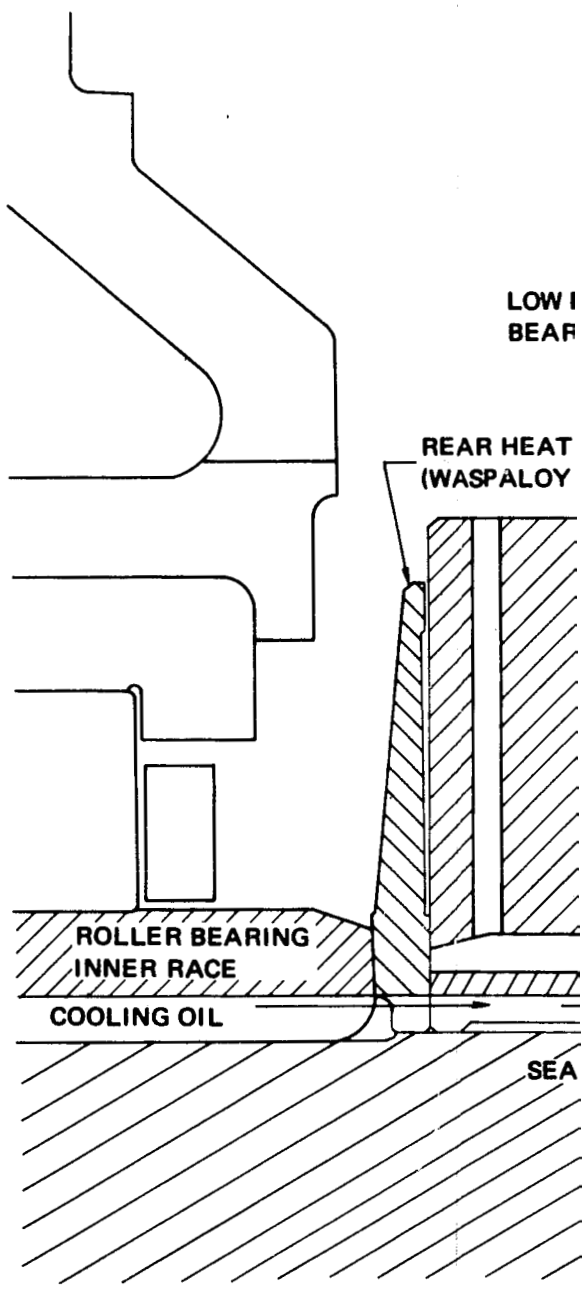

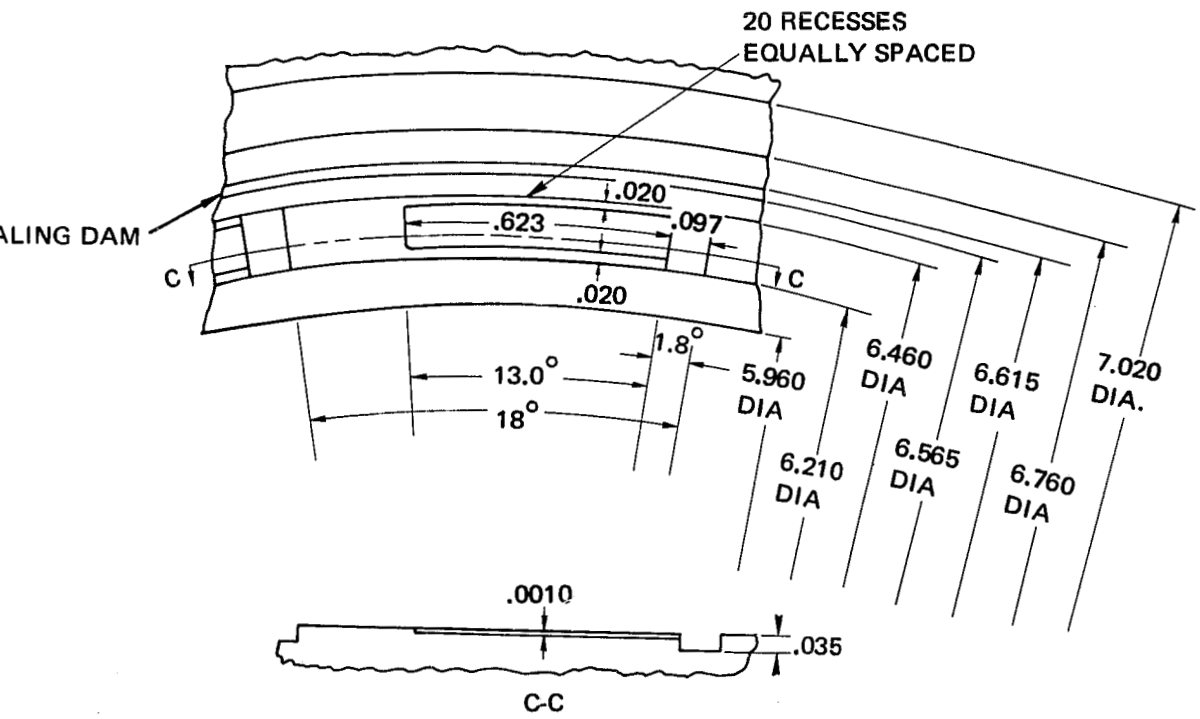

RAYLEIGH PAD AND
SEAL DAM DIMENSIONS

FOLDOUT FRAME 2

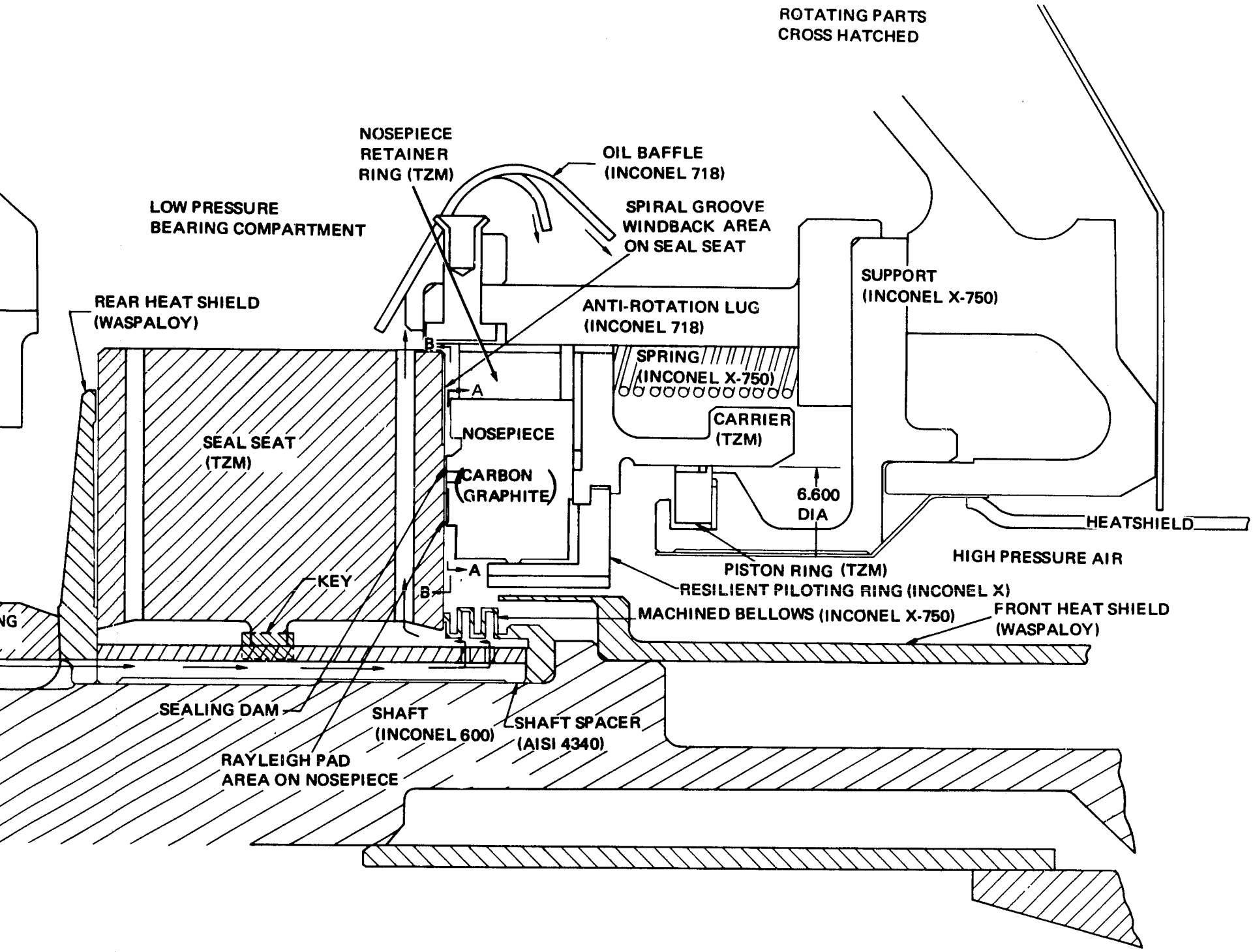

Figure 5 Design Features of the Narrow-Pad Seal

FOLDOUT FRAME 1

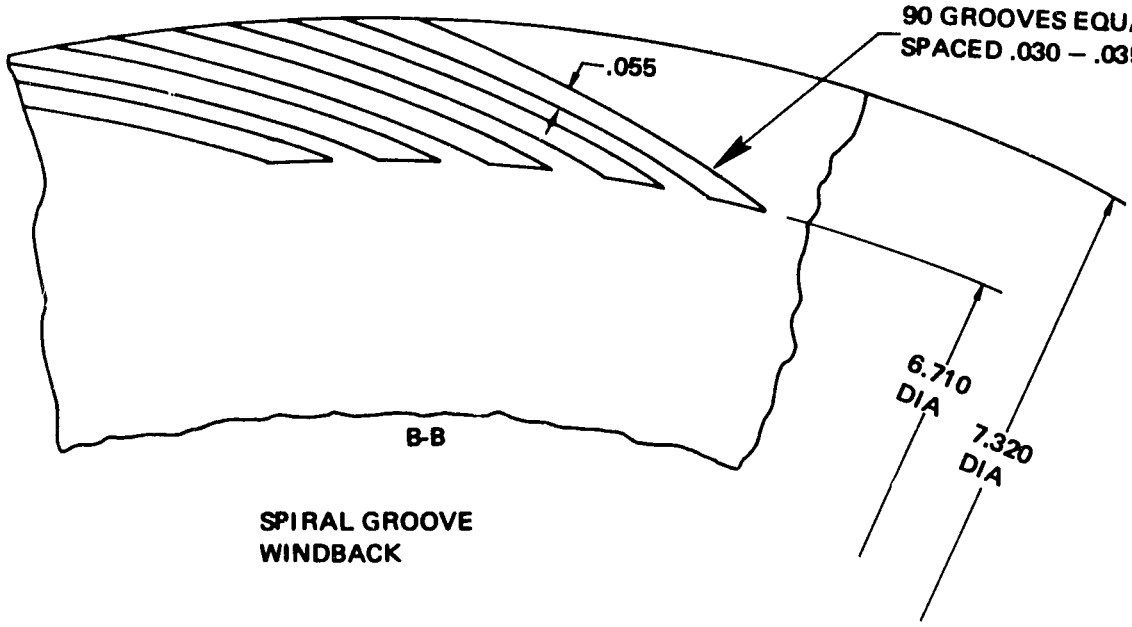

SPIRAL GROOVE
WINDBACK

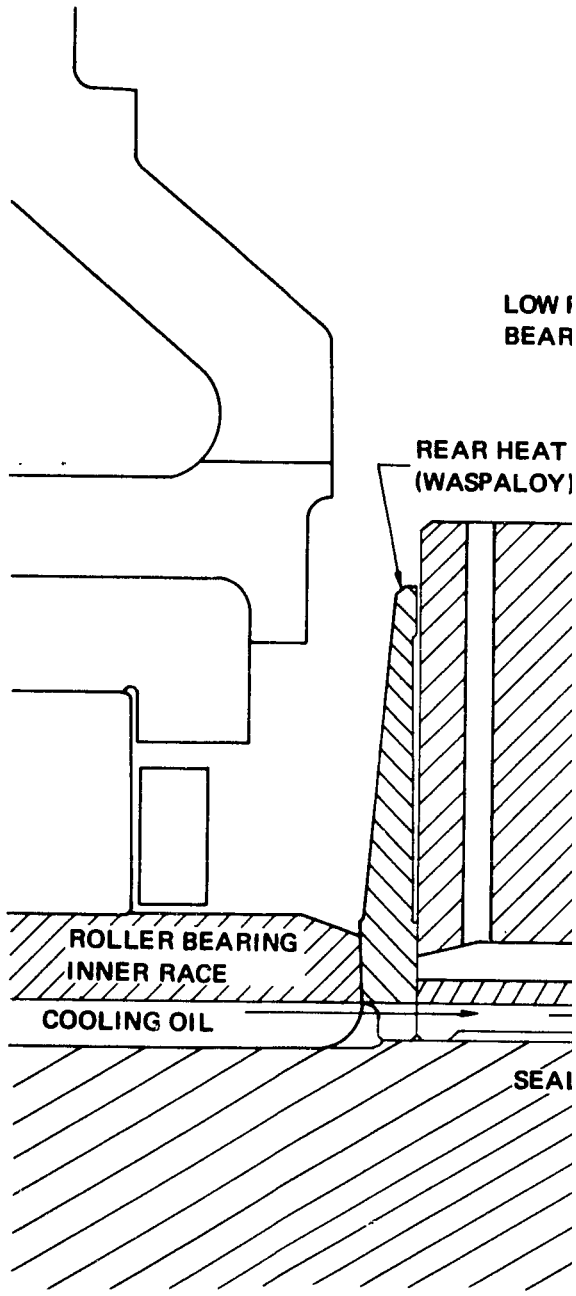

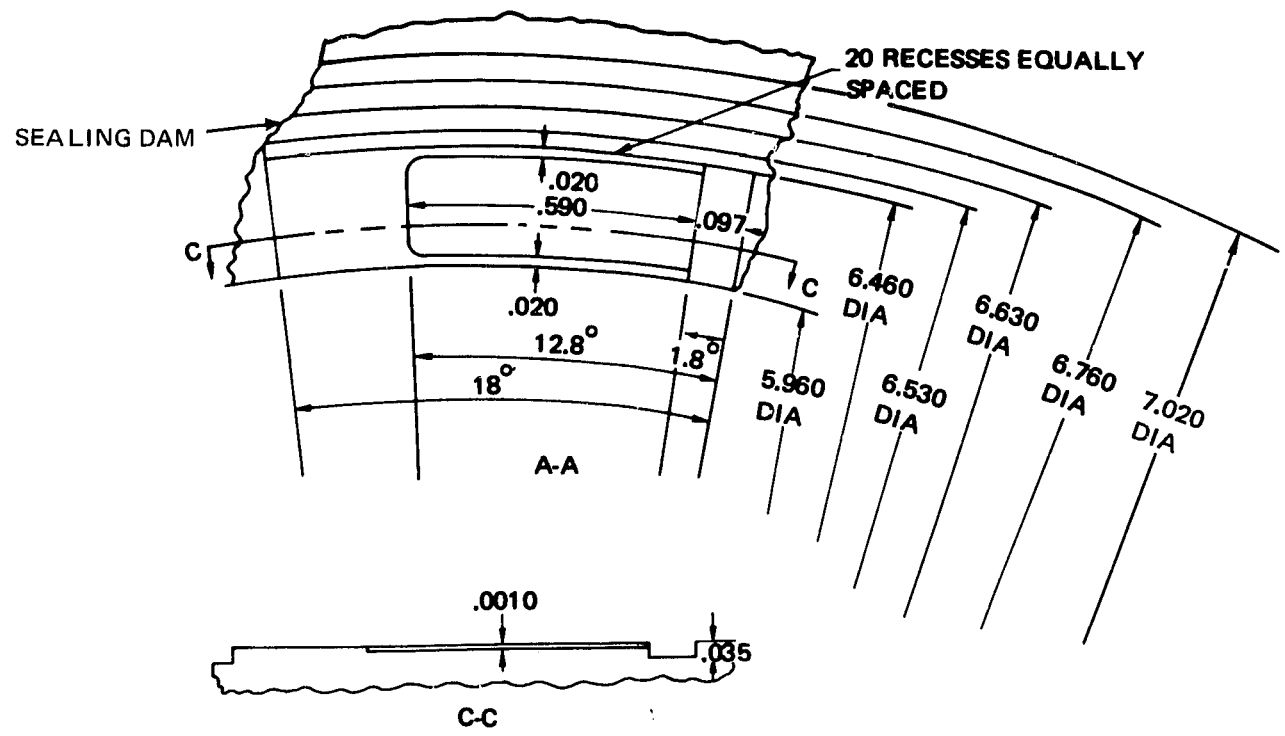

RAYLEIGH PAD AND
SEAL DAM DIMENSIONS

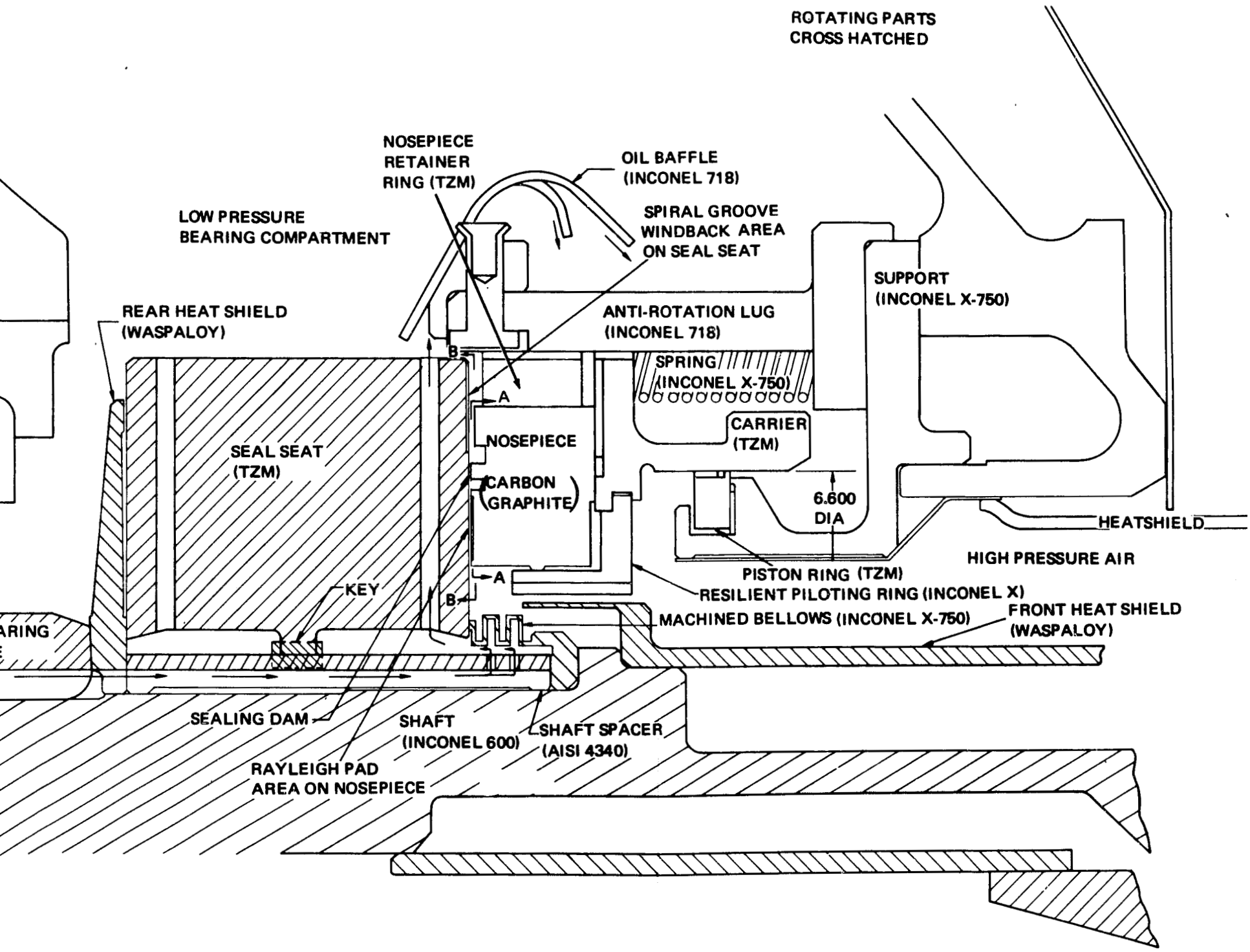

Figure 6 Design Features of the Wide-Pad Seal

FOLDOUT FRAME 1

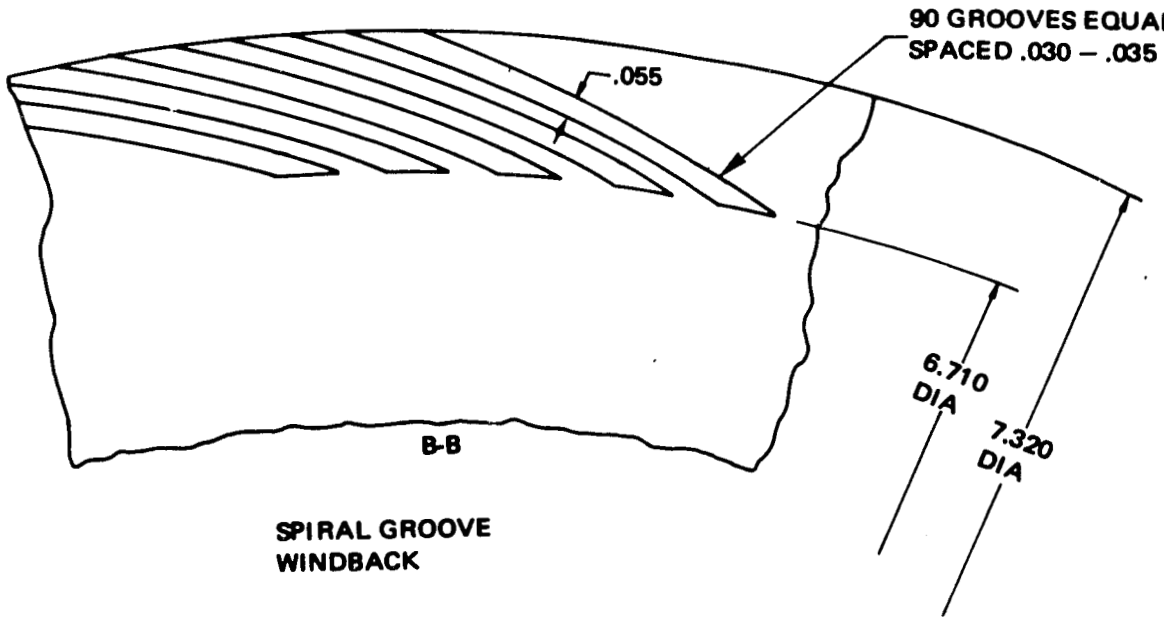

SPIRAL GROOVE
WINDBACK

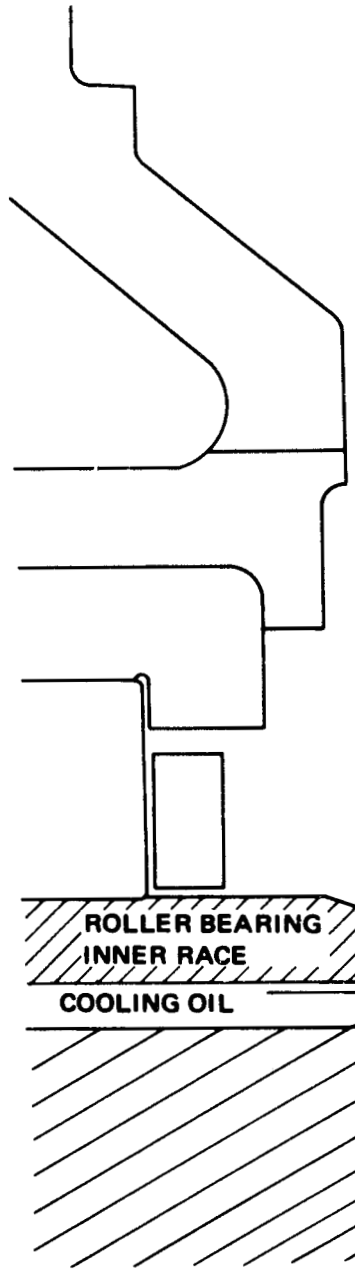

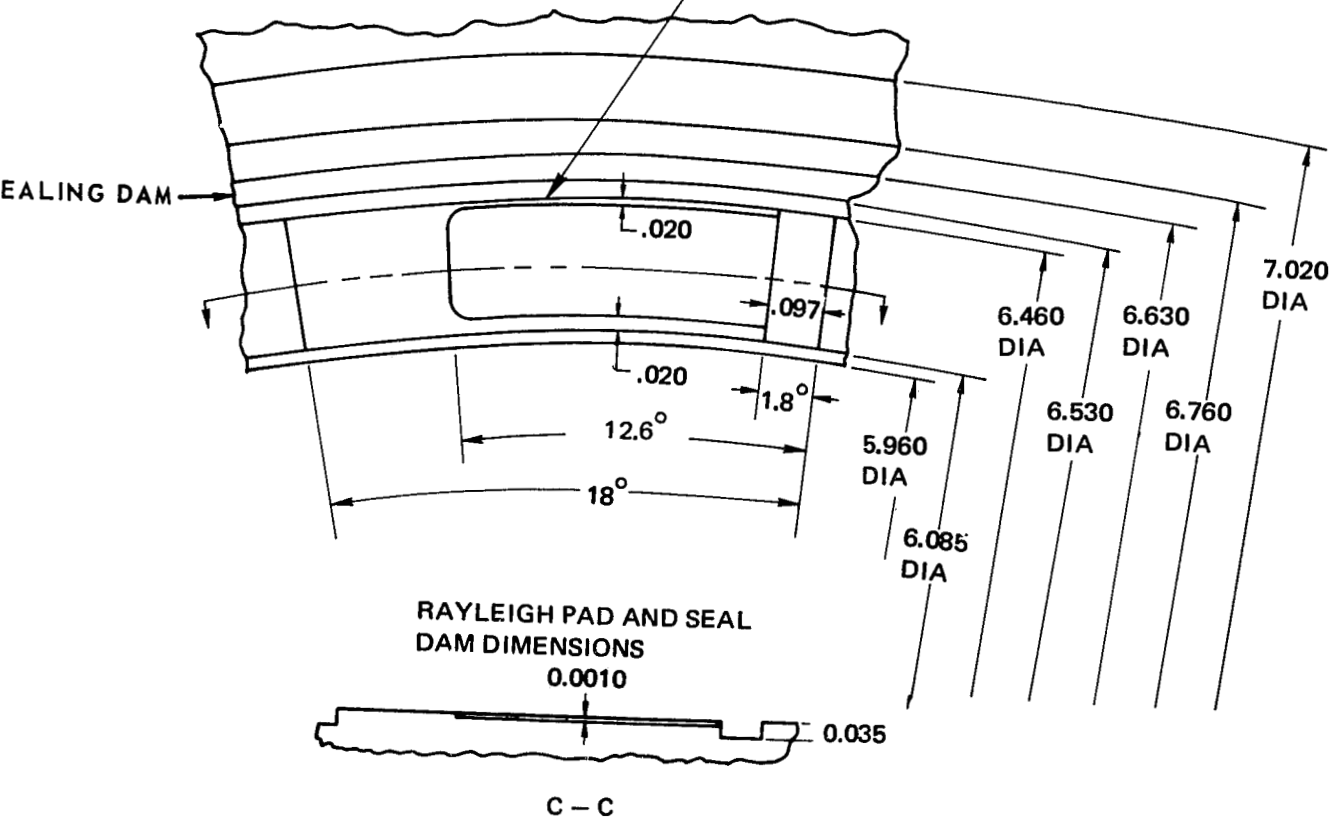

RAYLEIGH PAD AND SEAL
DAM DIMENSIONS

C – C

FOLDOUT FRAME 2

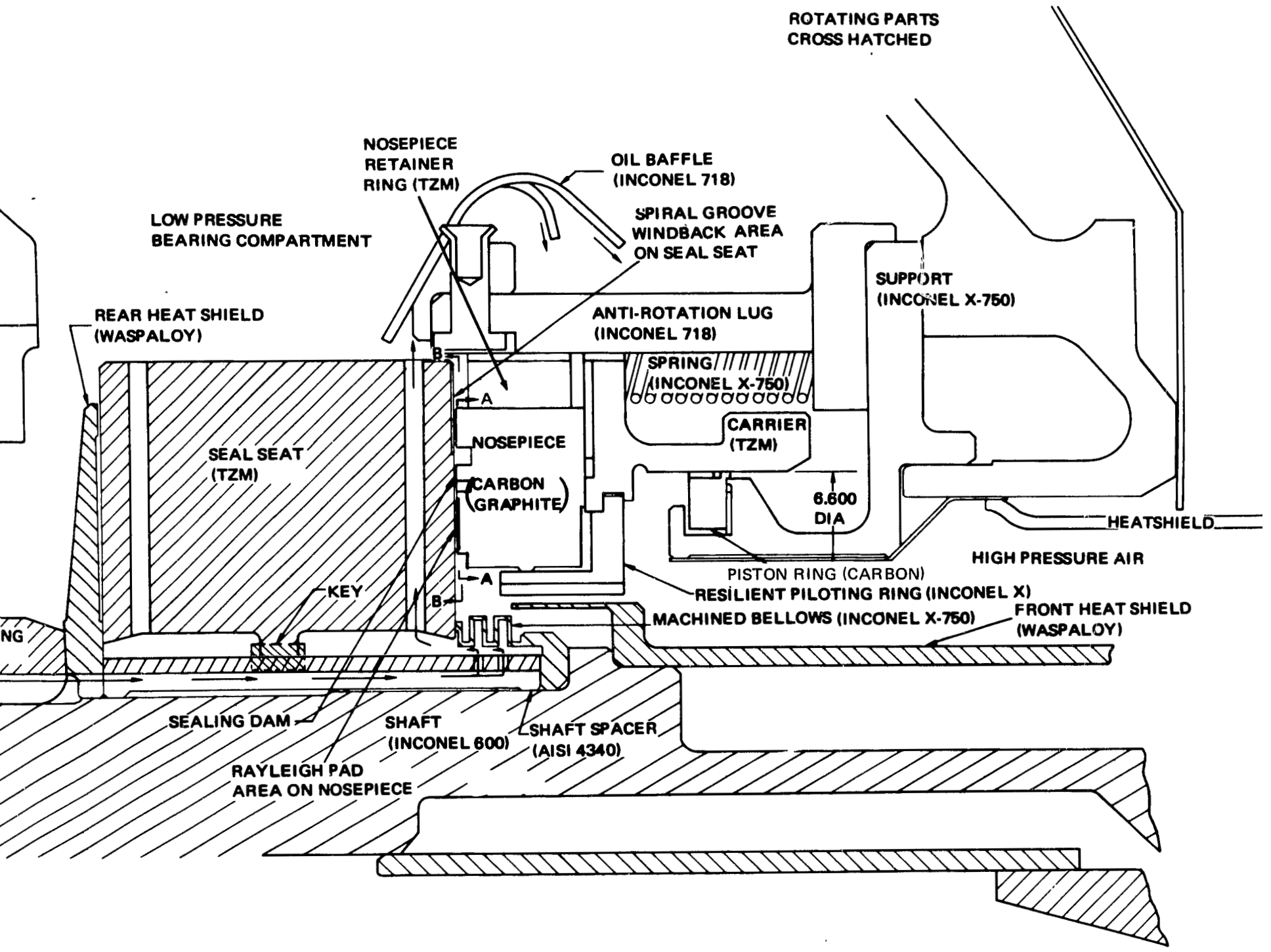

Figure 7 Design Features of the Revised Narrow-Pad Seal

FOLDOUT FRAME 1

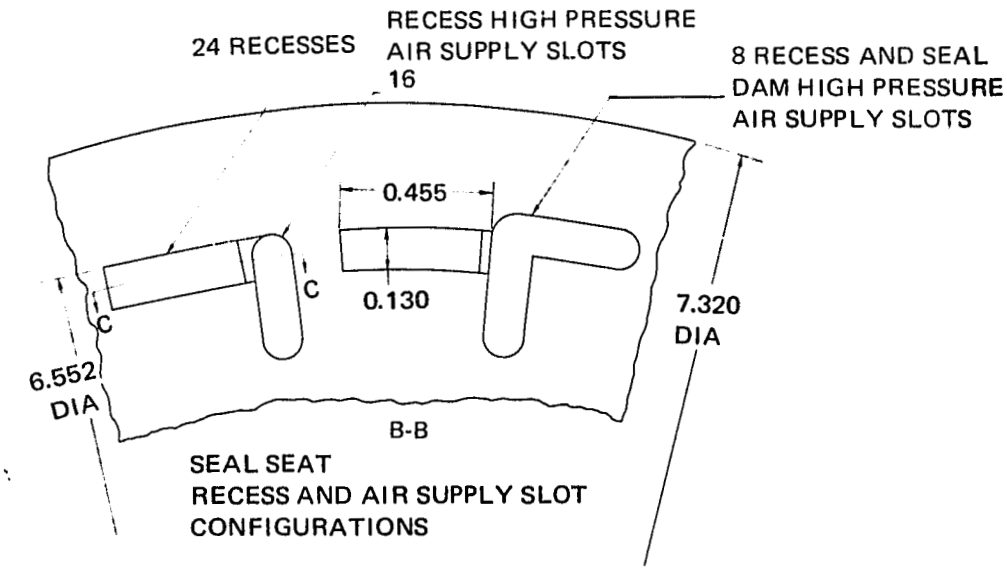

SEAL SEAT
RECESS AND AIR SUPPLY SLOT
CONFIGURATIONS

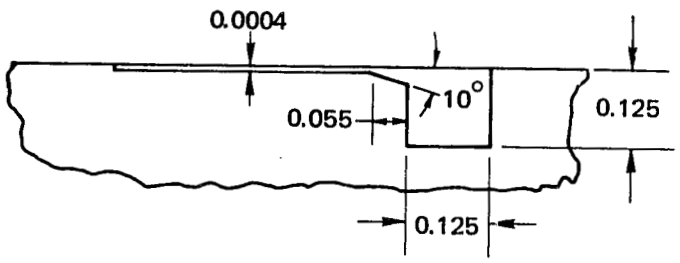

C-C

SEAL SEAT
RECESS DIMENSIONS

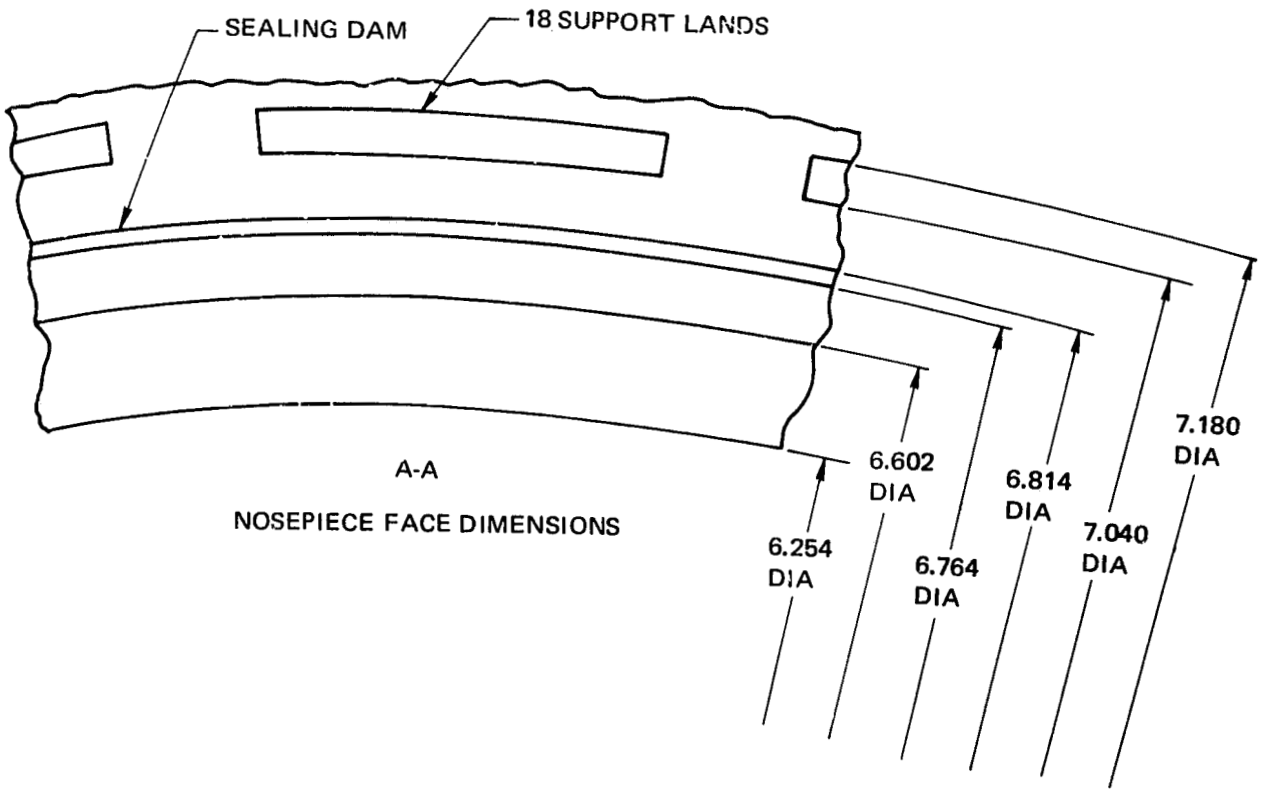

NOSEPIECE FACE DIMENSIONS

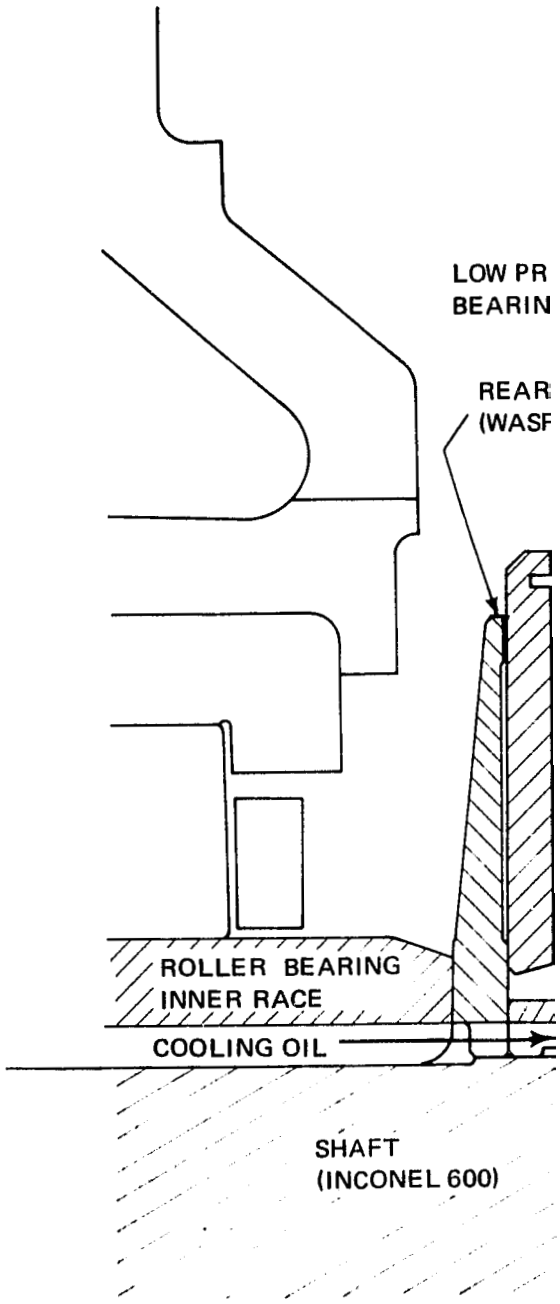

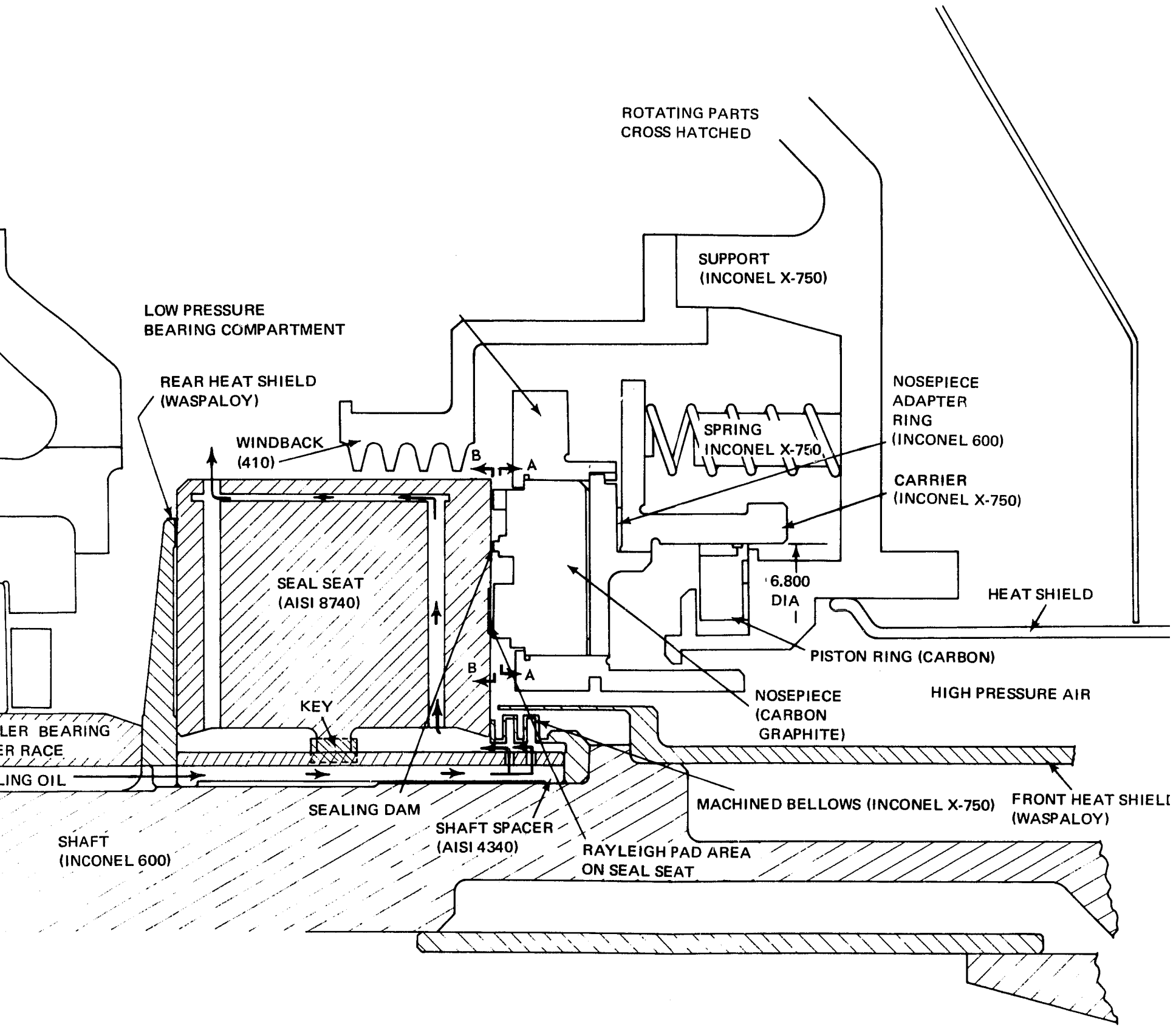

Figure 8 Design Features of the Recessed Seat Seal

PRECEDING PAGE BLANK NOT FILMED

TABLE I
SEAL CHARACTERISTICS

	Ceramic Seal	Narrow-Pad Seal	Wide-Pad Seal	Revised Narrow-Pad Seal	Recessed Seat Seal
Pad Width (in)	0.260	0.125	0.250	0.188	0.174
Pad Length (in)	0.541	0.995	0.985	0.985	– –
Number of Pads	36	20	20	20	8 sets of 3
Recess Depth (mils)	0.5	1.0	1.0	1.0	0.4
Ratio of Recess Length to Land Length	3.1	3.3	2	2	– –
Seal Dam Width (in)	0.050	0.025	0.050	0.050	0.025
Balance Diameter (in)	6.6	6.6	6.6	6.6	6.8
Percent Imbalance	70	70	70	70	72
Spring Load (lbs)	15.5	20	25	15	11.3
Film Thickness at 300 ft/sec, 50 psi, 150°F (mils)	0.28	0.13	0.27	0.18	0.21
Film Thickness at 300 ft/sec, 50 psi, 150°F (scfm)	0.96	0.21	0.28	0.24	0.78
Film Thickness at 500 ft/sec, 300 psi, 150°F (mils)	0.37	0.20	0.38	0.27	0.25
Leakage at 500 ft/sec, 300 psi, 150°F (scfm)	24	10	12	15	17

D. SEAL PERFORMANCE ANALYSES

For the five designs analyzed under Phase III, mean film thickness and primary air leakage were calculated by establishing a balance in the steady-state axial forces. These forces are dependent on seal surface speed, air pressure differential, air temperature, the deviation of the primary sealing surfaces from true parallelism, and the relationship between the diameters of the sealing dam and the secondary seal.

The steady-state axial forces acting on a seal nosepiece are shown in Figure 9. The mean operating film thickness was found by equating the opening forces with the closing forces:

$$F_P + F_D = F_B + F_S$$

where:

F_P = Rayleigh pad load capacity (lbs)
F_D = dam load capacity (lbs)
F_B = hydraulic balance load (lbs)
F_S = spring load (lbs)

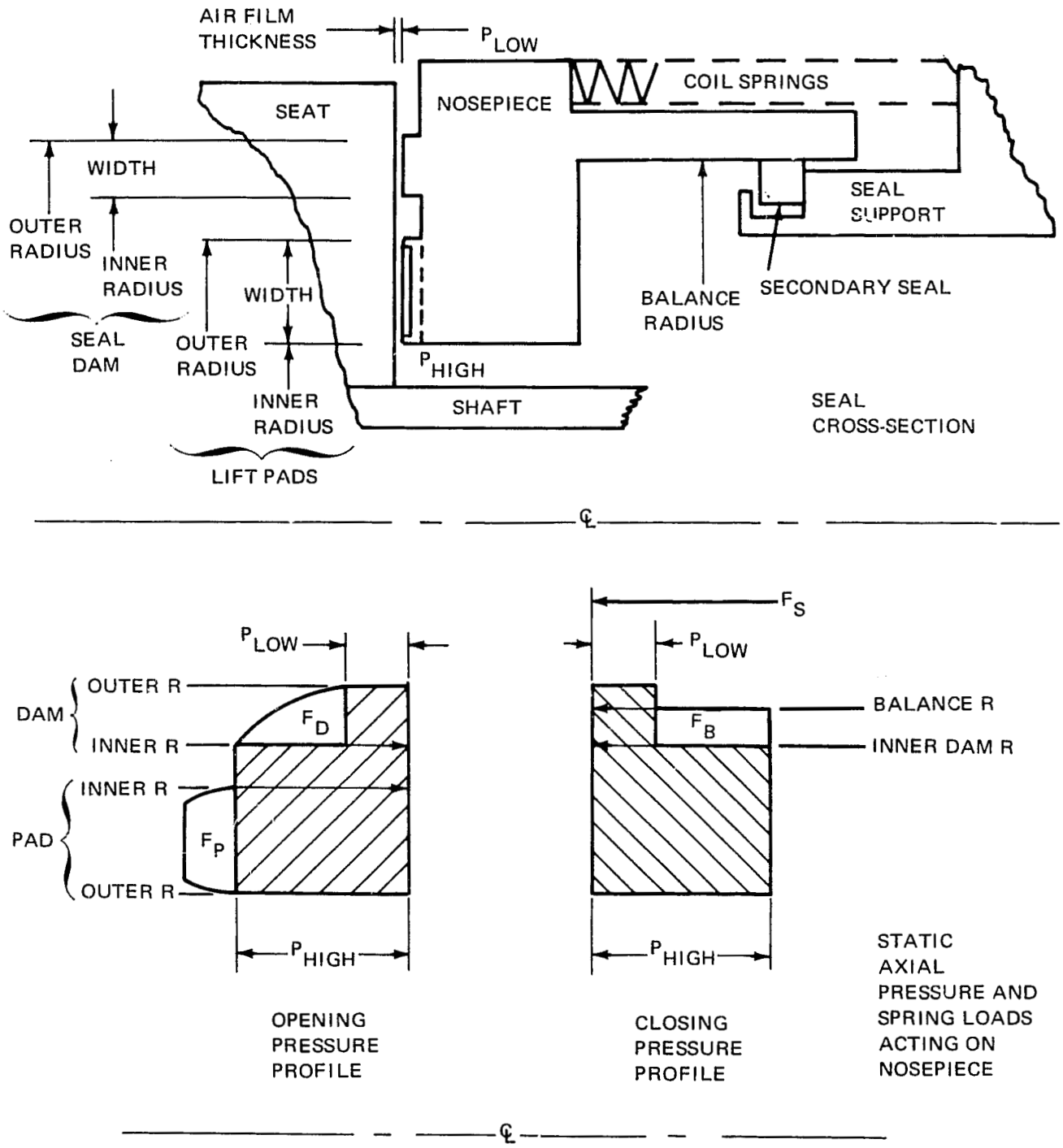

Figure 9 Schematic Diagram of the Steady-State Forces Acting on the Nosepiece and Seal Seat. Forces Represented by the Cross-Hatched Regions of the Axial Pressure Profiles are Equal and Opposite, and Therefore Omitted from the Equation

The pad load capacity is a function of speed, temperature, pad geometry, and air-film thickness; the dam load capacity is a function of the pressure differential across the seal, the dam geometry and the air film thickness. The hydraulic balance load is a function of the pressure differential across the seal, the balance radius, and the dam inner radius; and the spring load is a function of spring geometry, spring deflection, and the number of springs. The forces represented by the crosshatched regions of the axial pressure profiles in Figure 9 are equal and opposite, so they are omitted from the force-balance equation. Since both the Rayleigh pad load capacity and the seal dam load capacity vary significantly with film thickness, the force-balance equation was solved graphically.

The Rayleigh pad geometry used in each seal is fundamental to the seal design. The various seal designs have been identified by variations in pad width. All seals were made with nearly equal circumferential lengths so that pad width determined the pad area of each seal. Note that pad area controls the relative load capacity and stiffness levels of the seal air film.

Pad load capacity should be made high enough to allow for variations in seal force balance due to manufacturing tolerances and dimensional changes during operation. Pad stiffness must be high enough to cause the seal nosepiece to respond to runout of the seal seat so that heavy contact between the nosepiece and the seat is avoided. On the other hand, an increase in pad width leads to a corresponding increase in the air film thickness variation caused by a given amount of seal surface distortion.

Large pad widths also lead to seal designs which are too large and heavy for aircraft engine applications. The factors which determine the most suitable pad width for a given application are complex and subject to uncertainity. Pad width selection should be based on an accumulation of analytical and experimental background.

The selection of other pad design features was based on studies of the effects of pad geometry on load capacity. The number of pads and recess dimensions were chosen to provide maximum load capacity levels within the pad width constraints applied to each seal design. Practical considerations such as pad wear resistance and fabrication techniques also influenced pad design.

Figure 10 shows the combined effects of number of pads and recess depth on load capacity for a film thickness of 0.2 mil. It applies to the revised narrow pad seal at an air temperature of 150°F, but is typical of all padded seal designs operating over a wide range of conditions. The curves indicate that a large number of pads with shallow recesses produce the highest load capacity. The one mil recess depth used in the narrow-pad, wide-pad, and revised narrow-pad seal designs, however, is deeper than the optimum value. It was chosen to allow for a limited amount of wear and oxidation of the nosepiece surface. The selection of twenty pads followed from the choice of recess depth. When the pad recesses are placed in a more wear-resistant material, the recess depth may be reduced and the number of pads increased. The pad geometry selected for the ceramic seal and the recessed seat seal followed this practice, as shown in Table I.

The effect of recess length on pad load capacity is shown in Figure 11. The choice of recess length was influenced by the requirement that the land surface area be made large enough to ensure adequate pad wear resistance. A recess-to-land length ratio of two was selected for the carbon seal designs while a value of three was selected for the more wear-resistant ceramic seal. These values were chosen to balance the maximum load capacity requirements against the high wear resistance objectives which apply to the seal program.

After seal pad geometry had been established, the variation of pad load capacity with changes in film thickness, air temperature, and seal surface speed was determined. Curves of load capacity versus film thickness were generated for each of the five seals for sliding speeds from 300 to 500 ft/sec. They are shown in Figures 12 through 20. In order to standardize the performance predictions for the various seal designs, the nominal seal sliding speed was established using a 6.6 inch diameter as the reference point.

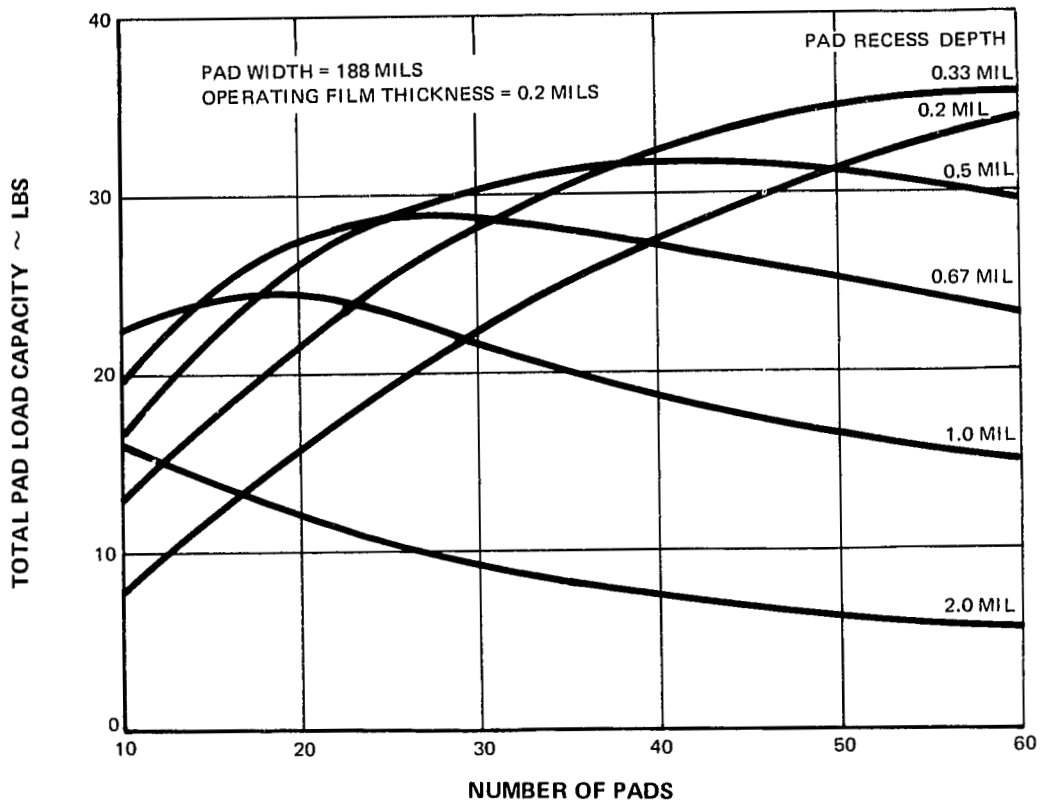

Figure 10 Effect of Recess Depth and Number of Pads on Total Load Capacity

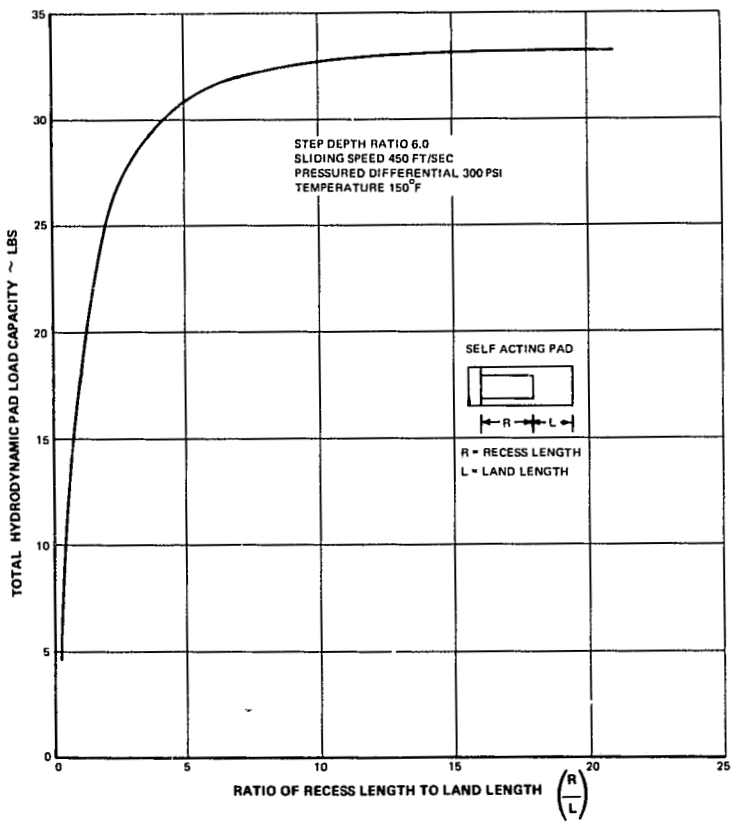

Figure 11 Relationship Between Total Hydrodynamic Pad Load Capacity and Ratio of Recess Length to Land Length

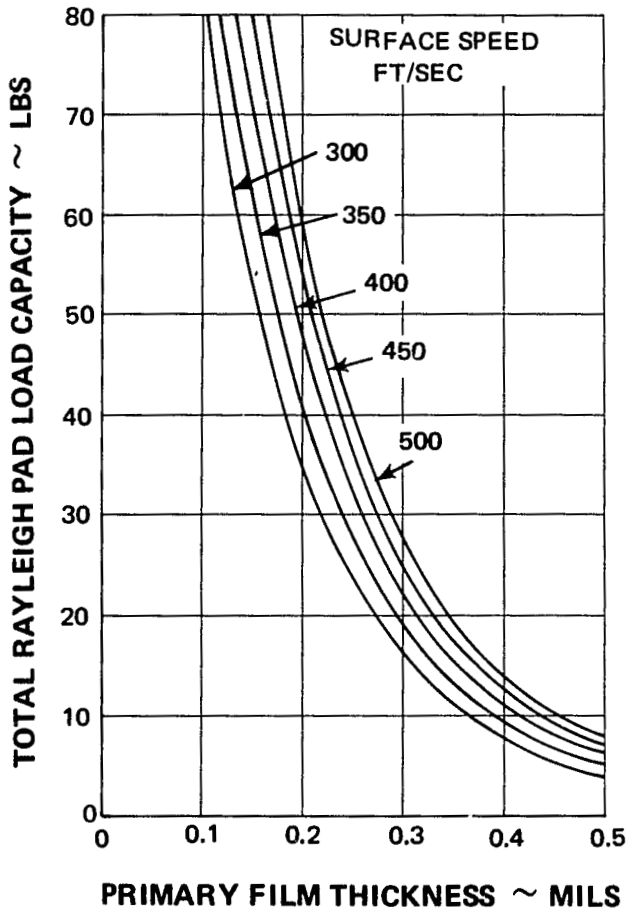

Figure 12 Load Capacity of the Rayleigh Pads in the Ceramic Seal at an Air Temperature of 150°F

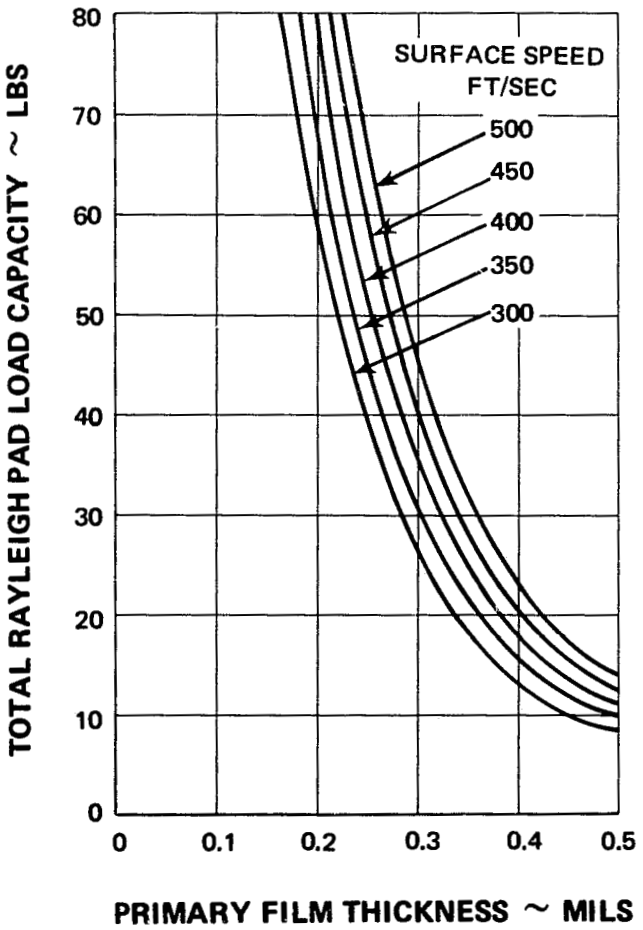

Figure 13 Load Capacity of the Rayleigh Pads in the Ceramic Seal at an Air Temperature of 800°F

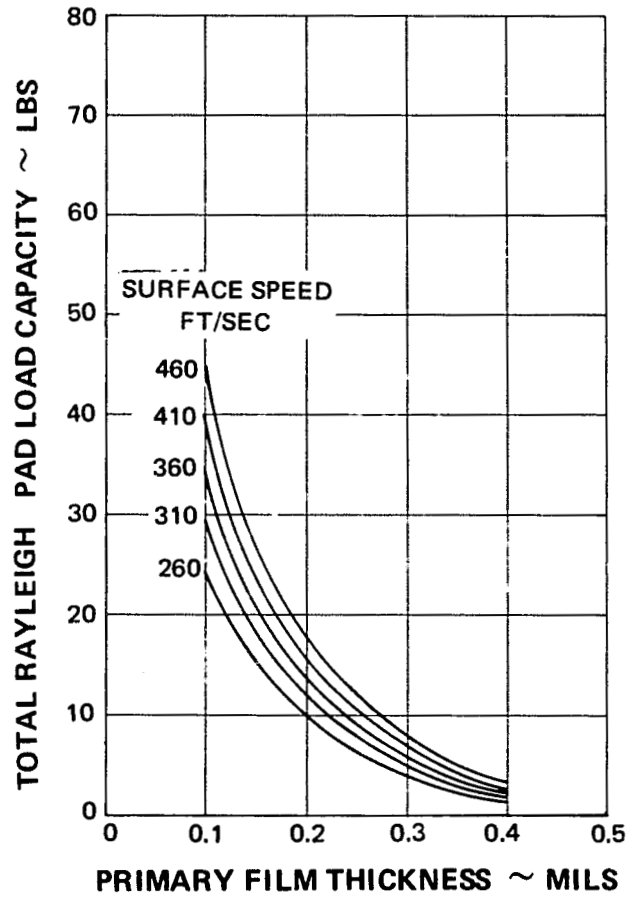

Figure 14 Load Capacity of the Rayleigh Pads in the Narrow-Pad Seal at an Air Temperature of 150°F

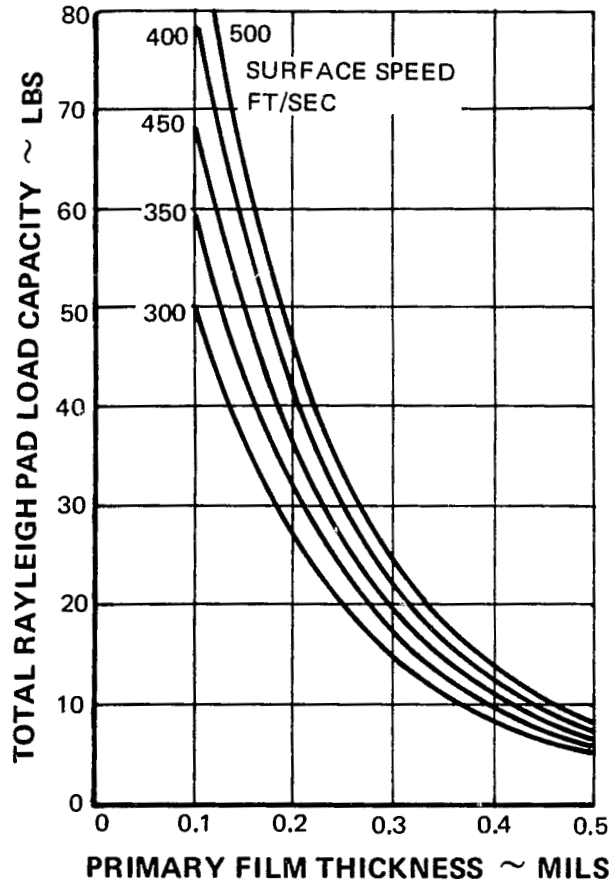

Figure 15 Load Capacity of the Rayleigh Pads in the Wide-Pad Seal at an Air Temperature of 150°F

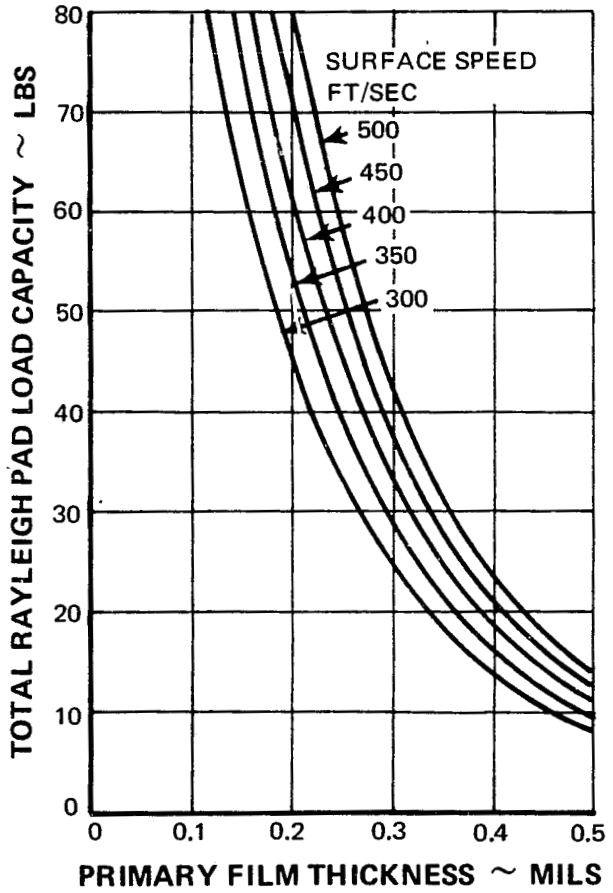

Figure 16 Load Capacity of the Rayleigh Pads in the Wide-Pad Seal at an Air Temperature of 800°F

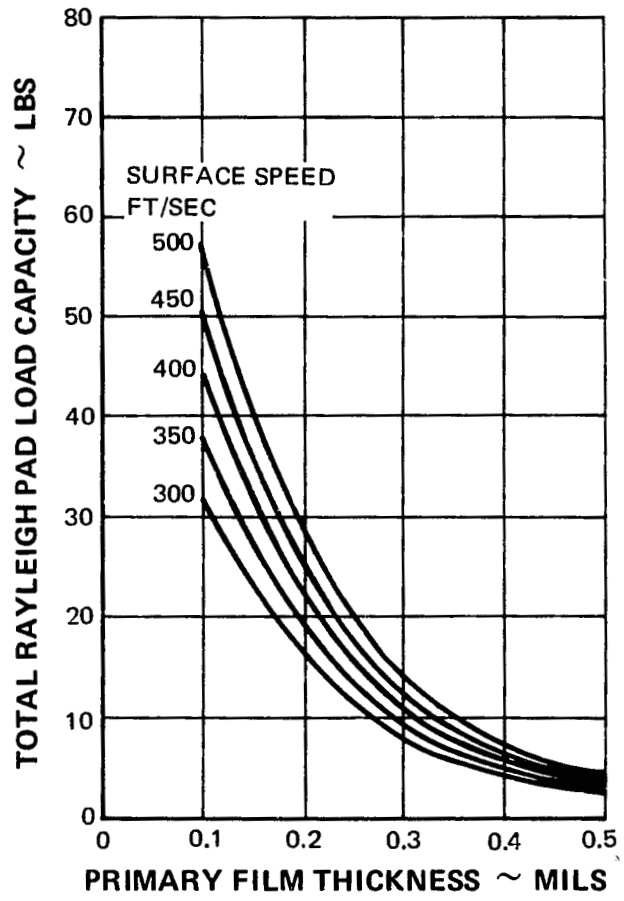

Figure 17 Load Capacity of the Rayleigh Pads in the Revised Narrow-Pad Seal at an Air Temperature of 150°F

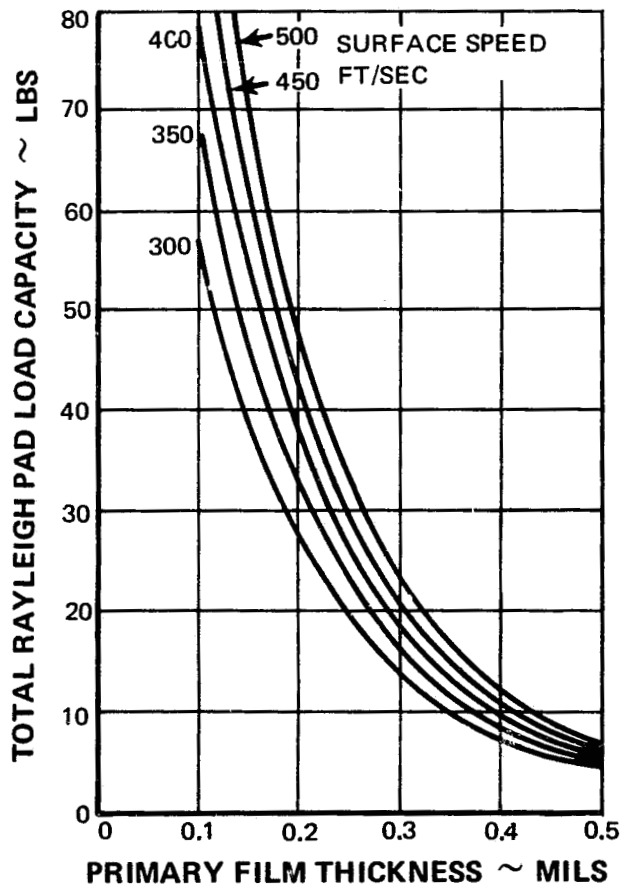

Figure 18 Load Capacity of the Rayleigh Pads in the Revised Narrow-Pad Seal at an Air Temperature of 800°F

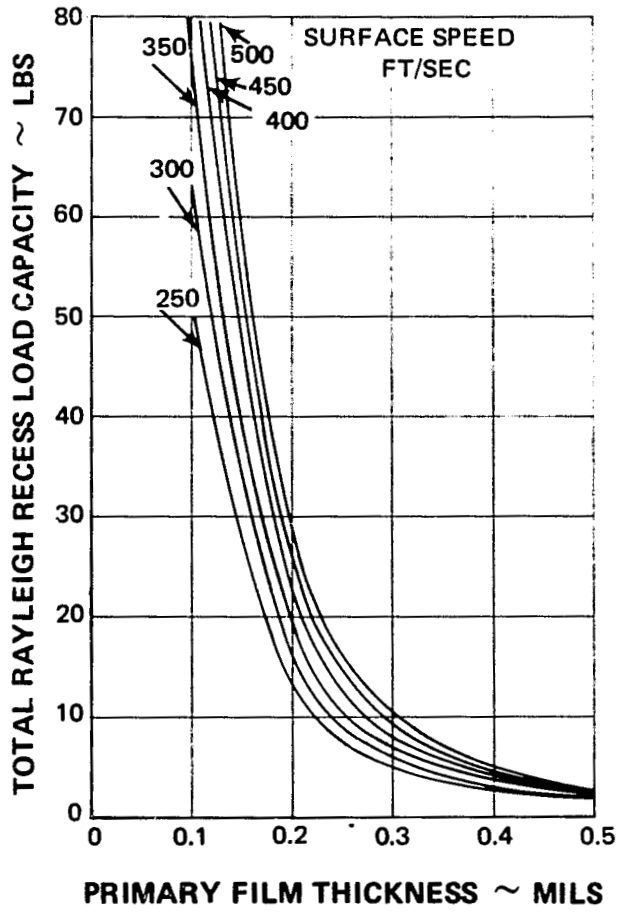

Figure 19 Load Capacity of the Rayleigh Pads in the Recessed Seat Seal at an Air Temperature of 150°F

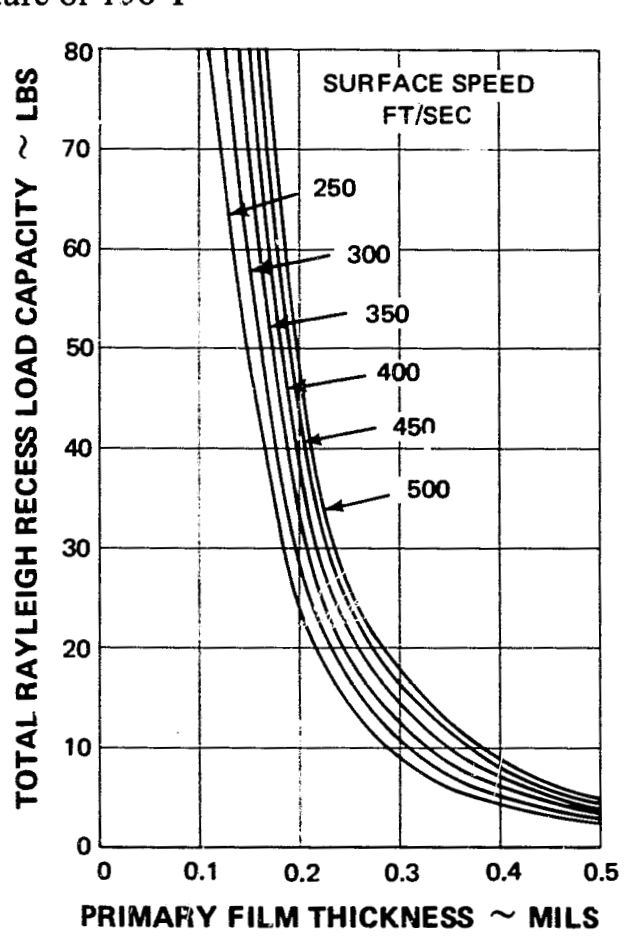

Figure 20 Load Capacity of the Rayleigh Pads in the Recessed Seat Seal at an Air Temperature of 800°F

All calculations to determine Rayleigh pad design and operating characteristics were done with the aid of the computer program described in Appendix B of Reference 1 and Appendix A of Reference 2. The program produces an iterative solution for a two dimensional compressible fluid flow matrix with variable flow areas in both flow directions.

The load capacity of the seal dam was determined with a computer program titled "Quasi-One-Dimensional Compressible Flow Across Face Seals and Narrow Slots", described in Reference 4. The program considers fluid inertia, viscous friction, and entrance loss effects for subsonic and choked-flow conditions in both laminar and turbulent flow regimes. Curves of load capacity versus film thickness were calculated for seal differential pressures from 50 to 300 psi, and are shown in Figures 21, 22, and 23. The ceramic seal, the wide-pad seal, and the revised narrow-pad seal all have the same seal dam dimensions. Their calculated dam load capacities are identical, as shown on Figure 21. Since the dam widths for the narrow-pad seal and the recessed seat seal are the same but their locations are slightly different, there are some slight differences in their load capacities, as shown in Figures 22 and 23. Comparing Figures 21, 22, and 23, it can be seen that the principal factors which affect seal dam load capacity are dam width and pressure differential, with load capacity being roughly proportional to both of those factors. The slight increase in load capacity with increasing film thickness, more evident at the high pressures, is indicative of the transition in flow regimes from laminar to turbulent.

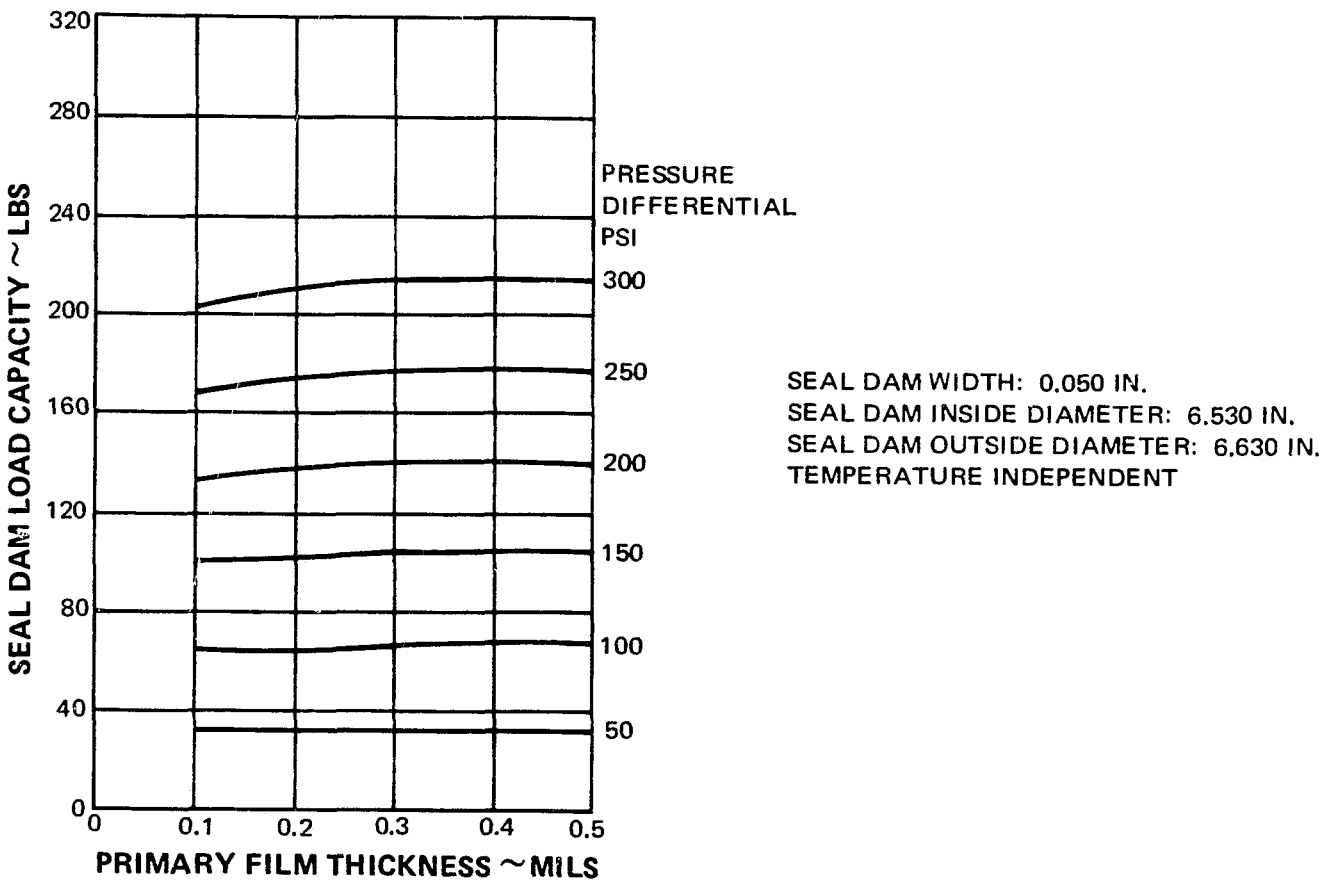

Figure 21 Seal Dam Load Capacity for the Ceramic Seal, Wide-Pad Seal, and the Revised Narrow-Pad Seal

SEAL DAM WIDTH: 0.025 IN.
SEAL DAM INSIDE DIAMETER: 6.565 IN.
SEAL DAM OUTSIDE DIAMETER: 6.615 IN.
TEMPERATURE INDEPENDENT

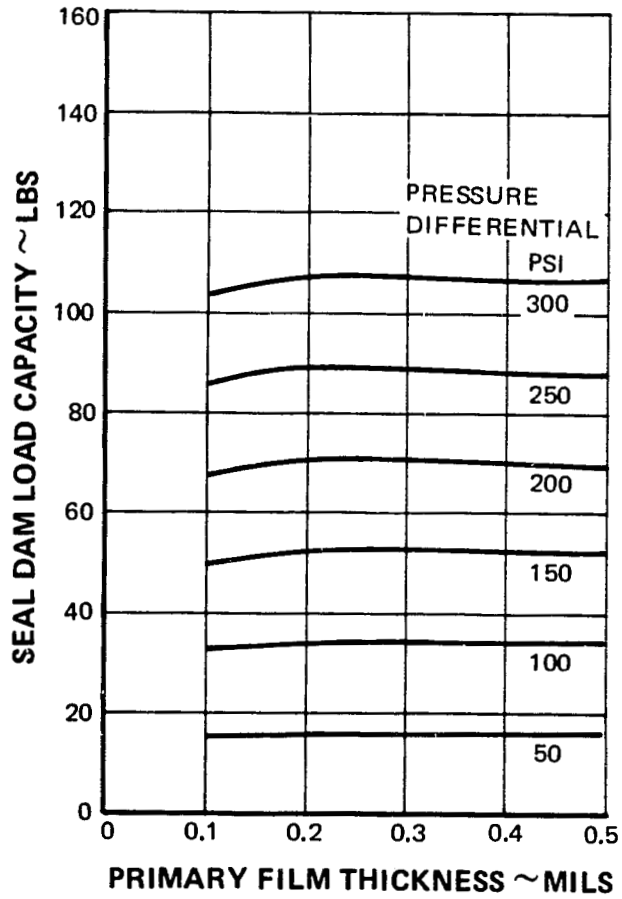

Figure 22 Seal Dam Load Capacity for the Narrow-Pad Seal

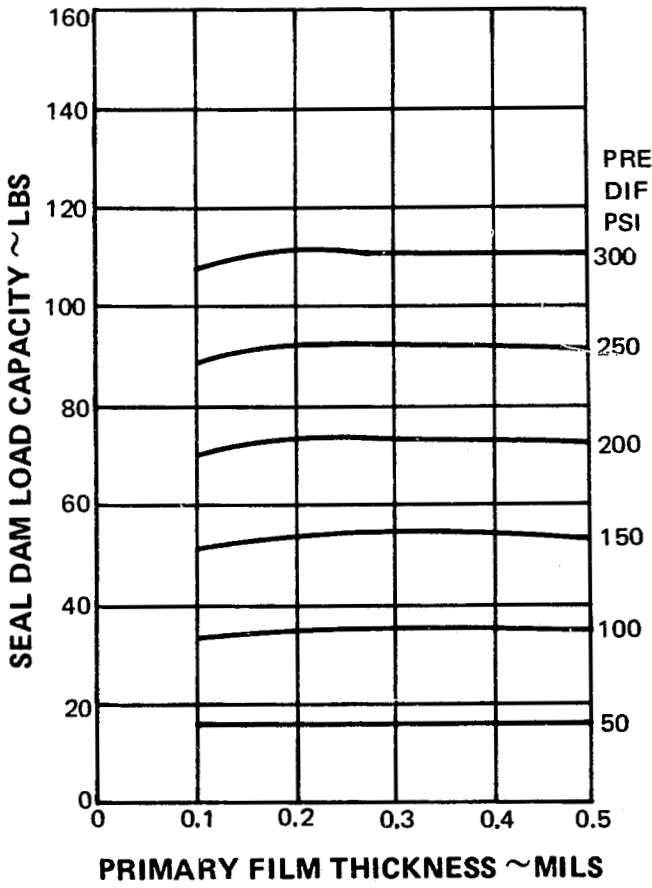

SEAL DAM WIDTH: 0.025 IN.
SEAL DAM INSIDE DIAMETER: 6.814 IN.
SEAL DAM OUTSIDE DIAMETER: 6.764 IN.
TEMPERATURE INDEPENDENT

Figure 23 Seal Dam Load Capacity for the Recessed Seat Seal

The operational film thickness for a seal depends on the balance between the total opening force on the seal and the total closing force. As discussed above, the opening forces on the seal are the Rayleigh pad load capacity and the seal dam load capacity (F_D and F_P). The closing forces on the seal are the spring force (F_S) and the hydraulic balance load (F_B). The hydraulic balance load is the force resulting from the pressure differential across the seal, and can be calculated by multiplying the seal pressure drop by the annular area between the inner edge of the seal dam and the balance diameter of the secondary seal. Table II gives the hydraulic balance load, spring force, and the total closing force for all five designs.

TABLE II
TOTAL CLOSING FORCES

Seal	Pressure Differential (psi)	Hydraulic Balance Load (lbs)	Spring Force (lbs)	Total Closing Force (lbs)
Ceramic Seal	50	36.1	15.5	51.6
	100	72.2	15.5	87.7
	150	108.3	15.5	123.8
	200	144.4	15.5	159.9
	250	180.5	15.5	196.0
	300	216.5	15.5	232.0
Narrow-Pad Seal	50	18.1	8	26.1
	100	36.2	8	44.2
	150	54.3	8	62.2
	200	72.4	8	82.4
	250	90.5	8	98.5
	300	108.6	8	116.6
Wide-Pad Seal	50	36.1	25	61.1
	100	72.2	25	97.2
	150	108.3	25	133.3
	200	144.4	25	169.4
	250	180.5	25	205.5
	300	216.5	25	241.5
Revised Narrow-pad Seal	50	36.1	15	51.1
	100	72.2	15	87.2
	150	108.3	15	123.3
	200	144.4	15	159.4
	250	180.5	15	195.5
	300	216.5	15	231.5
Recessed Seat Seal	50	19.4	11.3	30.7
	100	38.8	11.3	50.1
	150	58.2	11.3	69.5
	200	77.6	11.3	88.9
	250	96.8	11.3	108.1
	300	116.4	11.3	127.7

To determine the operational film thicknesses, the total closing force can be cross-plotted against the total seal load capacity for a given set of conditions. A typical cross plot for the revised narrow-pad seal is shown in Figure 24. It should be noted that the curves shown in Figure 24 are valid only for the conditions specified; raising the pressure differential, for example, would raise both the total closing force and the total seal load capacity.

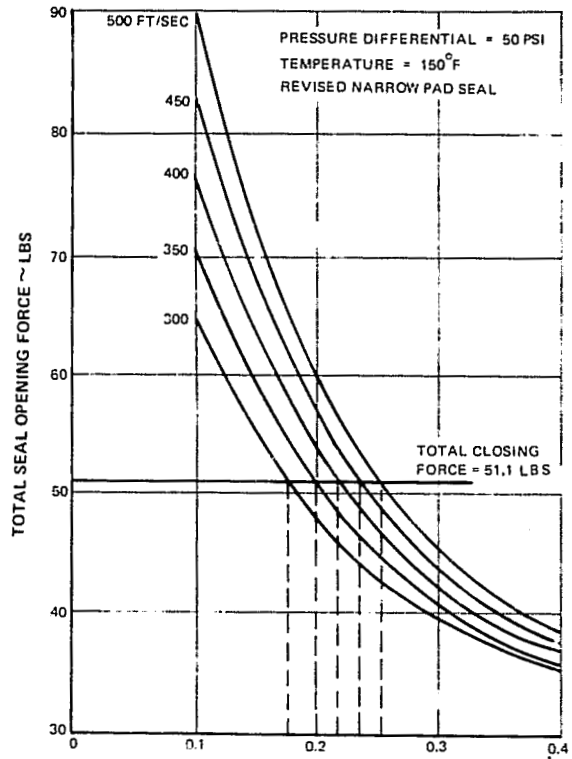

Figure 24 Typical Seal Force Balance Diagram

The compressible fluid flow program used to determine seal dam load also computes leakage past the primary seal as a function of film thickness. Figures 25 through 33 are plots of air leakage as a function of film thickness for the five seals. Cross-plotted over the leakage curves are the operating film thicknesses for constant operating speeds, as determine from the total load capacity plots. The pressure drop across the seal has a major effect on leakage and only a small effect on primary film thickness, while the seal surface speed has its major effect on film thickness with a relatively small effect on air leakage. The effect of spring load can be clearly seen in Figure 27. While increasing spring load decreases the primary film thickness, it also inceases the primary film stiffness, as can be seen by comparing Figure 27 with Figure 14. Looking at Figure 27, it can be seen that at 50 psi and a surface speed of 260 ft/sec, increasing the spring load from 0 to 20 pounds decreases the film thickness from 0.37 mil to 0.12 mil. From Figure 14 it is obvious that the slope of the load capacity curve is much steeper at a film thickness of 0.12 mil than at 0.37 mil. Since the stiffness of the film is the rate of change of load capacity with film thickness, the stiffness is greater at the lower film thickness (corresponding to the higher spring load).

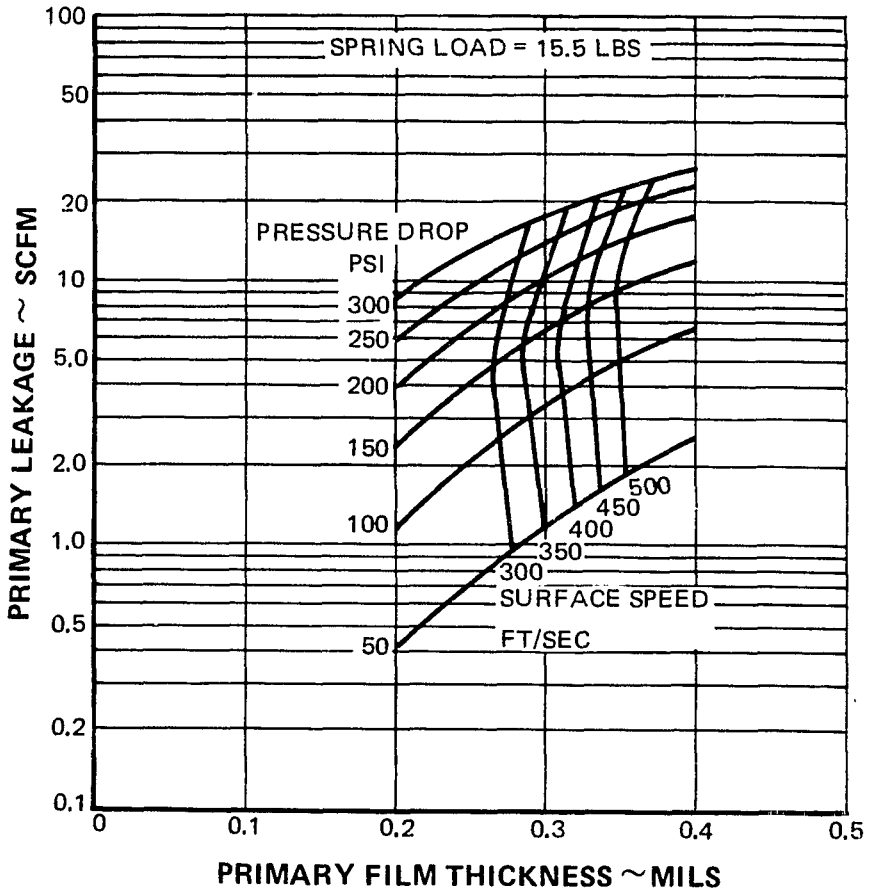

Figure 25 Calculated Primary Leakage and Film Thickness for the Ceramic Seal with Air at 150°F

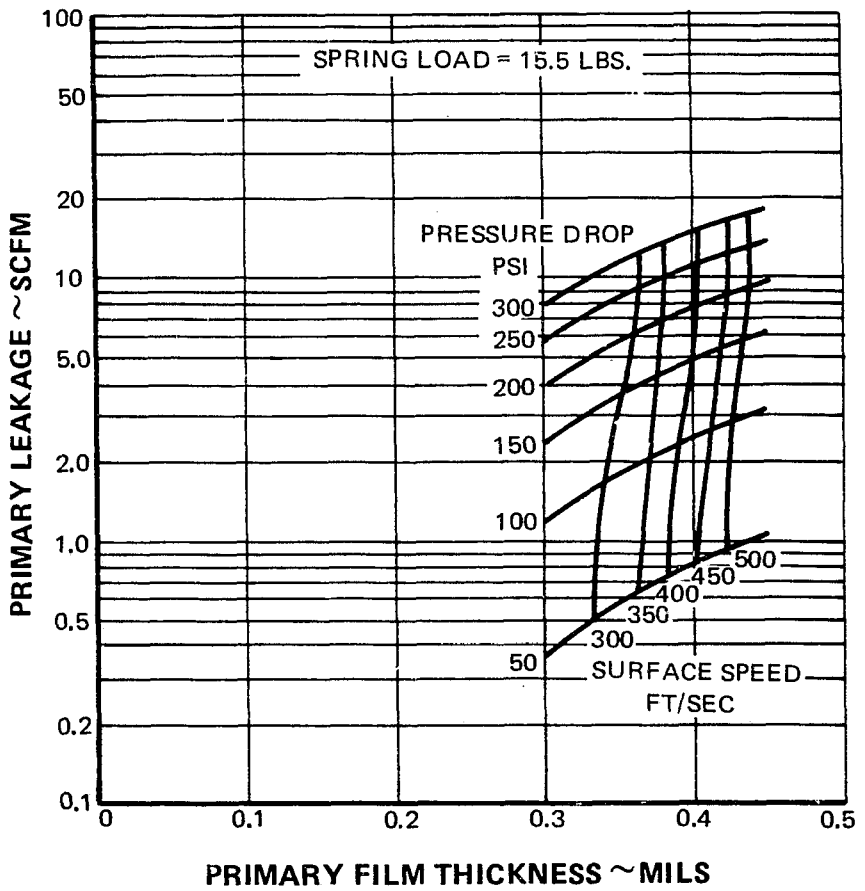

Figure 26 Calculated Primary Leakage and Film Thickness for the Ceramic Seal with Air at 800°F

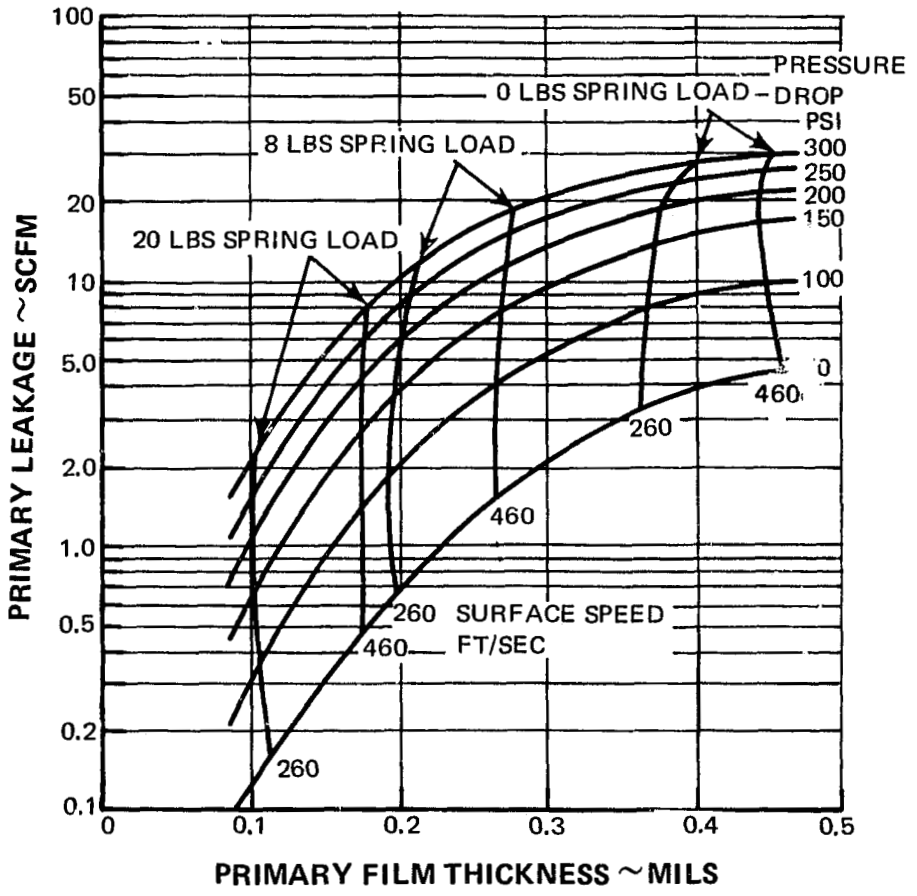

Figure 27 Calculated Primary Leakage and Film Thickness for the Narrow-Pad Seal with Air at 150°F

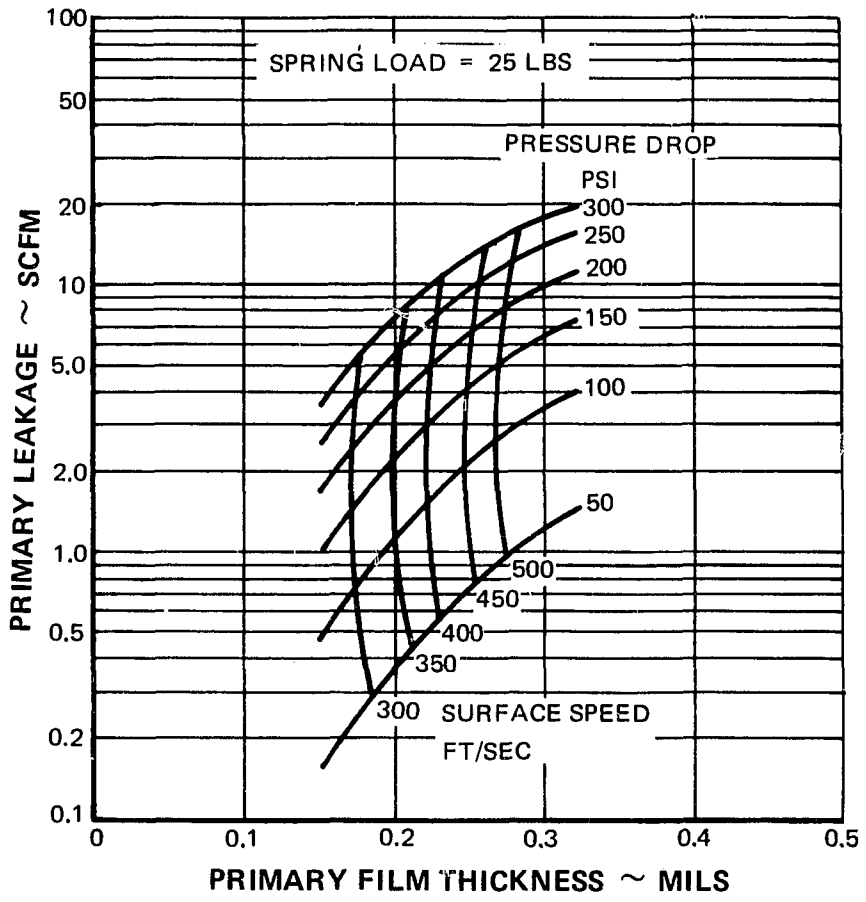

Figure 28 Calculated Primary Leakage and Film Thickness for the Wide-Pad Seal with Air at 150°F

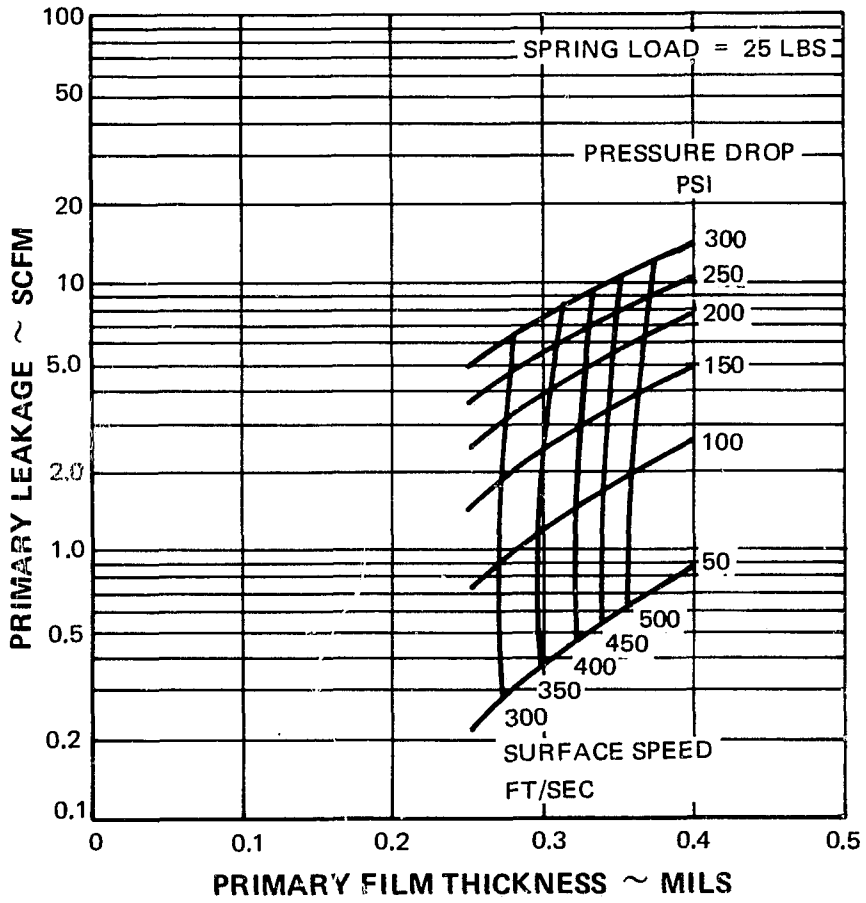

Figure 29 Calculated Primary Leakage and Film Thickness for the Wide-Pad Seal with Air at 800°F

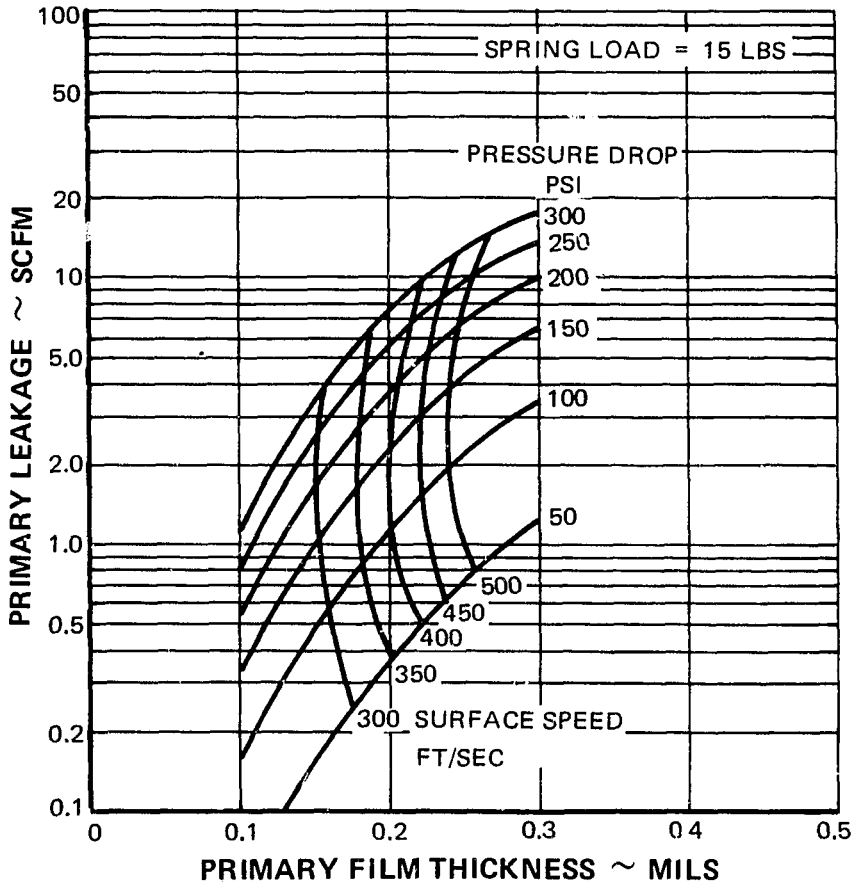

Figure 30 Calculated Primary Leakage and Film Thickness for the Revised Narrow-Pad Seal with Air at 150°F

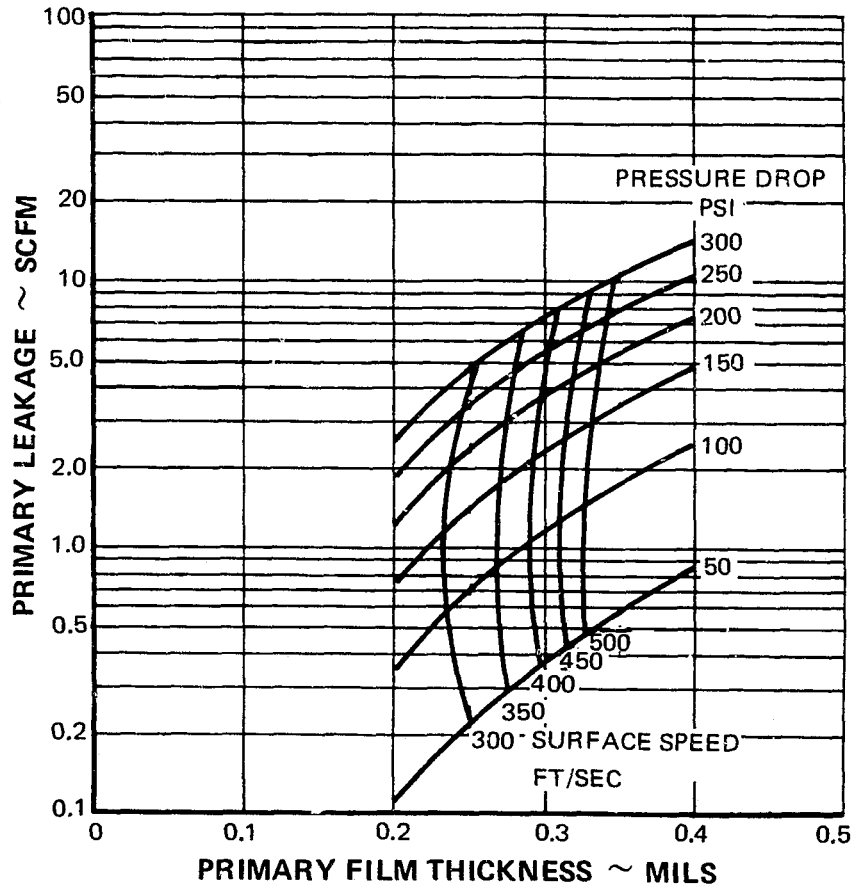

Figure 31 Calculated Primary Leakage and Film Thickness for the Revised Narrow-Pad Seal with Air at 800°F

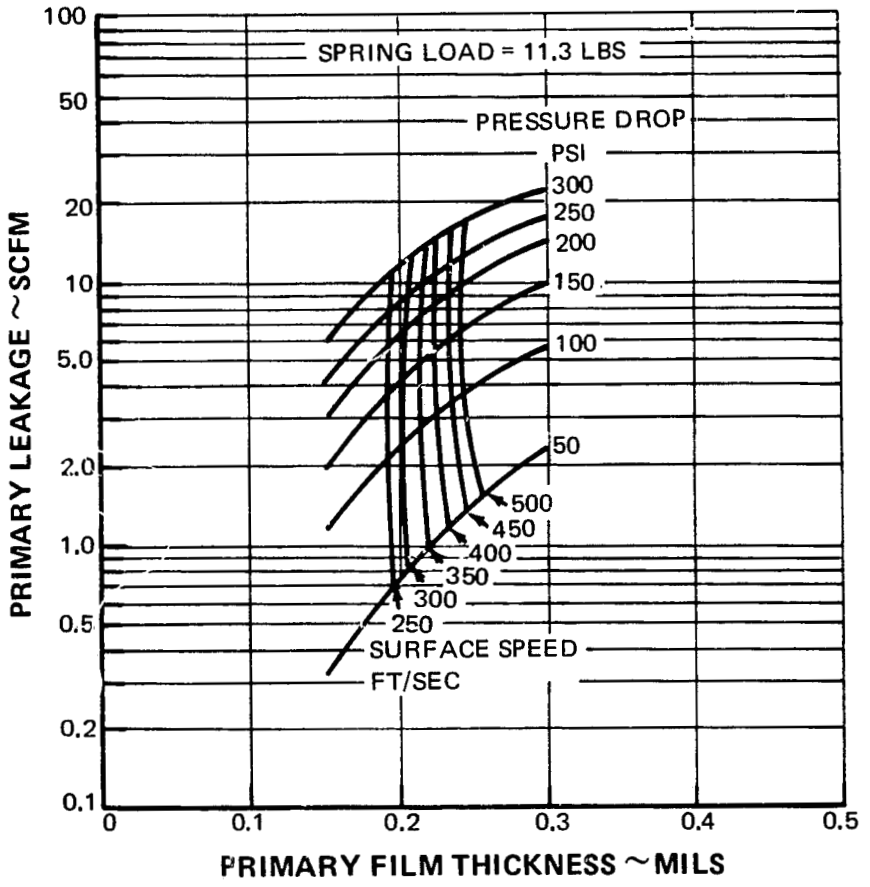

Figure 32 Calculated Primary Leakage and Film Thickness for the Recessed Seat Seal with Air at 150°F

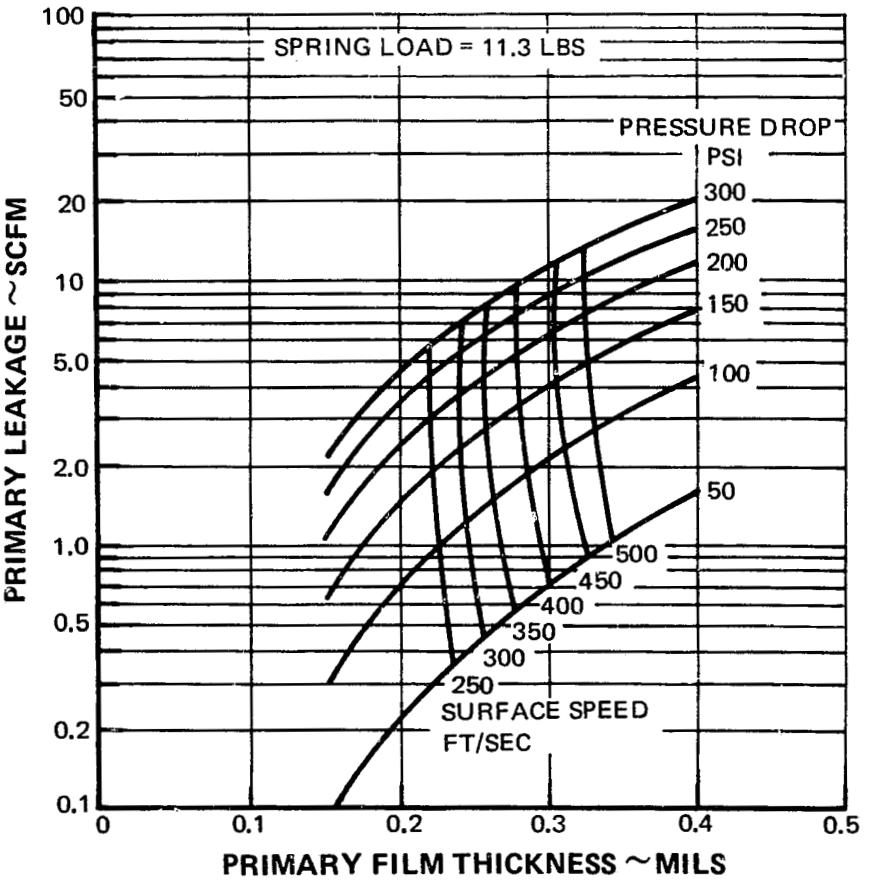

Figure 33 Calculated Primary Leakage and Film Thickness for the Recessed Seat Seal with Air at 800°F

Total air leakage for the seal is composed of leakage past the primary seal and leakage past the secondary seal. The test equipment used in this program was not capable of separating the primary and secondary leakages and purely analytical techniques have not been developed to predict the secondary air leakage over the range of operating conditions planned for Phase III, but it was found possible to use the static room-temperature leakage as a basis for estimates of secondary seal leakage. At these conditions the primary leakage is very small. The secondary leakage is made up of two components: sealing dam leakage and gap leakage. By correcting each of these components for higher air temperatures, curves of secondary seal air leakage could be developed as functions of air temperature for the range of pressure differentials across the seal. Such curves for the two piston rings used in Phase III are shown in Figure 34. It was also necessary to relate the air temperature at the piston rings to the seal air temperature. This relationship is shown in Figure 35, and the seal air temperatures are shown as a secondary (and nonlinear) scale at the right of Figure 34. These data were based on testing of gas-film seals in Phase I (Reference 7) and Phase II (Reference 3).

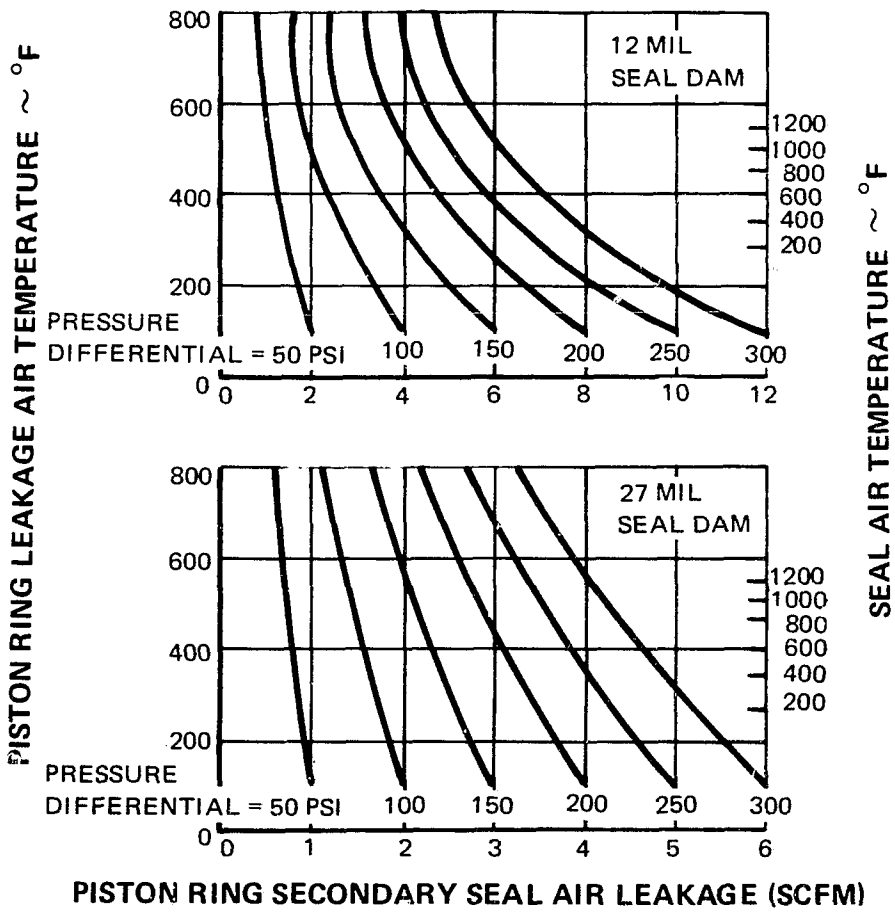

Figure 34 Air Leakage Past the Secondary Seals

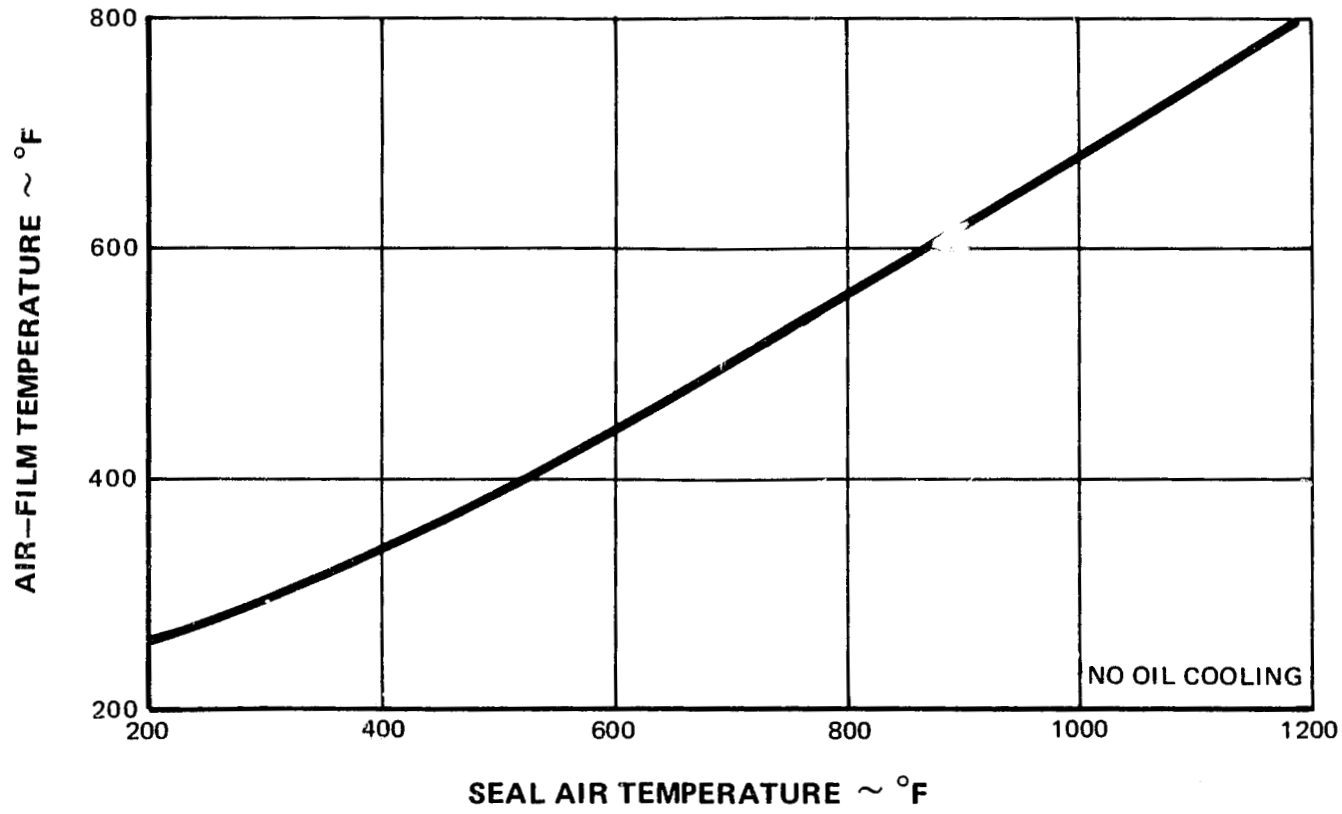

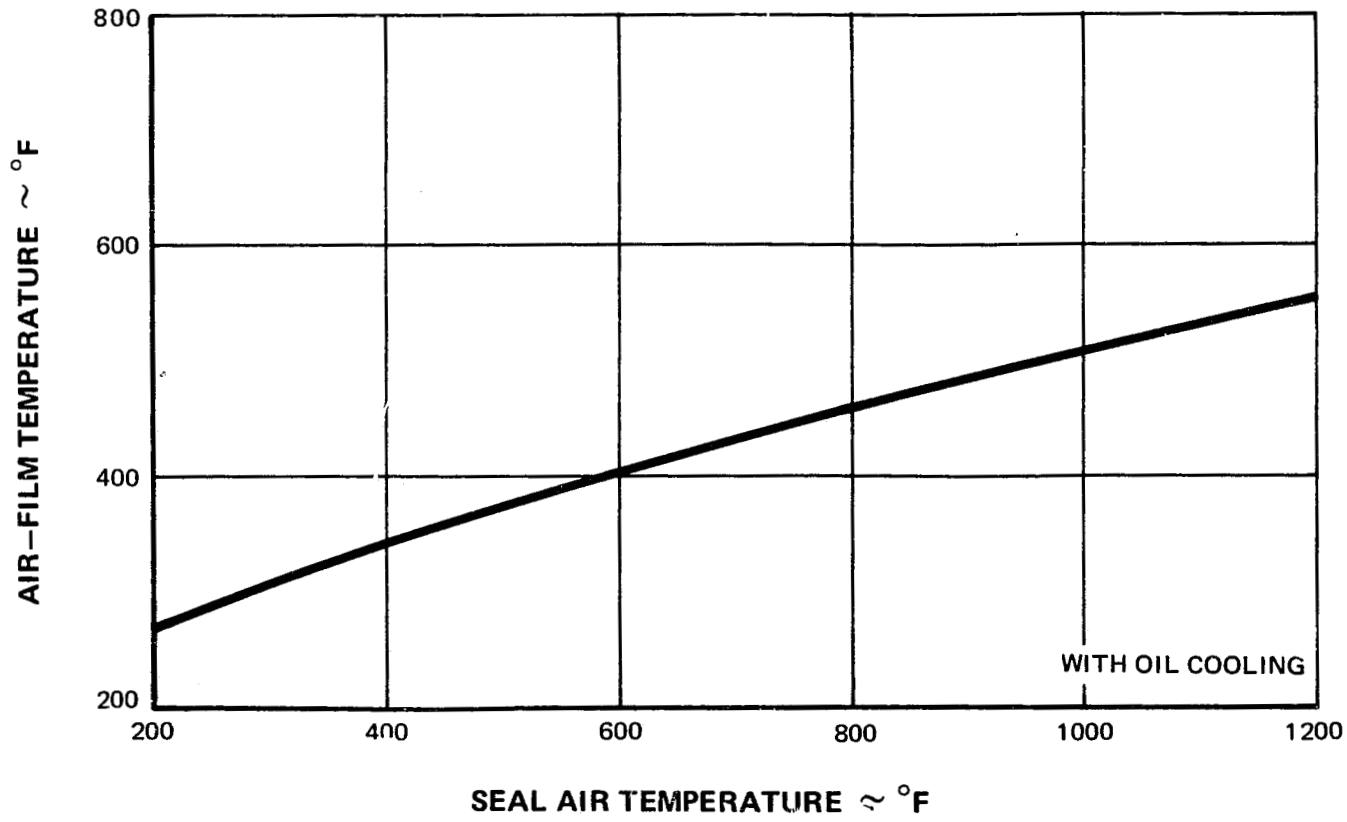

Figure 35 Estimated Air-Film Temperature as a Function of Seal Air Temperature

SECTION IV
EXPERIMENTAL EVALUATION OF THE CERAMIC SEAL

The ceramic seal is described in Section III of this report, and a layout drawing of the seal is shown in Figure 4. The ceramic nosepiece was used because it will tolerate higher temperatures than carbon without oxidizing. In addition, the ceramic material was expected to provide more resistance to erosion and wear of the seal nosepiece.

The five builds of the ceramic seal underwent a total of 27.7 hours of preliminary dynamic checkout testing. During that time its air leakage was in reasonable agreement with the predicted values, but it suffered from unstable operation and contact between the ceramic nosepiece and the chrome-carbide coated seal seat, as shown in Table III. The preliminary dynamic checkouts on the ceramic seal were terminated after Build 5 because contact between the nosepiece and the seal seat had fractured the edges of two of the Rayleigh pads on the nosepiece, reducing their self-acting capability; further testing would only have resulted in further damage to the seal seat and the nosepiece.

TABLE III
CERAMIC SEAL TEST SUMMARY

Build No.	Nosepiece	Seal Seat	Piston Ring	Carrier	Spring Load (lbs)	Other Special Features	Type of Test	Reason For Test Termination	Condition After Test: Nosepiece Face	Condition After Test: Seal Seat Face	Total Bld End Hours	Total Bld Hours
1	New	New	New	New	15.5	Coatings: Seal Seat Face - Chrome Carbide Piston Ring - Chrome Flash Carrier Bore - Chrome Carbide	PC*	Unstable Operation	Discolored, Flat Within 0.06 Mils, Some Chipping Of Edges	Wear Marks 0.45 Mils Deep In Seal Dam Wear Track	0	.5
2	Used From Bld 1	New	Used From Bld 1	Used From Bld 1	22.9		PC	Indications of Incipient Rubbing contact	Evidence of Light Contact With Seal Seat	Evidence of Light Contact With Nosepiece Seal Dam	0	1.8
3	Relapped From Bld 2	Used From Bld 2	Used From Bld 2	Used From Bld 2	15.5		PC	Unstable Operation At High Speeds	Evidence of Light Contact With Seal Seat	Evidence of Light Contact With Nosepiece	0	13.4
4	Used From Bld 3	Used From Bld 3	Used From Bld 3	New	15.5	Carrier Material Changed To 410 S.S., Carrier Bore Coating: Chrome Plate	PC	Unstable Operation At Low Pressure/High Speed Condition	Evidence Of Light Contact With Seal Seat	Evidence of Light Contact With Nosepiece	0	7.7
5	Used From Bld 4	Used From Bld 4	Used From Bld 4	Used From Bld 4	22.9		PC	Excessive Air Leakage Due To Fracture Of Rayleigh Pad Edges	Scratches 0.2 Mils Deep. Edge Fractures	Wear Marks 1.25 Mils Deep In Seal Dam Wear Track, Contact With Outer Edge Of Rayleigh Pads.	0	4.3
											0	27.7

*PC = Preliminary Dynamic Checkout

A. PRELIMINARY DYNAMIC CHECKOUT - BUILD 1

The ceramic nosepiece used in this seal was fabricated during Phase II (Reference 3) of this contract for what was then called the Type A-1 seal (see Reference 3). A close-up of the nosepiece is shown in Figure 36 and the seal is shown assembled prior to testing in Figure 37. A surface analyzer was used to take profile measurements of the nosepiece before testing in order to provide a clear record of the actual condition of the surface. A representative trace is shown in Figure 38, with a sketch of the nosepiece to show the relationship between the trace and the geometry of the nosepiece. The average depth of the recess was 0.5 mil.

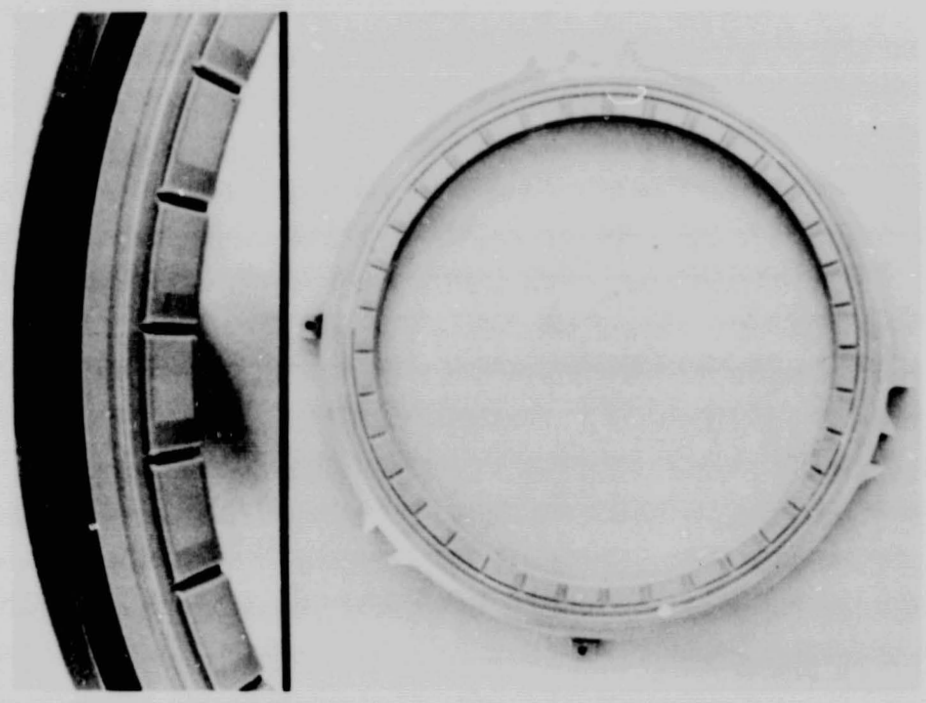

Figure 36 Completed Ceramic Nosepiece Ring Assembly with Close-Up of Ceramic Ring (CN-23132 & 23133)

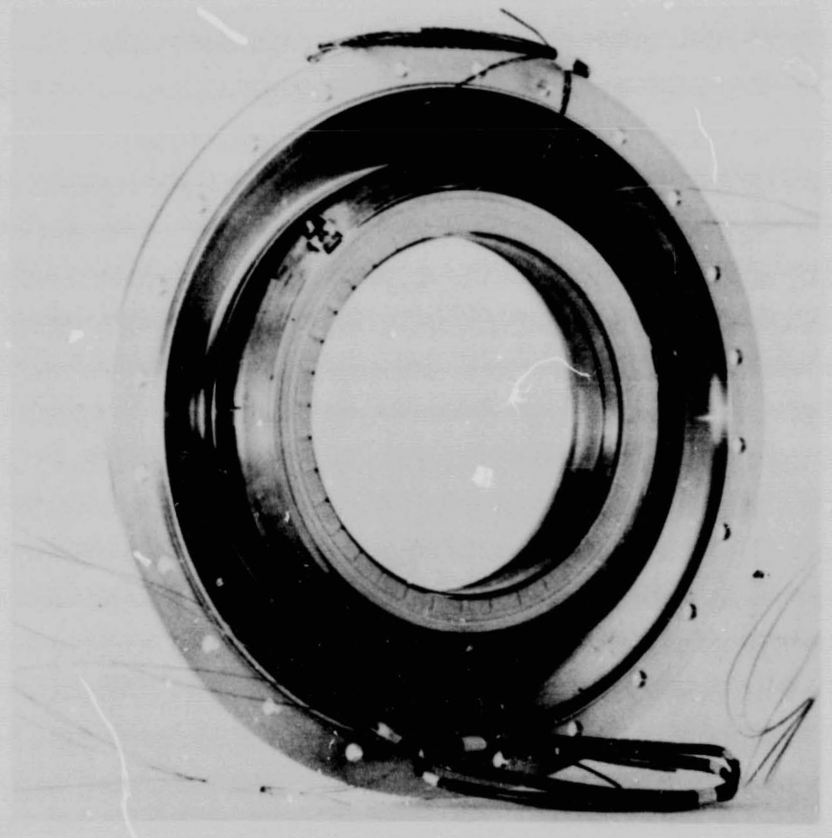

Figure 37 Ceramic Nosepiece Seal Assembly Before Testing (CN-25781)

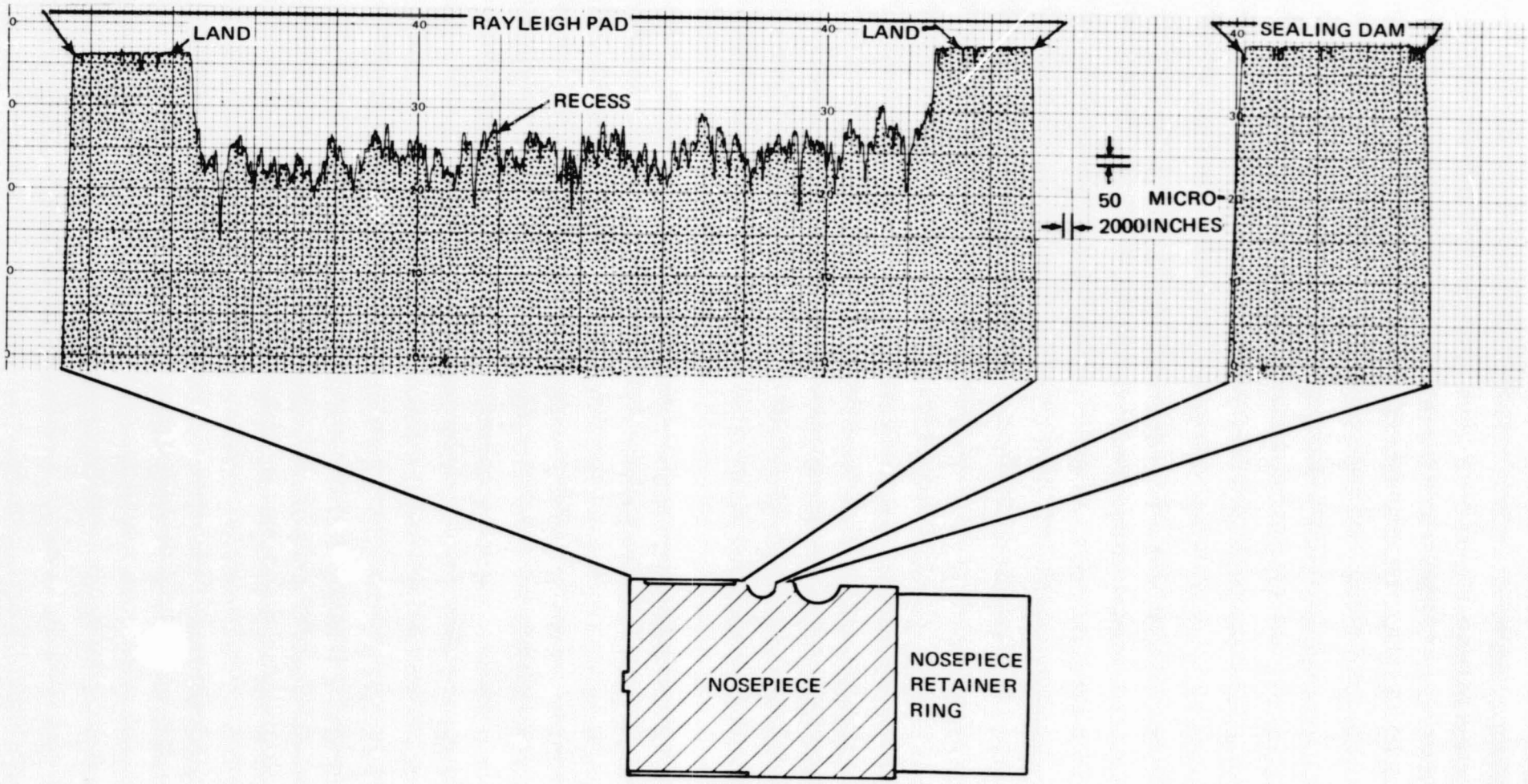

Figure 38 Representative Profile Trace Taken Radially Across the Face of the Ceramic Nosepiece Before Testing in Build 1.

The first point of the preliminary dynamic checkout program was a seal sliding speed of 260 ft/sec and a pressure differential of 50 psi. For the first three minutes of operation at that point, the air leakage was approximately 4 scfm. The air leakage then increased and varied between 8 and 10 scfm for the remaining 27 minutes of operation at that point. As the second point (sliding speed 310 ft/second, pressure differential 50 psi) was being set, the air leakage increased rapidly from 13.9 scfm to 22.0 scfm. At that time the test rig was disengaged from the drive engine and the test was terminated. The air leakage results are shown in Figure 39. The total air leakage is the sum of leakage past the primary and secondary seals.

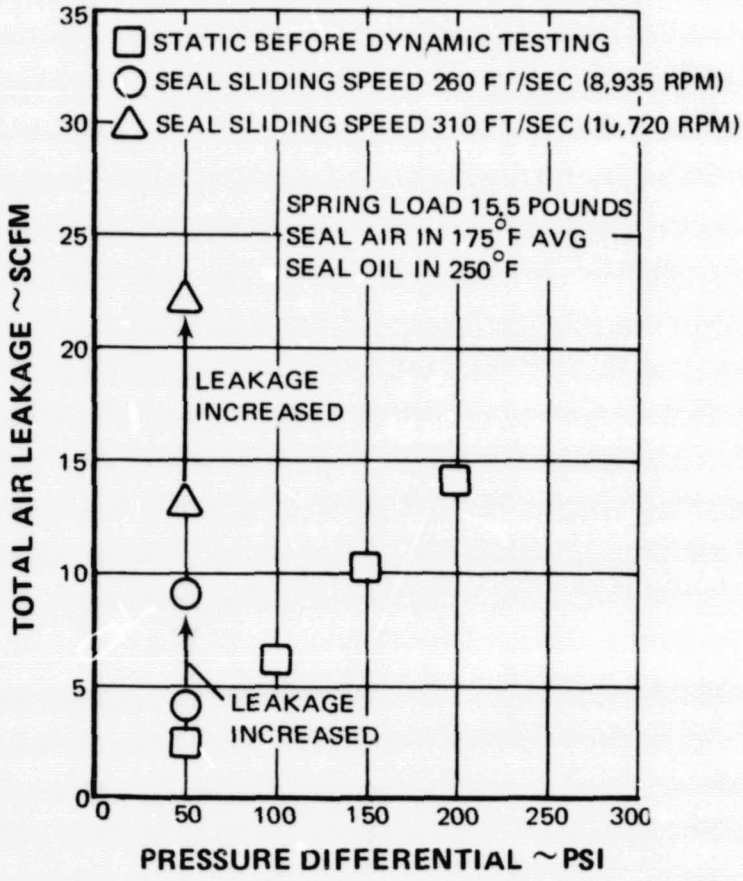

Figure 39 Air Leakage Past Build 1 of the Ceramic Nosepiece Seal

Disassembly revealed that the nosepiece had rubbed against the seal seat. The wear marks on the seal seat are shown in Figure 40. Profile traces across the seal dam and Rayleigh pad wear track on the seal seat revealed that the rub-mark scratches were as deep as 0.45 mil. A representative profile trace across the seal seat is shown in Figure 41.

Although discolored, the face of the ceramic nosepiece was flat within 5 helium light bands and was considered to be reusable. An overall view of the ceramic nosepiece after Build 1 testing is shown in Figure 42, and a closeup of one of the discolored areas is shown in Figure 43. Note the slight chipping at the edge of the Rayleigh pad.

Analysis of the Build 1 test results indicated that the relatively low thrust load on the test rig thrust bearings caused by low air pressures produced a shaft vibration and a corresponding axial runout or wobble in the seal seat. The wobble may have exceeded the amplitude which could be followed by the nosepiece.

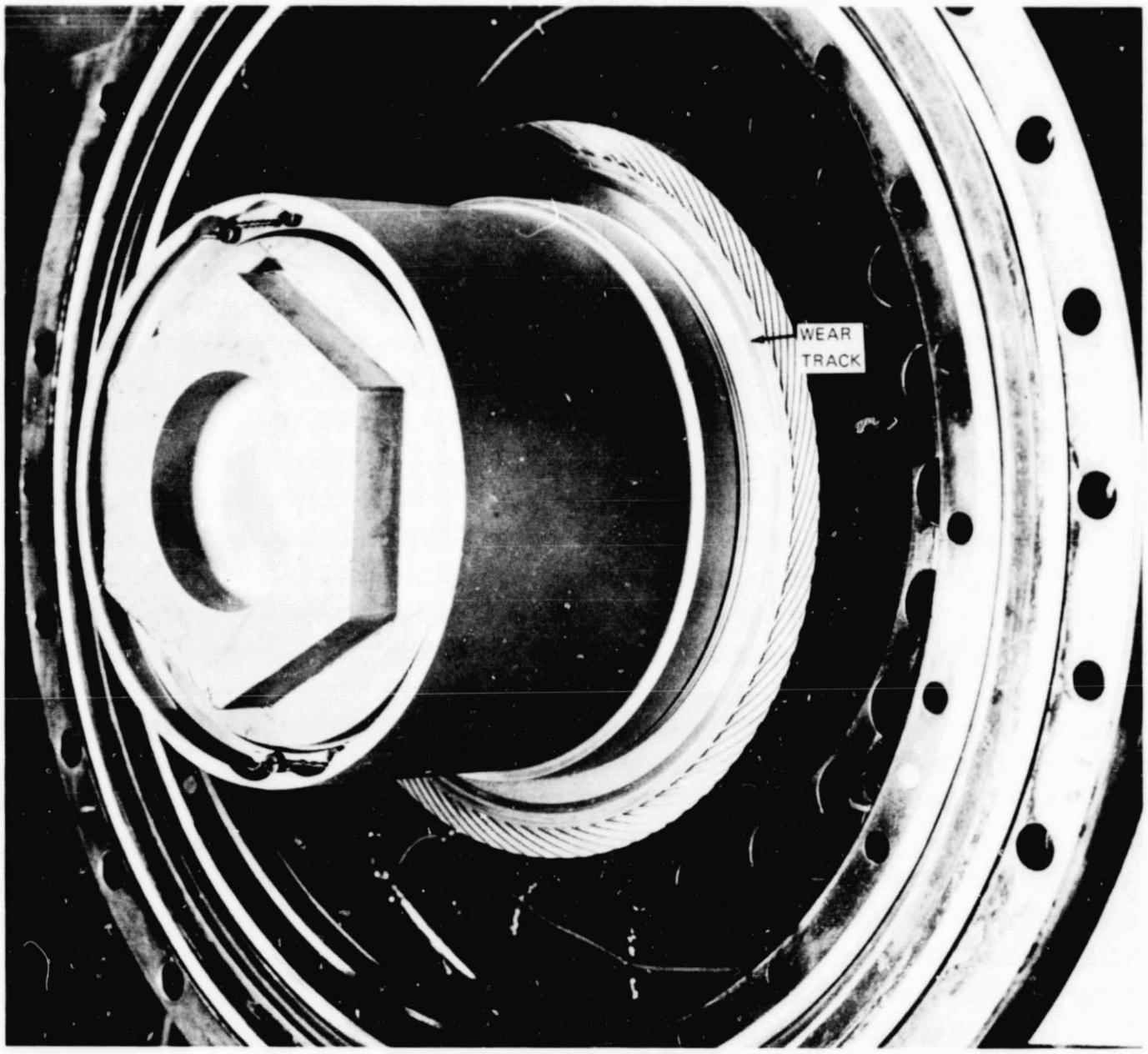

Figure 40 Seal Seat After Build 1 Testing of the Ceramic Nosepiece Seal (CN-25820)

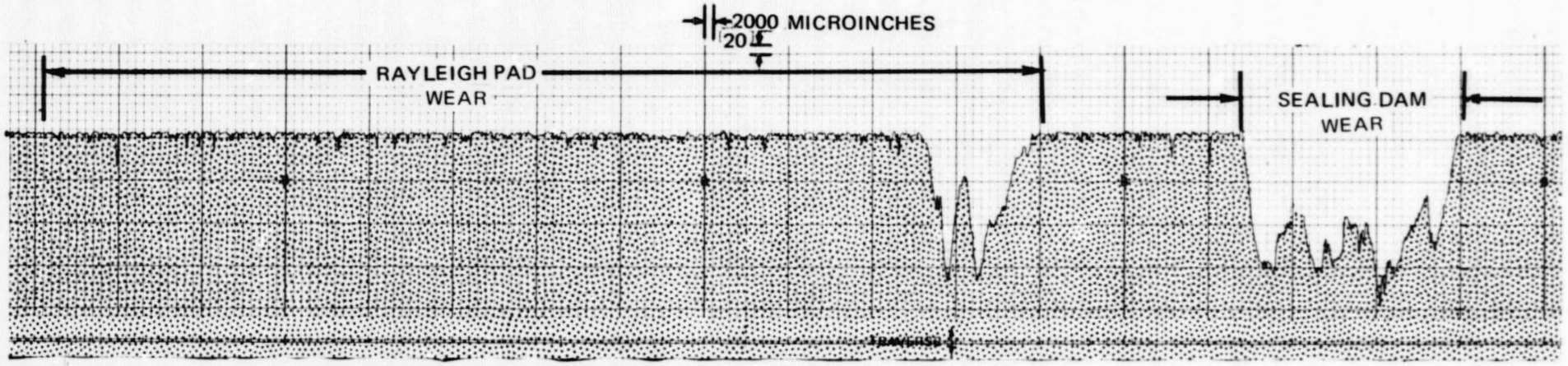

Figure 41 Profile Trace Taken Radially Across the Face of the Seal Seat Showing Wear Track After 0.5 Hour of Build 1 Testing

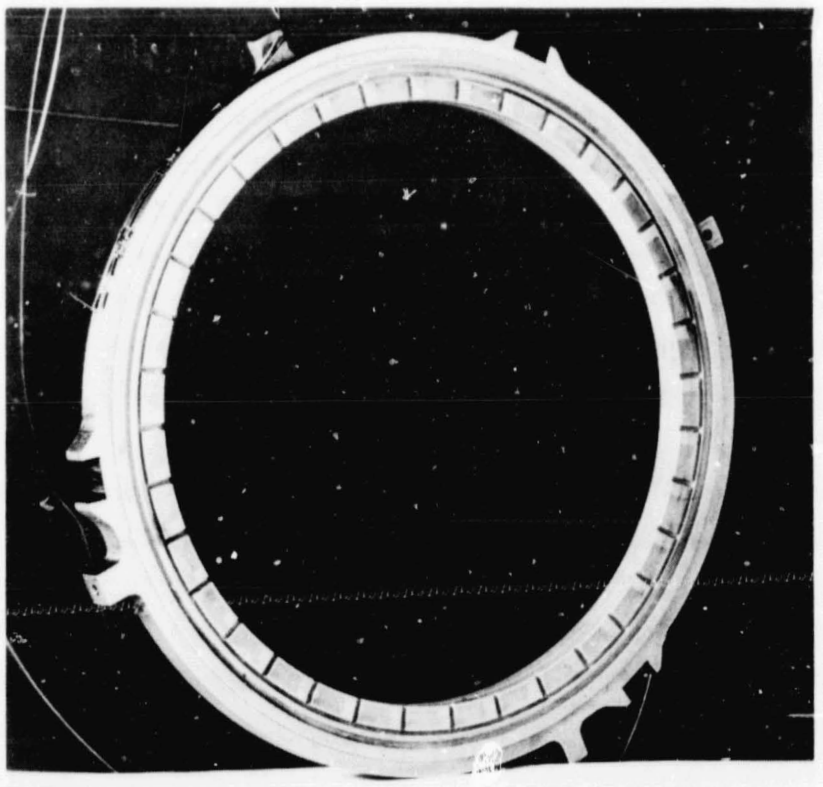

Figure 42 Ceramic Nosepiece After Build 1 Testing
(CN-25825)

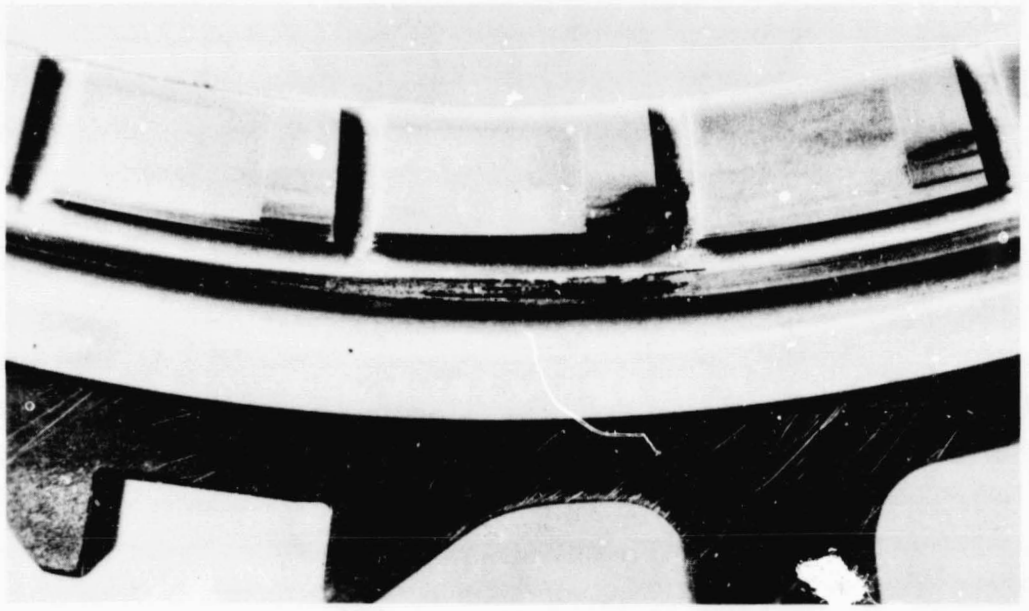

Figure 43 Close-Up of the Ceramic Nosepiece After Build 1 Testing
(CN-25824)

2 9

B. PRELIMINARY DYNAMIC CHECKOUT - BUILD 2

Two changes were made for the Build 2 configuration. The spring load on the seal at the operating position was increased from 15.5 to 22.9 pounds to improve the tracking dynamics of the seal; and the two-point preloaded roller bearing in the forward end of the test rig was replaced with a redesigned three-point preloaded roller bearing to reduce rig vibration. In addition, the worn seal seat from Build 1 was replaced when the test rig was reassembled for Build 2.

The preliminary dynamic checkout of Build 2 was performed at the following sliding velocities and pressure differentials:

Seal Velocity (ft/sec)	Pressure Differential (psi)
260	50
310	50, 100, 150, 200

The air leakages measured are shown in Figure 44. The dynamic leakages were approximately the same as the static leakages, indicating that the seal was operating at very low film thicknesses. Disassembly and inspection after 1.8 hours of dynamic testing revealed signs of light contact between the nosepiece and seal plate, although neither was damaged.

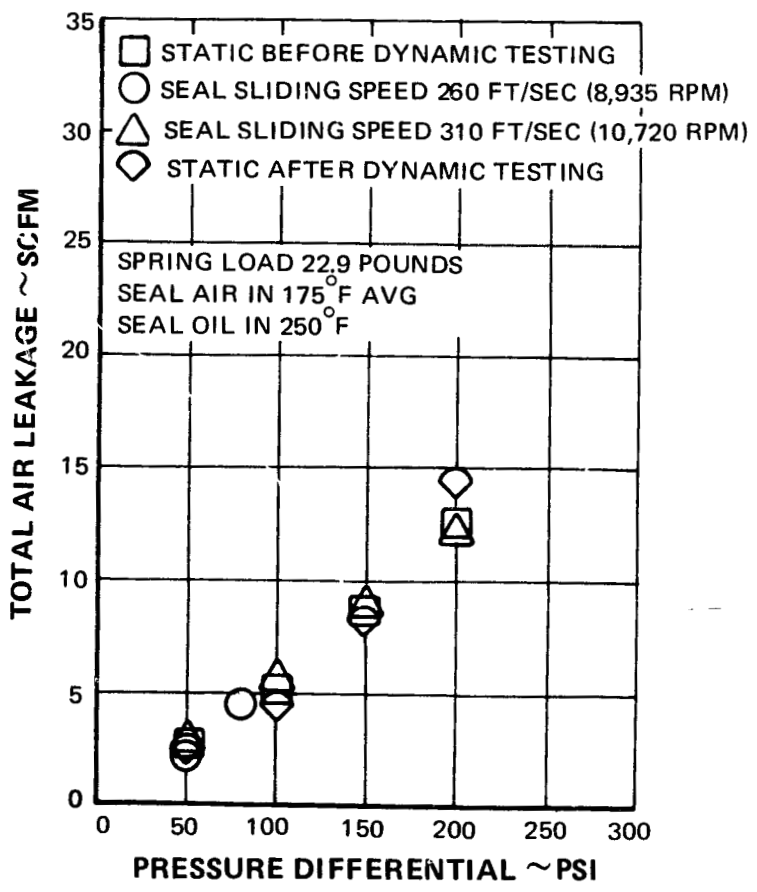

Figure 44

Air Leakage Past Build 2 of the Ceramic Nosepiece Seal

It was observed during Build 2 testing that the rig vibration level was greatly reduced by use of the three-point preloaded roller bearing. With the reduced vibration level, it became desirable to run the seal at the original design spring load, since this would improve the seal's lift-off characteristics.

C. PRELIMINARY DYNAMIC CHECKOUT - BUILD 3

Build 3 of the ceramic seal was assembled with a spring load of 15.5 pounds, the same as that used in Build 1. In addition, the face of the nosepiece was lapped slightly to reduce the dishing of the face from 5 to 3 helium light bands.

Build 3 underwent preliminary dynamic testing with ambient air at speeds between 260 and 410 ft/sec, and pressure differentials between 50 and 300 psi. The static and dynamic test results obtained during the testing are shown in Figure 45. It was found that the seal could not be operated at all the required test conditions. For a sliding speed of 360 ft/sec, operation was erratic at pressures below 100 psi. For a sliding speed of 410 ft/sec, it was erratic at pressures below 300 psi.

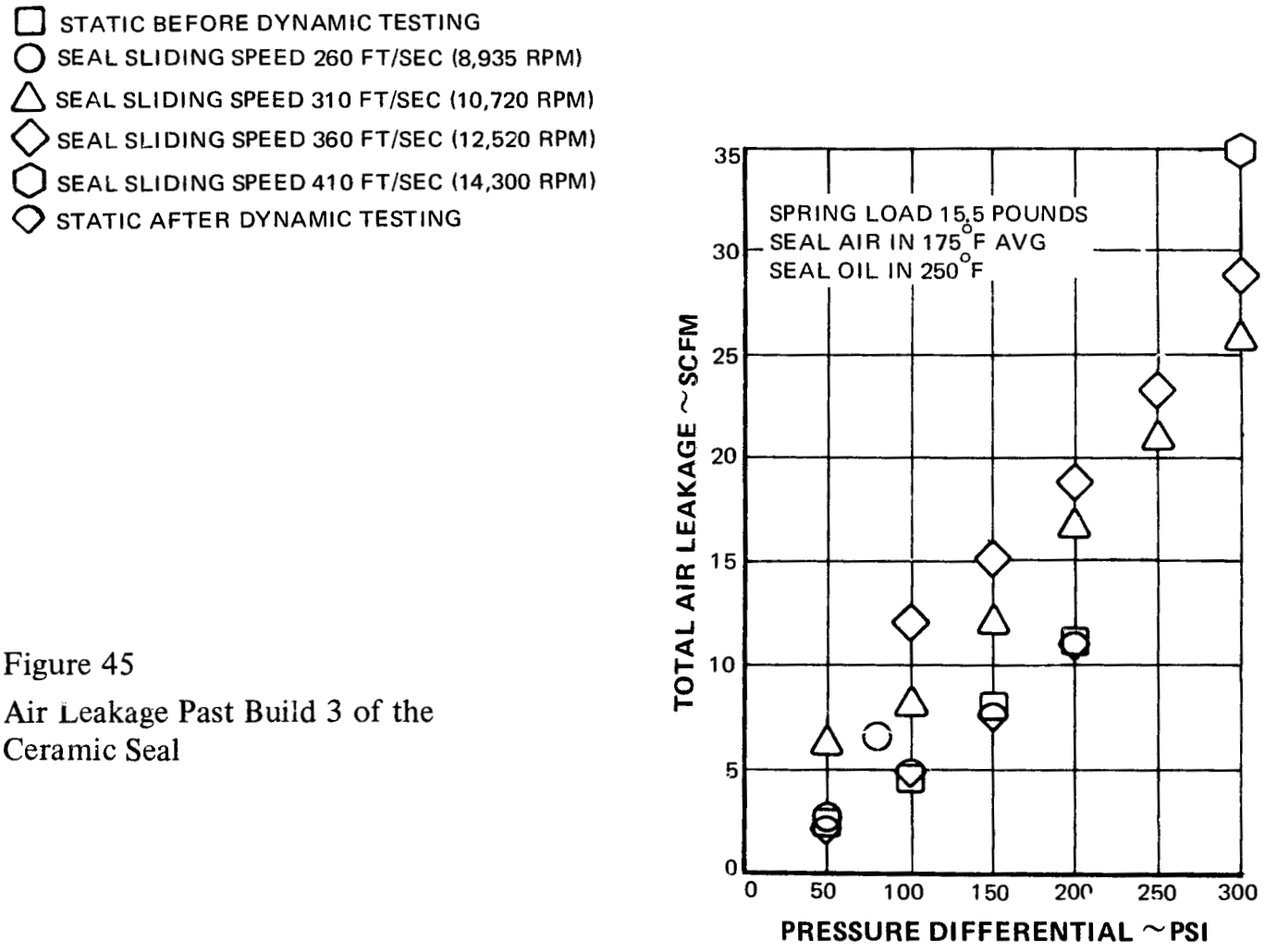

Figure 45

Air Leakage Past Build 3 of the Ceramic Seal

D. PRELIMINARY DYNAMIC CHECKOUT - BUILD 4

In Build 4, a 410 stainless steel seal carrier was substituted for the TZM seal carrier used in the three previous builds. This substitution reduced the weight of the nosepiece from 2.50 to 2.25 pounds, thereby reducing the effect of seal seat runout when the seal was operated at high speeds and low pressures. The spring load of 15.5 pounds used on the Build 3 seal was kept the same for the Build 4 seal.

The Build 4 preliminary dynamic checkout was performed at sliding speeds from 260 to 360 ft/sec and pressure differentials from 50 to 200 psi. The measured air leakages are presented in Figure 46. In the testing at 360 ft/sec and 100 psi, air leakage was initially slightly higher than expected. During continued operation leakage rose steadily, indicating unsatisfactory operation.

After the test, the seal assembly was removed from the rig for inspection. Evidence of light contact was visible on the nosepiece and seal seat, but neither was damaged. In general, testing of the Build 4 seal showed some improvement over Build 3, but there was not enough improvement to permit operation at all the required conditions of high speed and low pressure differentials.

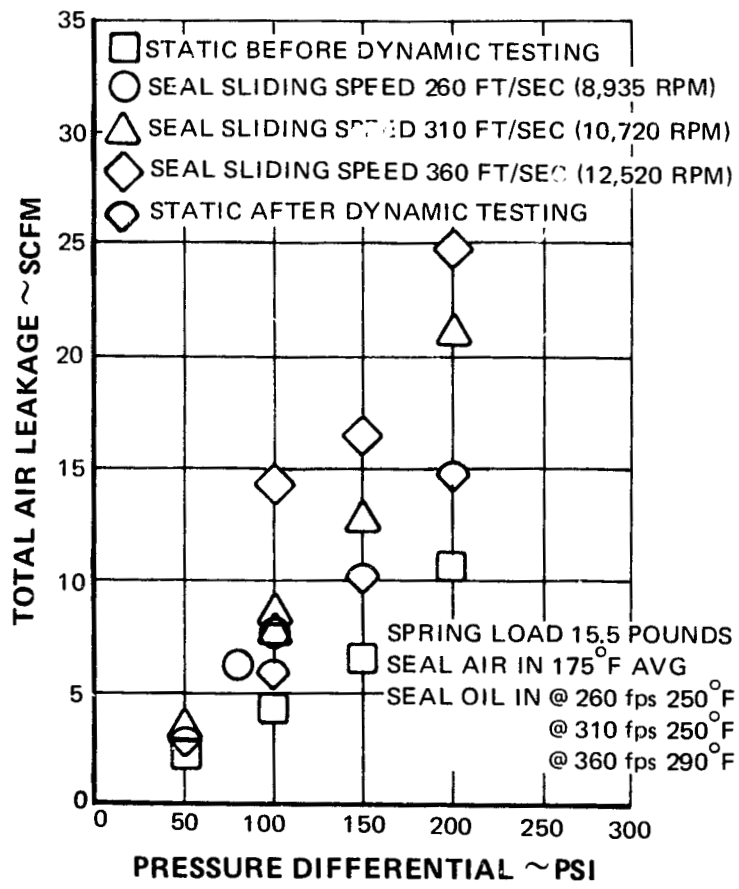

Figure 46 Air Leakage Past Build 4 of the Ceramic Nosepiece Seal

A comparison of theoretical and actual leakage for Builds 4 and 5 of the ceramic is presented in Figures 47 through 50. The theoretical curves were obtained by combining the calculated leakages at the primary seal with the static leakage obtained from actual tests, which was assumed to be identical with the leakage past the secondary seal during dynamic testing. Agreement between the theoretical and actual leakages was very good at test conditions where the seal was successfully operated. At certain other conditions seal performance was erratic, with actual seal leakage higher than theoretical.

The circumferential variation in film thickness because of seal seat runout and nosepiece inertia is probably significant when the seal operation is erratic. As the circumferential variation in film thickness increases the leakage rate increases, because leakage is approximately proportional to the third power of film thickness. Leakage increases in the regions of maximum film thickness are greater than the leakage decreases in the regions of minimum film thickness.

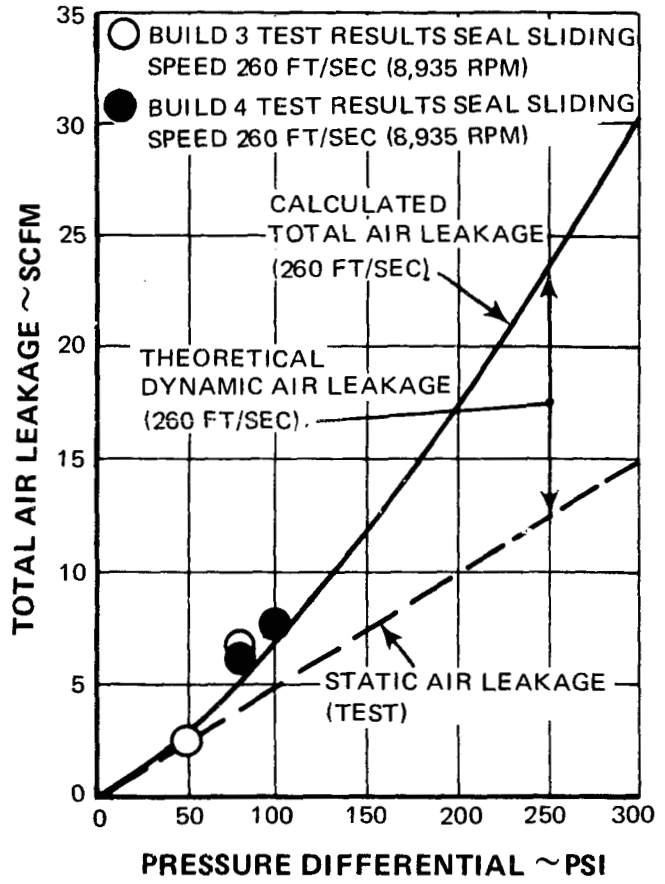

Figure 47 Calculated and Actual Air Leakage Past Build 3 of the Ceramic Seal At a Sliding Speed of 260 ft/sec with Ambient Air

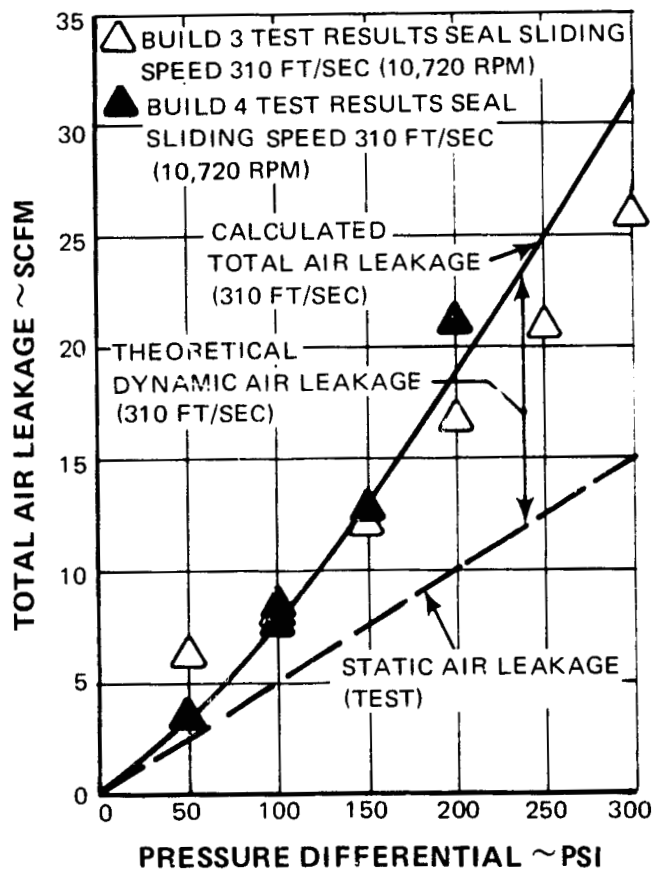

Figure 48

Calculated and Actual Air Leakage Past Builds 3 and 4 of the Ceramic Seal at a Sliding Speed of 310 ft/sec with Ambient Air

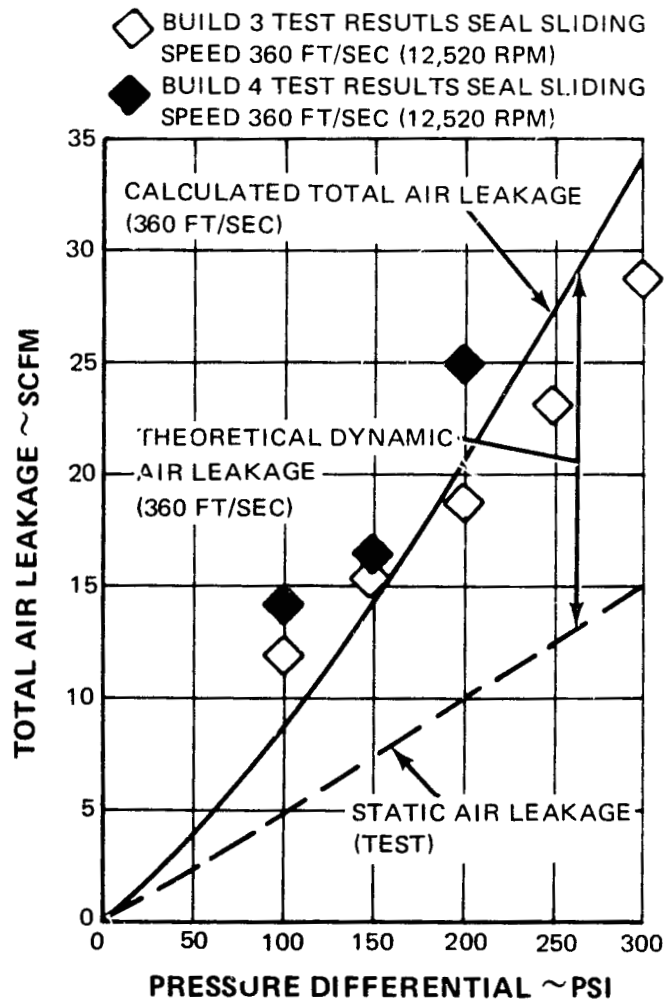

Figure 49

Calculated and Actual Air Leakage Past Builds 3 and 4 of the Ceramic Seal at a Sliding Speed of 360 ft/sec with Ambient Air

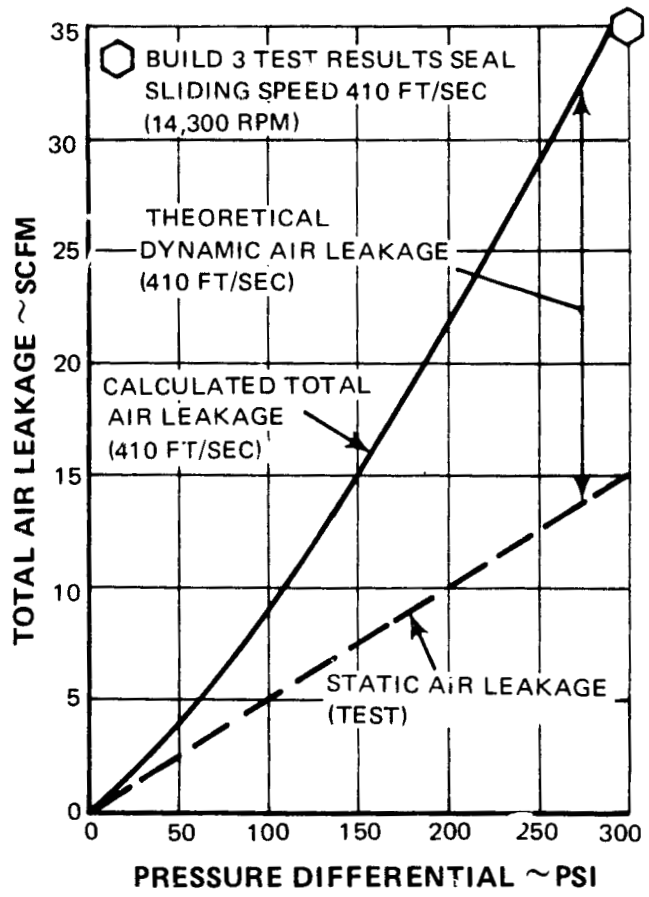

Figure 50 Calculated and Actual Air Leakage Past Build 3 of the Ceramic Seal at a Sliding Speed of 410 ft/sec with Ambient Air

E. PRELIMINARY DYNAMIC CHECKOUT - BUILD 5

In order to raise the gas-film stiffness at low-pressure operating conditions, Build 5 incorporated a nosepiece spring load of 22.9 pounds (the same as that for Build 2). The stainless steel carrier was retained from Build 4.

Build 5 was tested dynamically at a sliding speed of 360 ft/sec at pressure differentials from 50 to 250 psi. The test results are plotted in Figure 51. Operation at 360 ft/sec was successful at pressure differentials from 250 psi to 70 psi, but excessive air leakage was experienced at the final 50-psi point. During the testing operation was also attempted at a sliding speed of 410 ft/sec and a pressure differential of 250 psi, but leakage at that condition was excessive. As shown in Figure 51, the posttest static leakage was also high.

Disassembly and inspection of the seal revealed that there had been extensive contact between the nosepiece and the seal seat. The inner shroud and land of one Rayleigh pad had broken off. An overall view of the ceramic nosepiece is shown in Figure 52, and a close-up of the broken pad is shown in Figure 53. The wear marks on the seal seat are shown in Figure 54.

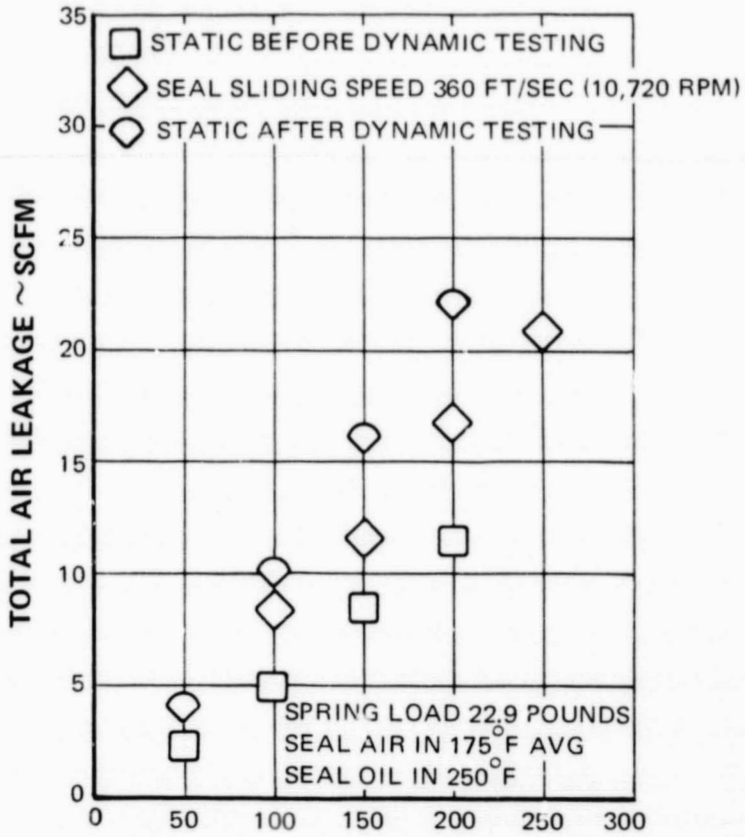

Figure 51 Air Leakage Past Build 5 of the Ceramic Nosepiece Seal (CN-26739)

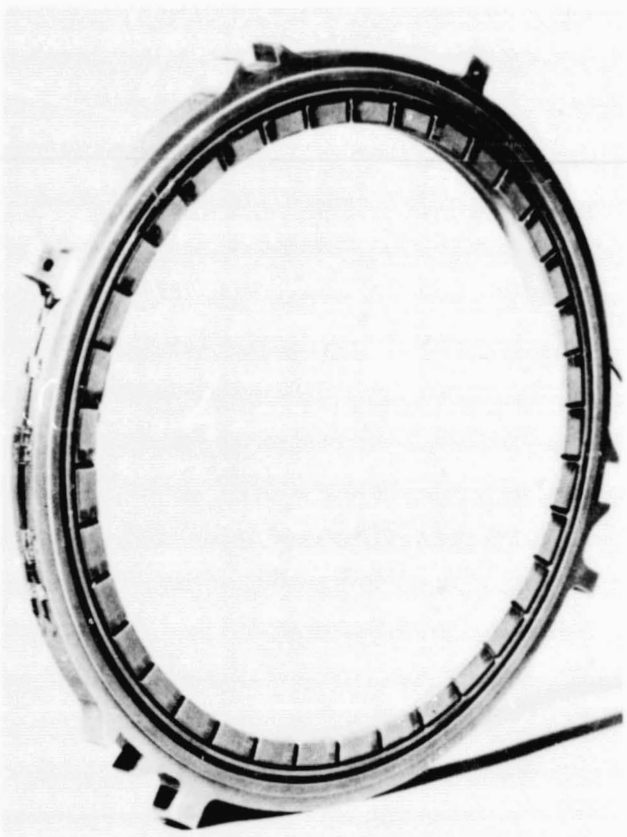

Figure 52 Ceramic Nosepiece After Build 5 Testing. Total Test Time 27.7 Hours

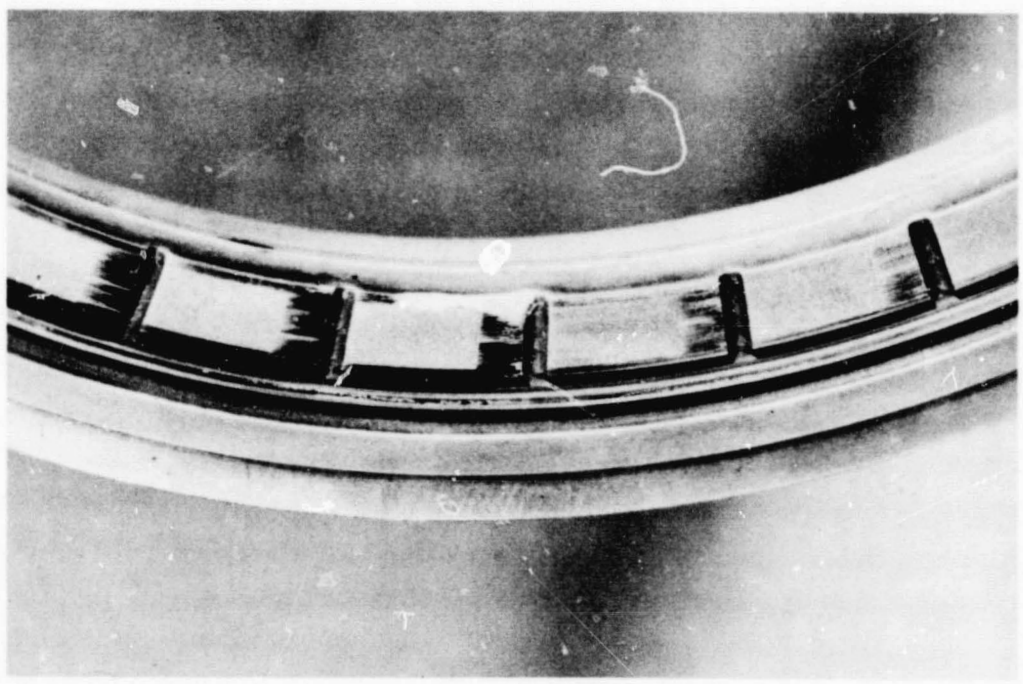

Figure 53 Close-Up of Ceramic Nosepiece After Build 5 Testing (CN-26740)

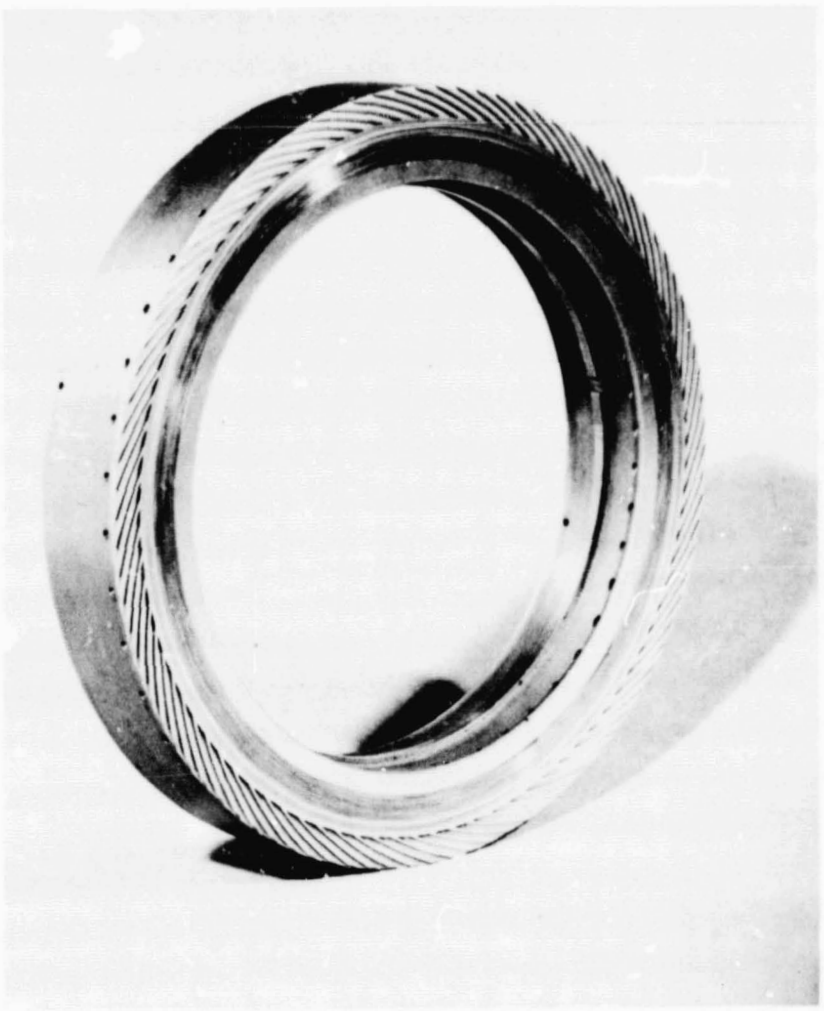

Figure 54 Seal Plate After Tests on Build 5 of the Ceramic Nosepiece Seal (CN-26741)

Profile traces across the seal seat showed scratches up to 1.25 mils deep in the area of the seat aligned with the nosepiece seal dam, as shown in Figure 55. Profile traces across the face of the ceramic nosepiece revealed scratches up to 0.2 mil deep, as shown in Figures 56 and 57. The total wear on the nosepiece can be seen by comparing Figure 56 with Figure 38. Both of these were taken at the same location, but Figure 38 was taken before the start of Build 1 testing.

Although the ceramic seal operated successfully at 410 ft/sec and 300 psi, there was too much intermittent contact between the nosepiece and seat, which resulted in edge fractures on the nosepiece and wear on the seat. This fracture failure mode of the ceramic nosepiece does not compare favorably with the wear-in properties of the carbon nosepieces.

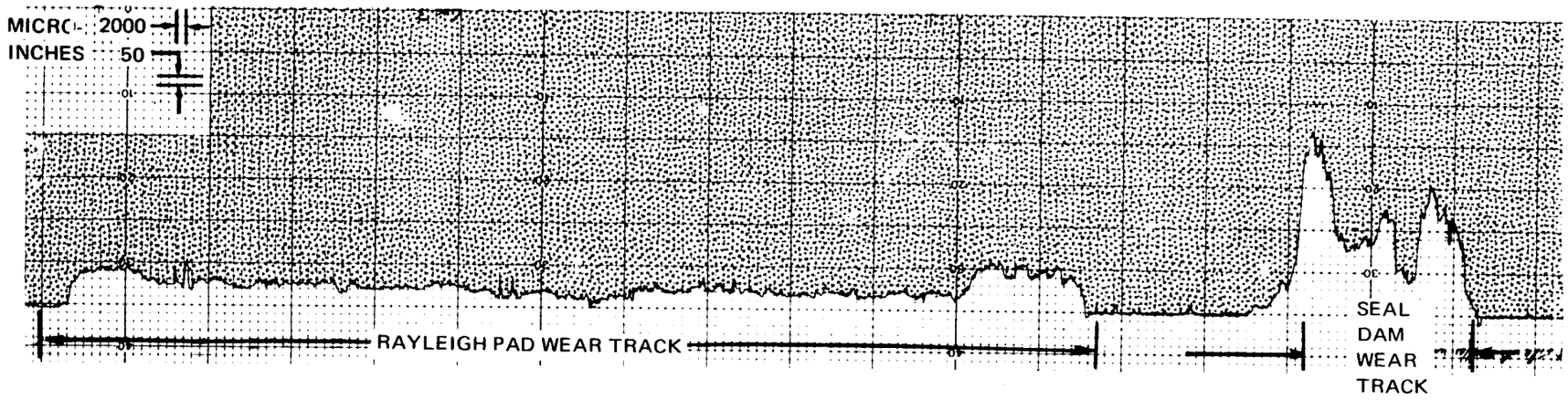

Figure 55 Profile Trace Taken Radially Across the Face of the Seal Seat Showing Ceramic Nosepiece Wear Track After 4.3 Hours of Build 5 Testing. Total Test Time on Seal 27.2 Hours.

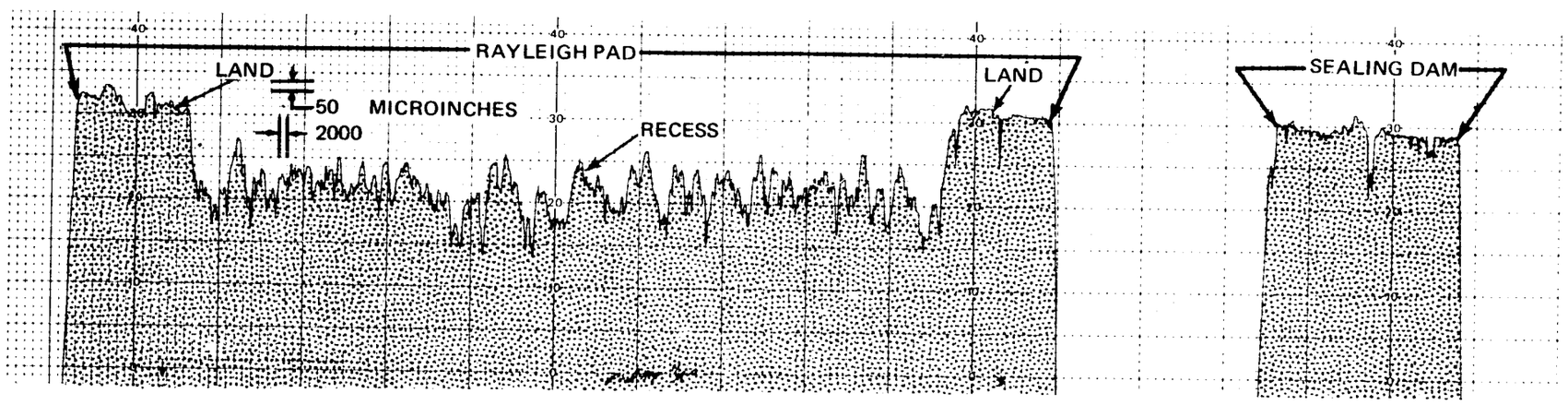

Figure 56 Representative Profile Trace Taken Radially Across the Face of the Ceramic Nosepiece After 4.3 Hours of Build 5 Testing. Total Time on Nosepiece 27.7 Hours

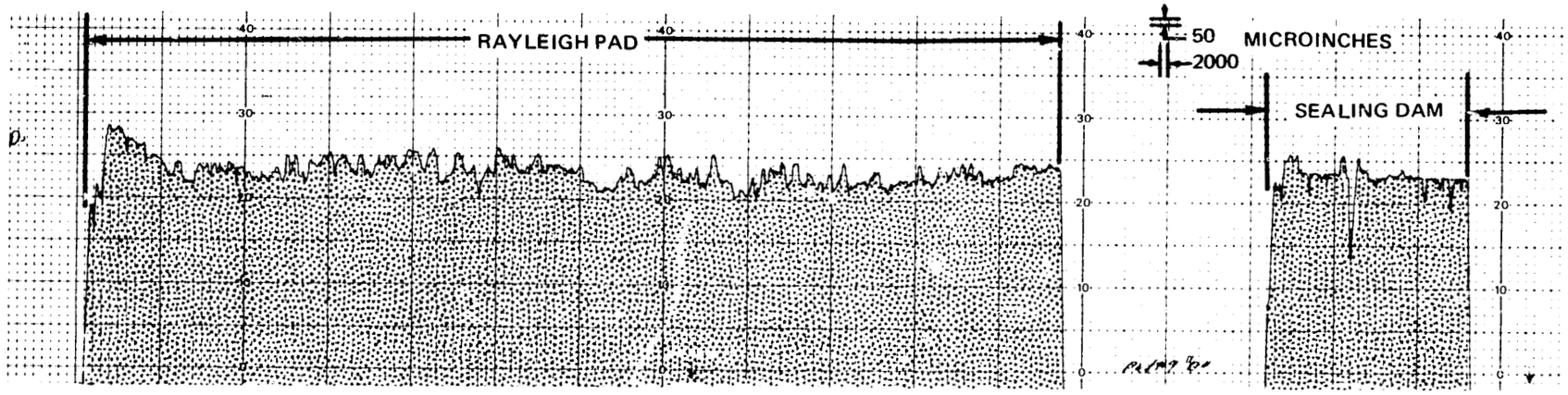

Figure 57 Profile Trace Taken Radially Across the Face of the Ceramic Nosepiece at a Rayleigh Pad Land After 4.3 Hours of Build 5 Testing. Total Time on Nosepiece 27.7 Hours.

PRECEDING PAGE BLANK NOT FILMED

SECTION V
EXPERIMENTAL EVALUATION OF THE NARROW-PAD SEAL

The narrow-pad seal is described in Section III of this report, and a layout of the seal is shown in Figure 5. One principal difference between the narrow-pad seal and the ceramic seal is that the nosepiece of the narrow-pad seal was made of carbon instead of ceramic. Also, the narrow-pad carbon nosepiece has a 25-mil wide dam instead of the 50-mil wide dam of the ceramic nosepiece, and its Rayleigh pads are 125 mils wide instead of 260 mils.

The three builds of the narrow-pad seal underwent a total of 70.2 hours of preliminary dynamic checkout and elevated-temperature testing. Although operation at speeds up to 360 ft/sec was generally satisfactory, attempts to run the seal at 410 ft/sec were unsuccessful and resulted in excessive air leakage. The test program on the narrow-pad seal is summarized in Table IV.

TABLE IV

NARROW-PAD SEAL TEST SUMMARY

Build No.	Carbon Nosepiece	Seal Seat	Piston Ring	Carrier	Spring Load (lbs)	Other Special Features	Type of Test	Reason for Test Termination	Condition After Test: Nosepiece Face	Condition After Test: Seal Seat Face	Total Bld. End, Hours	Total Bld. Hours
1	New	Relapped From Bld. 1 Ceramic Seal	New	Used From Bld 5 Ceramic	7.6	Coatings: Seal Seat Face - Chrome Carbide Piston Ring - Chrome Flash Carrier Bore - Chrome Carbide	PC*	Excessive Air Leakage At High Speeds	Excellent	Excellent		2.3
2	Used From Bld 1	Used From Bld 1	Used From Bld 1	Used From Bld 1	15.4		PC	Excessive Air Leakage At High Speeds	Excellent	Excellent		6.3
3	Used From Bld 2	Used From Bld 2	Used From Bld 2	Used From Bld 2	22.9		PC	Excessive Air Leakage At High Speeds	Approximately 0.05 Mil Wear for Total Builds 1, 2, 3, Test Time	Good		5.9
3-1	Used From Bld 3	Used From Bld 3	Used From Bld 3	Used From Bld 3	22.9		PC & FT**	Excessive Air Leakage At High Speeds and Air Temperatures	Tapered Face Wear: Average Rayleigh Pad Wear 0.2 Mil, Seal Dam Wear 0.3 Mil	Good	30.0	55.7
											30.0	70.2

*PC = Preliminary Dynamic Checkout Testing
**ET = Elevated Temperature Testing

A. PRELIMINARY DYNAMIC TESTING - BUILD 1

The carbon nosepiece for the narrow-pad seal is shown assembled before testing in Figure 58. A close-up of the nosepiece is shown in Figure 59. Profile traces across the seal face revealed an average pad depth of 0.8 mil. A typical trace is shown in Figure 60. The seal was assembled for Build 1 with a spring load of 7.8 pounds.

Preliminary dynamic checkouts were conducted at sliding speeds of 260 and 310 ft/sec and pressure differentials from 50 to 200 psi. Attempts to check out the seal at higher speeds were unsuccessful as indicated by excessive leakage. The test results are shown in Figure 61. A comparison of the actual and calculated leakages for the Build 1 seal is presented in Figure 62. Total air leakage is the sum of the primary and secondary leakages.

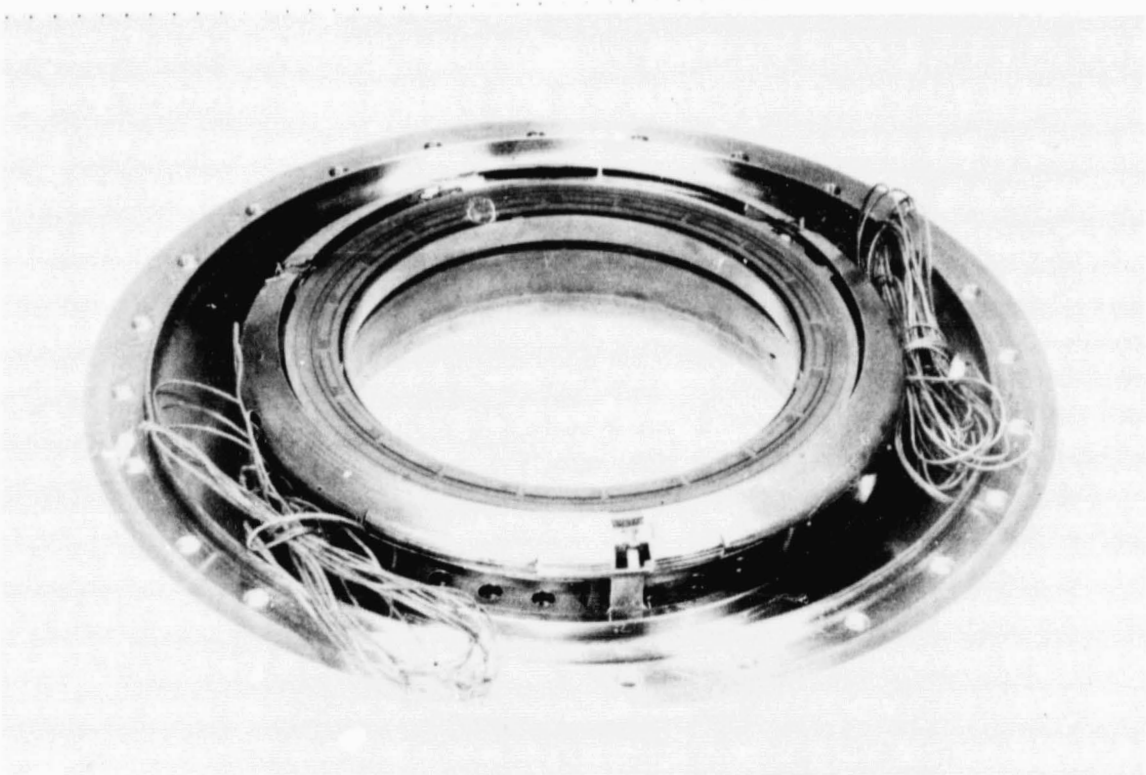

Figure 58 Nosepiece from the Narrow-Pad Seal Before Testing (XPN-11773)

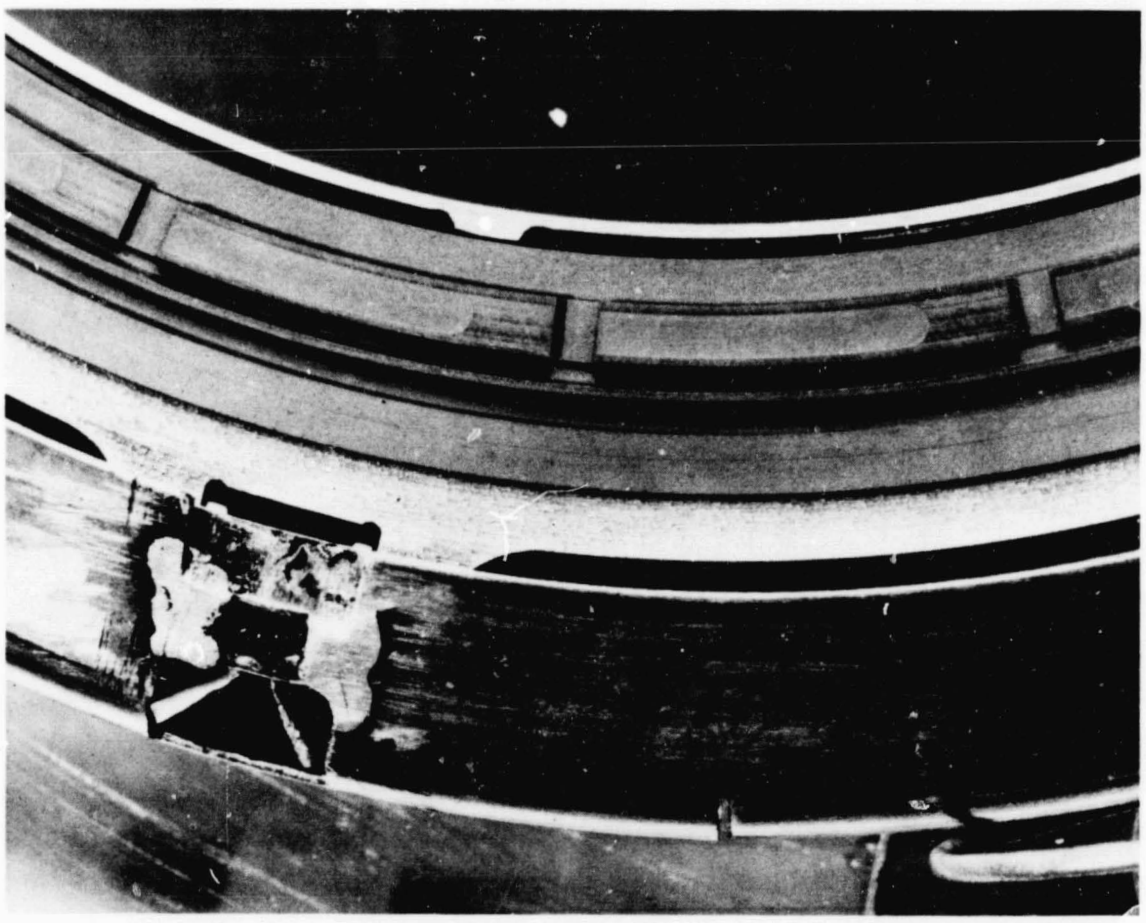

Figure 59 Close-Up of the Nosepiece from the Narrow-Pad Seal Before Testing (XPN-11772)

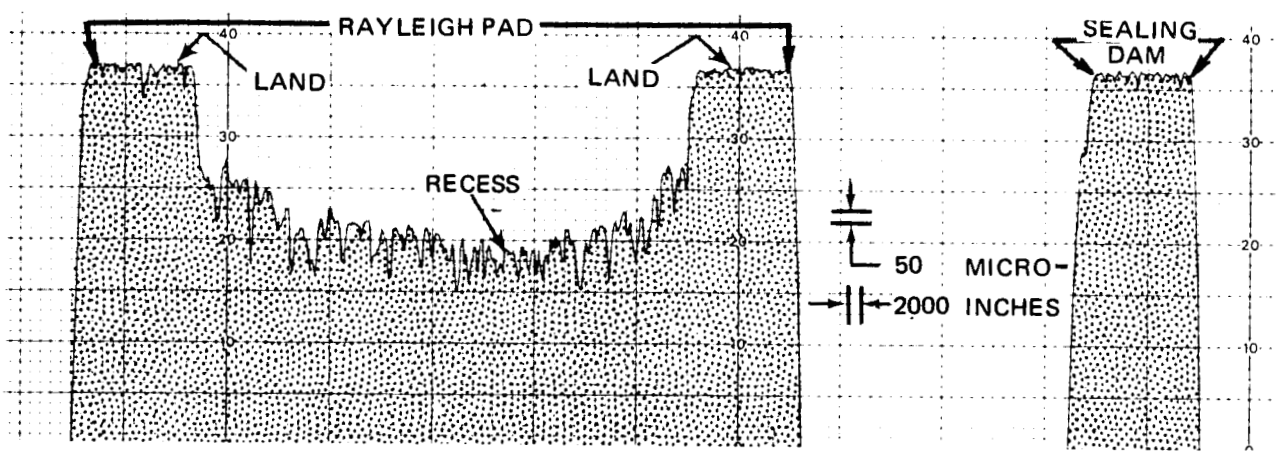

Figure 60 Representative Profile Trace Taken Radially Across the Face of the Carbon Nosepiece from the Narrow-Pad Seal Before Build 1 Testing

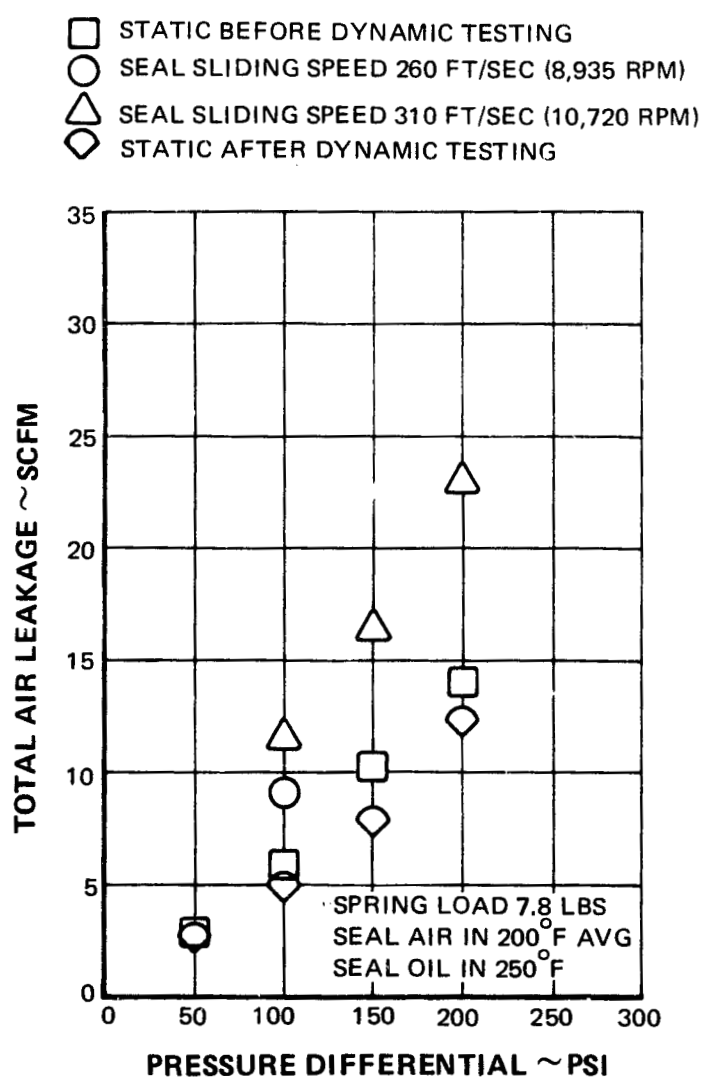

Figure 61 Air Leakage Past Build 1 of the Narrow-Pad Seal

The Build 1 leakage results indicated that the gas-film stiffness was insufficient to allow the nosepiece to follow the seal seat's runout at high speeds, although visual inspection showed that both the nosepiece and seat were in excellent condition after the Build 1 testing. In order to raise the gas-film stiffness at the seal operating conditions, the spring load was increased to 15.4 pounds for Build 2.

B. PRELIMINARY DYNAMIC CHECKOUT - BUILD 2

Except for the increased spring load, the Build 2 configuration was identical to the Build 1 configuration and used all of the parts from Build 1. The preliminary dynamic checkouts on Build 2 were successful at 260 and 310 ft/sec, but marginal at 335 ft/sec. Pressure differentials for these tests ranged from 50 to 250 psi. The test results are plotted in Figure 63. At 335 ft/sec operation at pressure differentials below 130 psi resulted in high air leakage, while attempts to run the seal at 360 ft/sec resulted in excessive air leakage. A comparison between the calculated and actual air leakages for a speed of 310 ft/sec is presented in Figure 64.

Disassembly and inspection after the tests showed that the nosepiece and seal seat were in excellent condition.

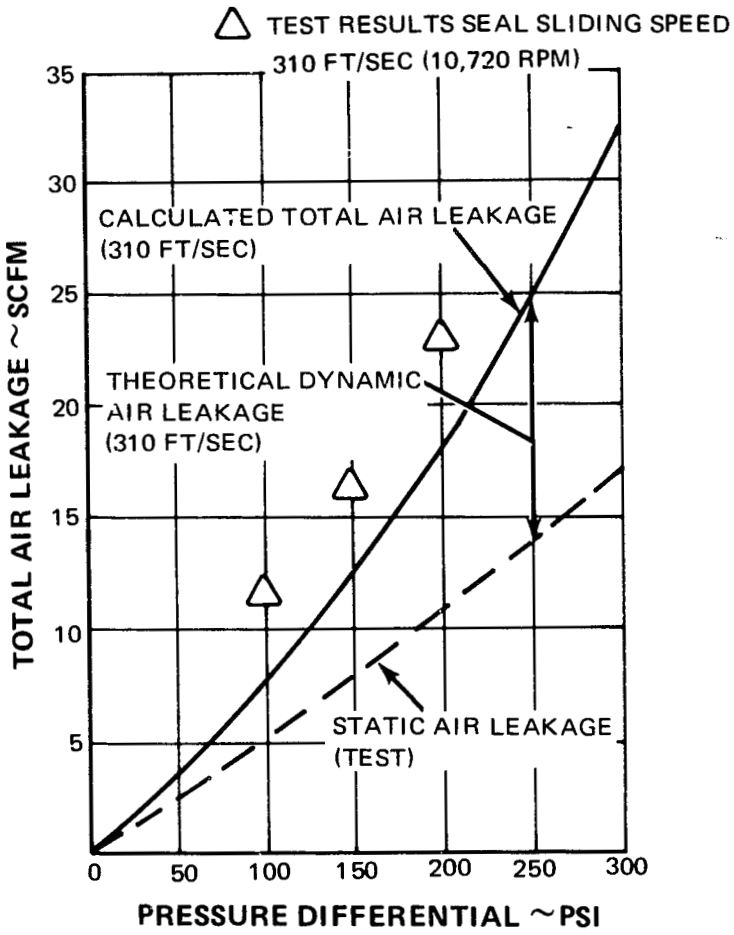

Figure 62 Calculated and Actual Air Leakage Past Build 1 of the Narrow-Pad Seal with Ambient Air

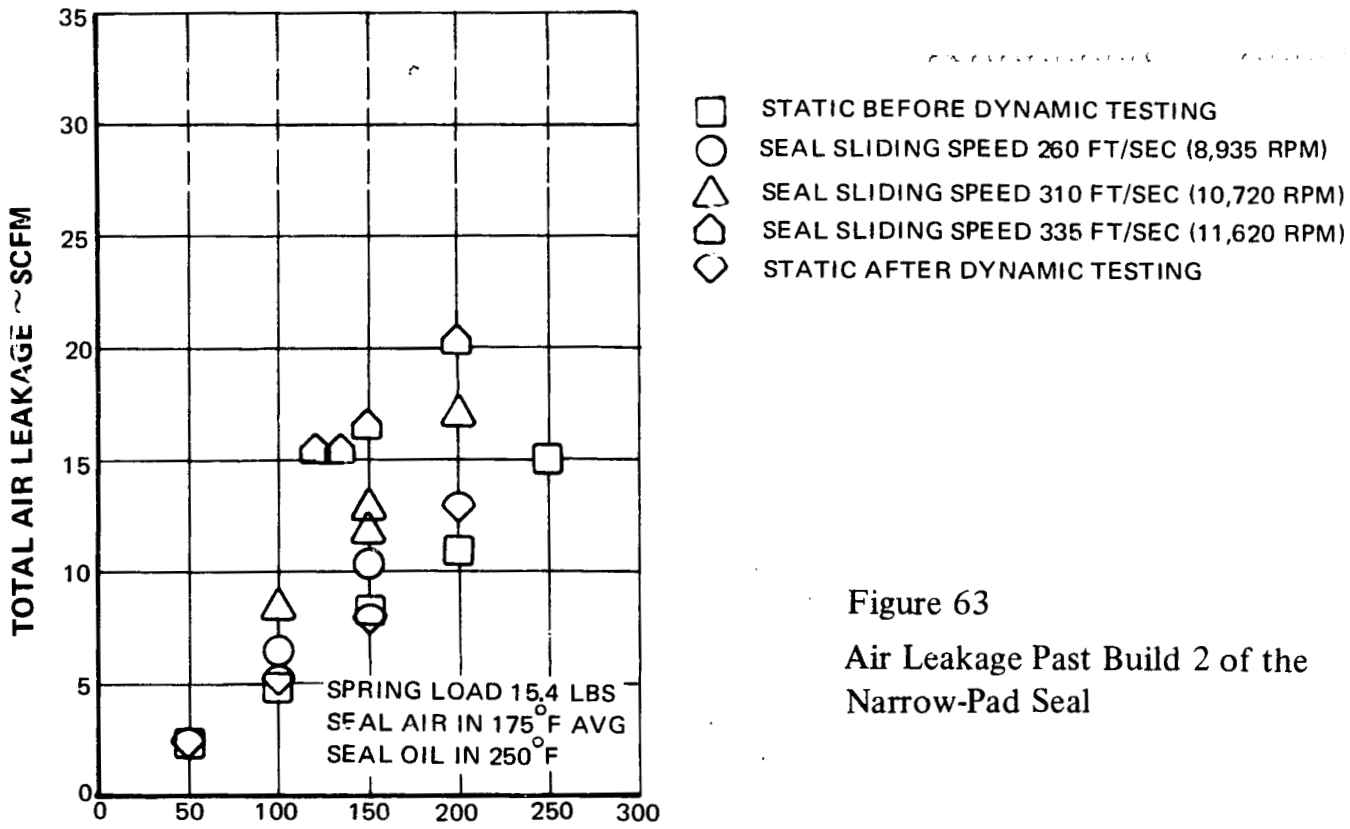

Figure 63

Air Leakage Past Build 2 of the Narrow-Pad Seal

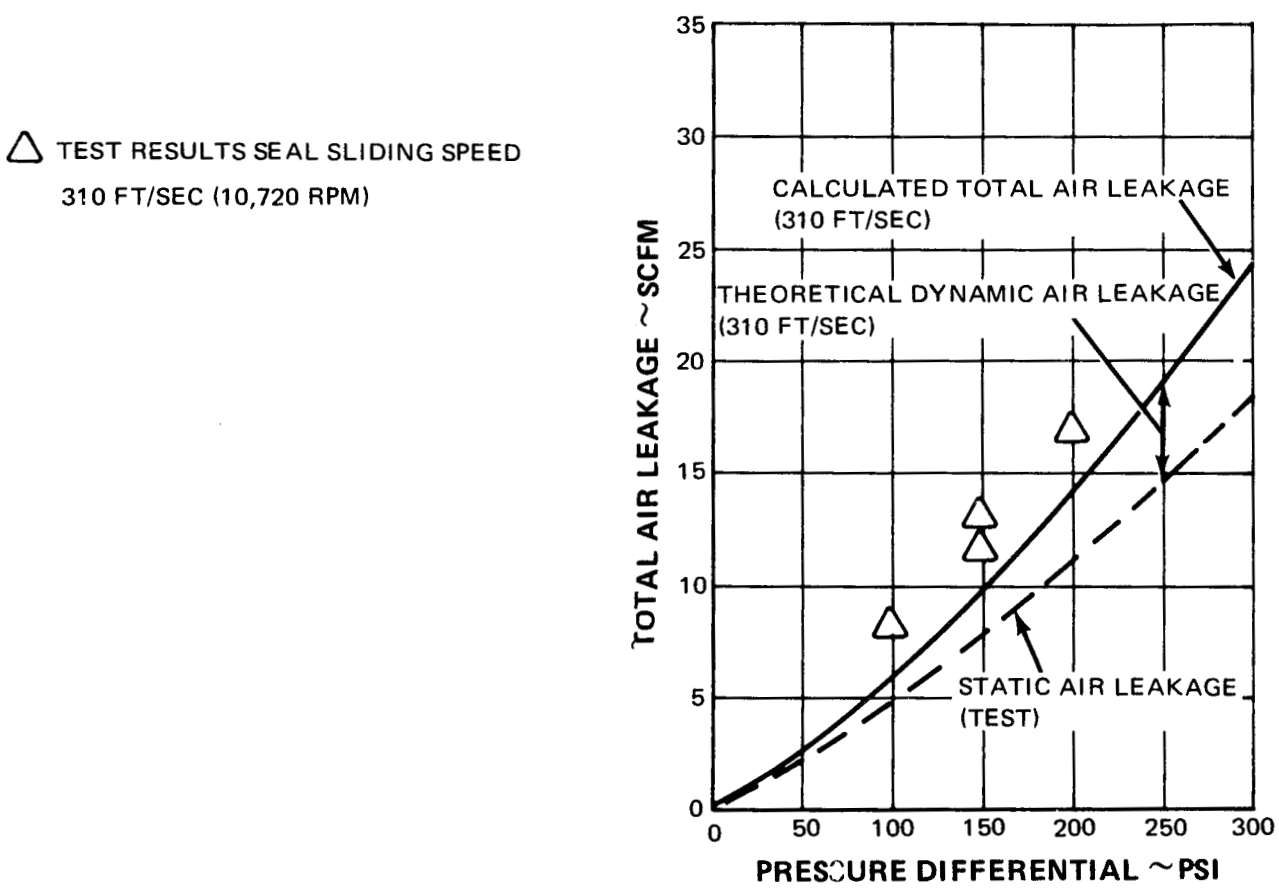

Figure 64 Calculated and Actual Air Leakage Past Build 2 of the Narrow-Pad Seal with Ambient Air

C. PRELIMINARY DYNAMIC CHECKOUT - BUILD 3

In order to increase the stiffness of the gas film still further, the spring load for Build 3 was increased to 22.9 pounds. All other parts in Build 3 were used parts from Build 2.

The preliminary dynamic checkouts of Build 3 covered sliding speeds from 260 to 360 ft/sec and pressure differentials from 50 to 250 psi. In general, the Build 3 test results were very similar to those from Build 2. The Build 3 test results are shown in Figure 65, and a comparison of theoretical and actual air leakage at 310 ft/sec is shown in Figure 66. At that speed, the theoretical and actual leakages correlated quite well.

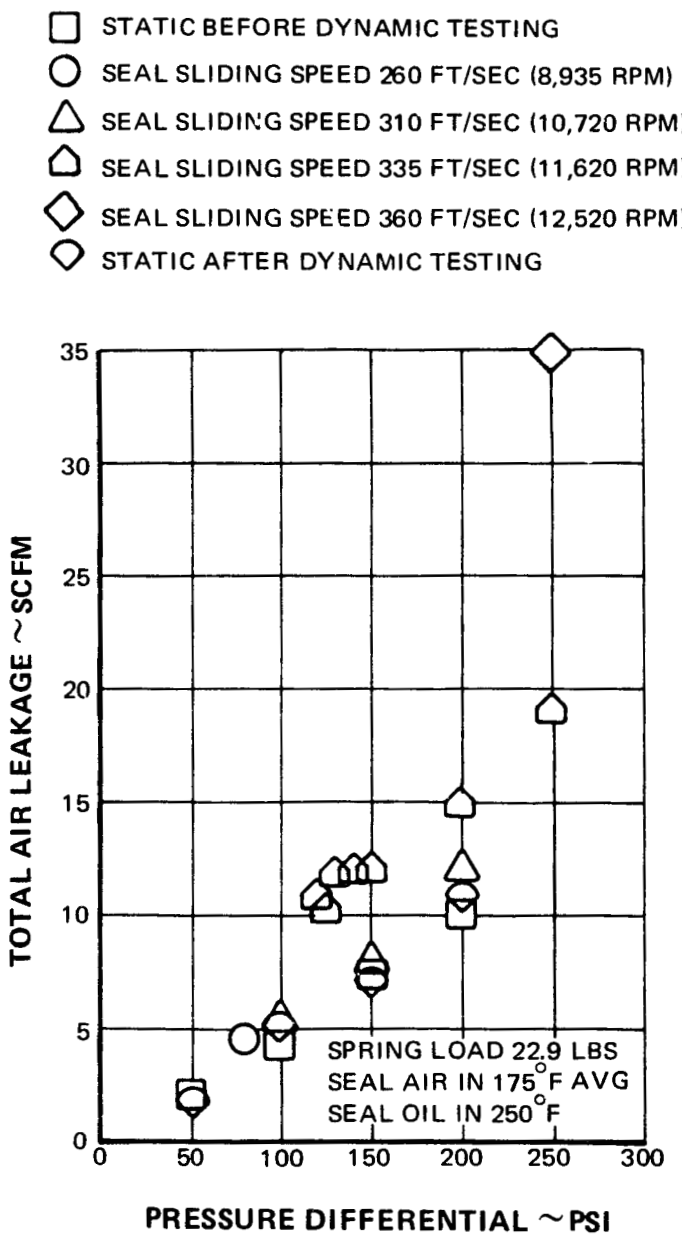

Figure 65 Air Leakage Past Build 3 of the Narrow-Pad Seal

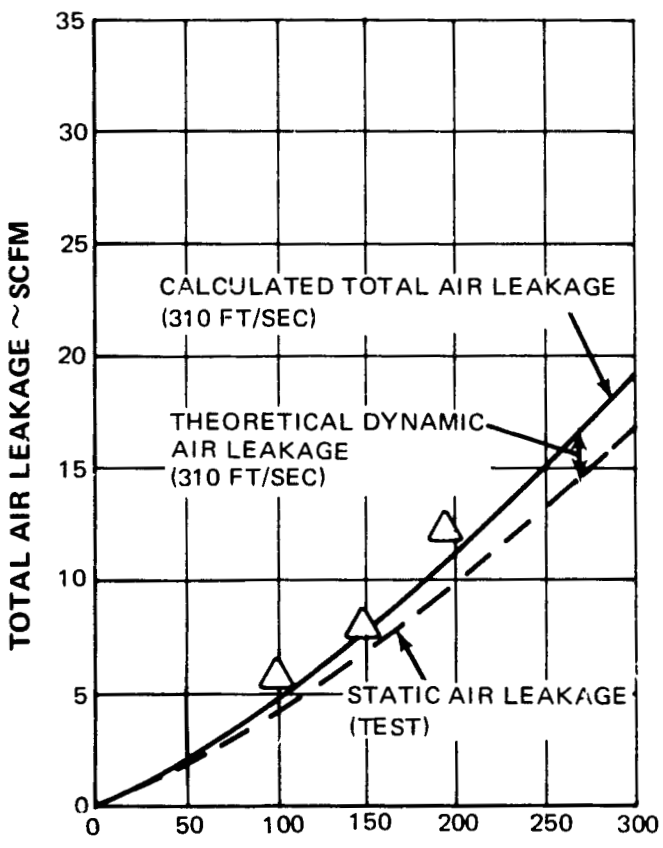

Figure 66 Calculated and Actuai Air Leakage Past Build 3 of the Narrow-Pad Seal with Ambient Air

Disassembly and inspection showed that the seal seat and nosepiece were in excellent condition. Profile traces across the carbon nosepiece indicated that the face wear was approximately 0.05 mil for the total test time (Builds 1, 2, and 3) of 14.5 hours. A representative profile trace is shown in Figure 67. The trace in Figure 67 was taken at the same location as the pretest trace shown in Figure 60.

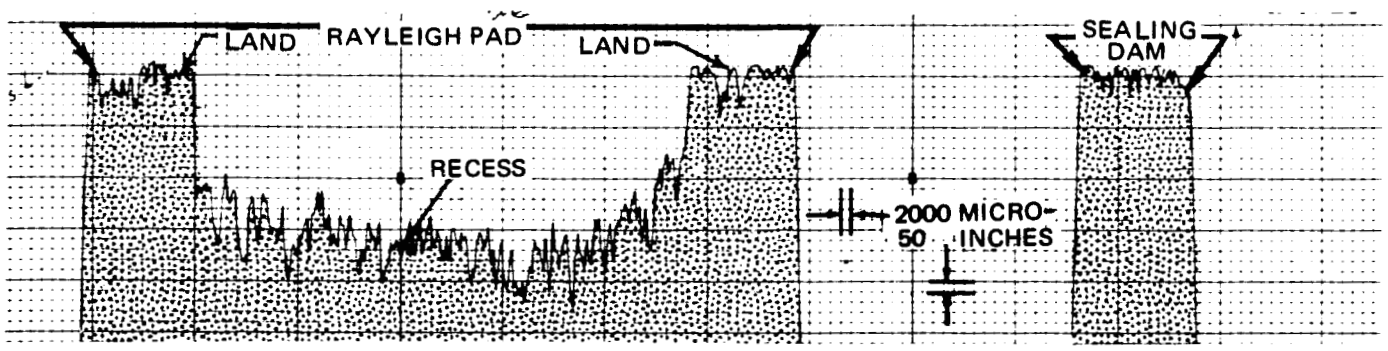

Figure 67 Representative Profile Trace Taken Radially Across the Face of the Carbon Nosepiece from the Narrow-Pad Seal after 5.9 Hours of Build 3 Testing. Total Time on Nosepiece 14.5 Hours

Because air leakages past the test seals were consistently high at speeds above 335 ft/sec, it was decided to recheck the test rig. To recheck the rig, the wide-pad Type A carbon nosepiece from Phase II (Reference 3) of this contract was rerun, resulting in high leakages above a sliding speed of 360 ft/sec. These high leakages indicated that the rig was not performing properly. The test rig was disassembled and the rotor was found to be unbalanced by 3.5 oz-in, which was considered to be excessive. With the rotor unbalanced by 3.5 oz-in the vibration level of the rig was raised to excessive levels and the shaft may have been vibrating in a conical whirl mode. The conical whirl mode would have produced an angular displacement of the shaft centerline and a corresponding angular displacement of the seal seat, resutling in a seal seat axial runout. This dynamic runout would be superimposed in the axial runout measured when the shaft assembly was examined prior to each test.

D. PRELIMINARY DYNAMIC CHECKOUT - BUILD 3-1

The rig shaft assembly was rebalanced for Build 3-1, reducing the shaft imbalance to 0.5 oz-in. In addition, the static axial runout of the seal seat was reduced from 1.2 to 0.8 mil. Otherwise, the Build 3-1 seal was the same as the Build 3 seal.

Build 3-1 was operated successfully at speeds from 260 to 360 ft/sec, and pressure differentials from 50 to 250 psi. Operation was also attempted at 410 ft/sec, but excessive air leakage was encountered. After the attempted operation at 410 ft/sec a test point at 360 ft/sec and 100 psi was rerun. For the first ten minutes at that point air leakage was acceptable, but after ten minutes the leakage increased to unacceptable levels. The results of the preliminary dynamic testing are shown in Figure 68. Comparisons of calculated and actual air leakages for speeds of 310 and 360 ft/sec are shown in Figures 69 and 70. When the seal assembly was removed from the rig for inspection it was found that the seal nosepiece and seal seat were in excellent condition.

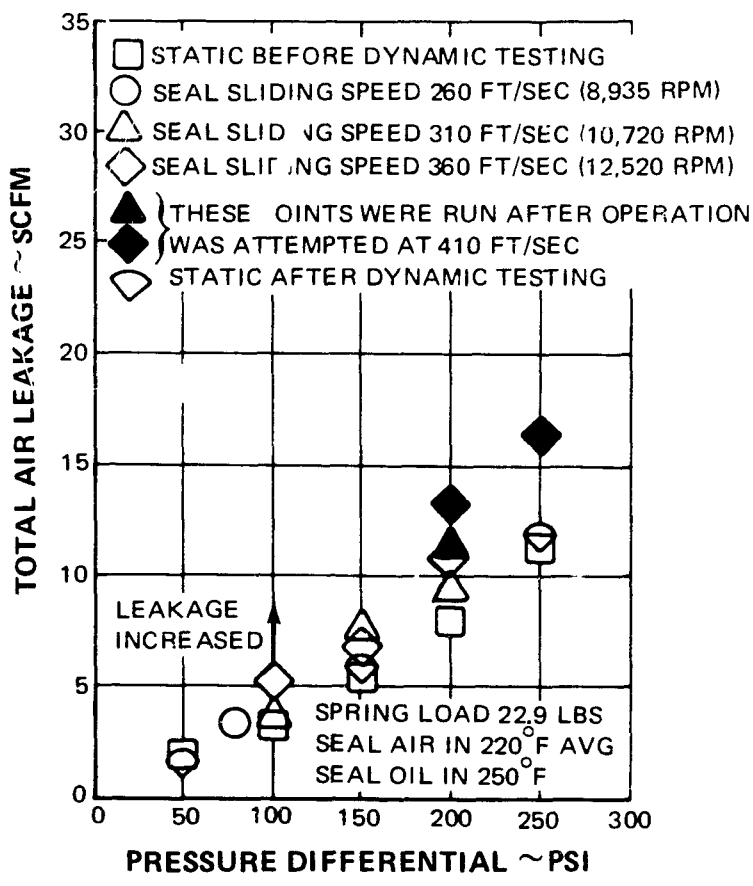

Figure 68

Air Leakage Past Build 3 of the Narrow-Pad Seal

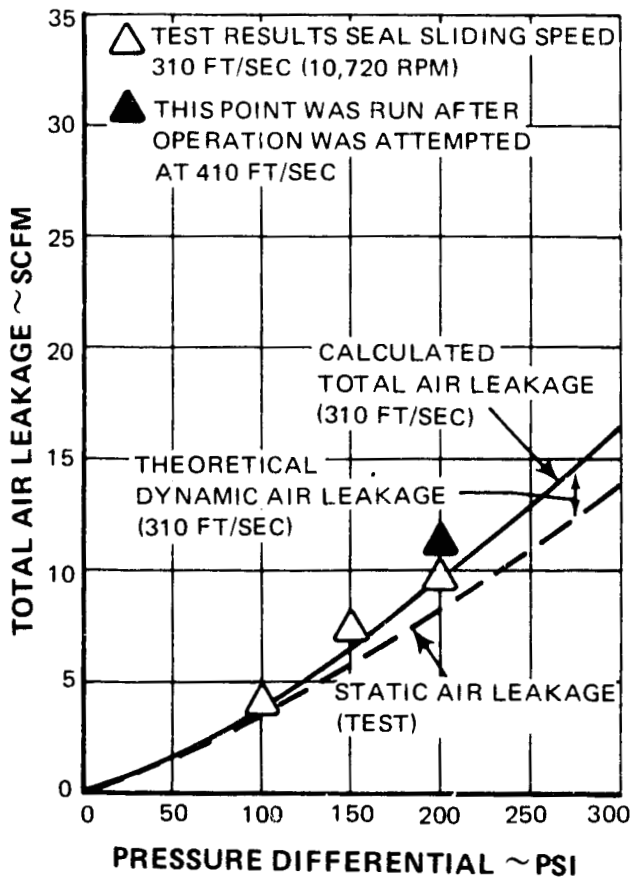

Figure 69 Calculated and Actual Air Leakage Past Build 3-1 of the Narrow-Pad Seal at a Sliding Speed of 310 ft/sec with Ambient Air

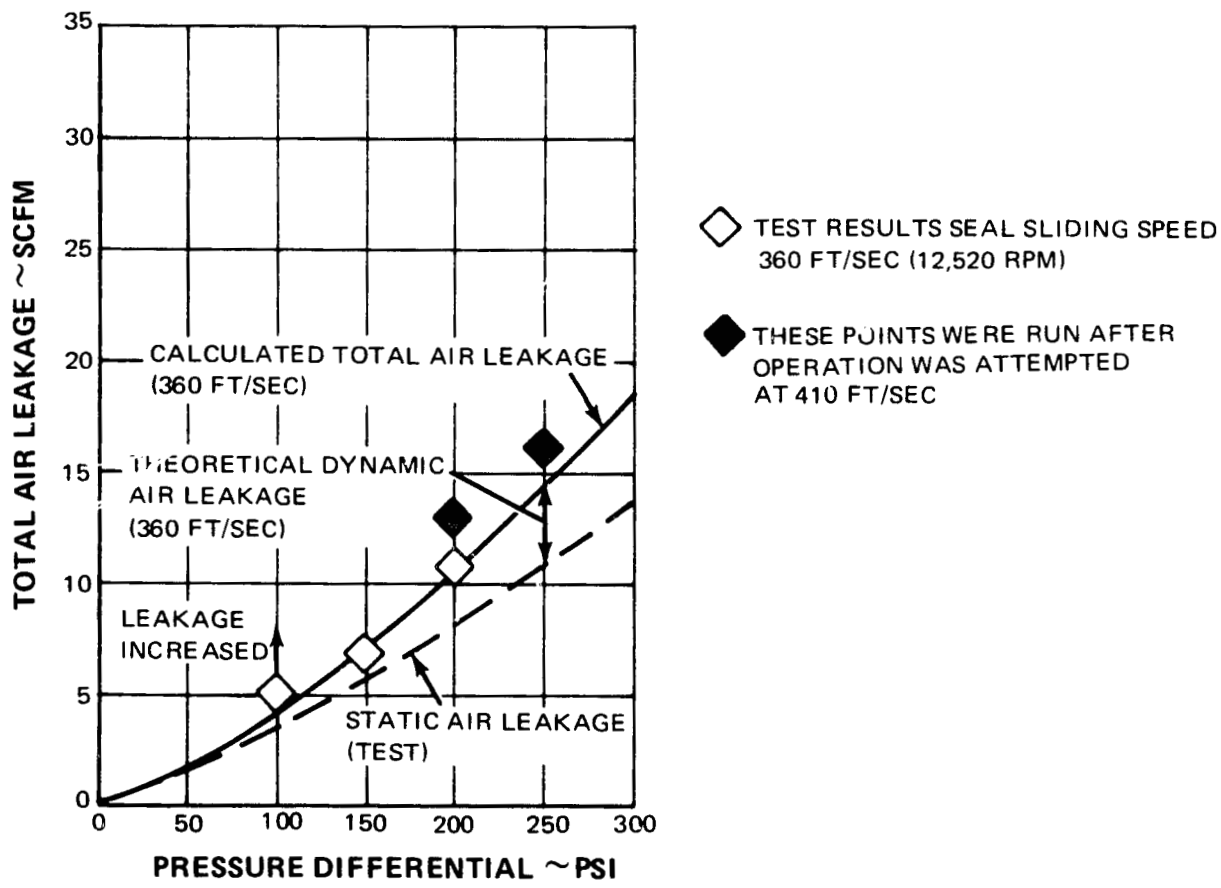

Figure 70 Calculated and Actual Air Leakage Past Build 3-1 of the Narrow-Pad Seal at a Sliding Speed of 360 ft/sec with Ambient Air

E. ELEVATED-TEMPERATURE TESTING - BUILD 3-1

Despite the marginal performance of the narrow-pad seal on the preliminary dynamic check-outs, it was decided to proceed with elevated temperatures. Higher temperatures provide the seal with higher load capacity and increased film thickness because the viscosity of air increases with increasing temperature. The increased film thickness was expected to give the seal a greater tolerance for distortion and seal seat runout.

Elevated-temperature testing was completed on the narrow-pad seal at the following conditions:

Time (hrs)	Seal Sliding Speed (ft/sec)	Seal Pressure Differential (psi)	Seal Air Temperature (°F)	Seal Oil-In Temperature (°F)	Average Air Leakage (scfm)
5	360	150	600	250	10.3
Testing interrupted for seal inspection					
5	360	150	800	250	12.4
20	360	200	750	250	13.0

After the first five hours of endurance testing the seal was removed for inspection. As shown in Figure 71 (taken at the same location as Figures 60 and 67), profile traces taken across the nosepiece revealed tapered wear. After a total time of 29.9 hours on the nosepiece there had been an average wear of 0.10 mil at the inner edge of the Rayleigh pad, 0.15 mil at its outer edge, and a wear of 0.18 mil on the seal dam.

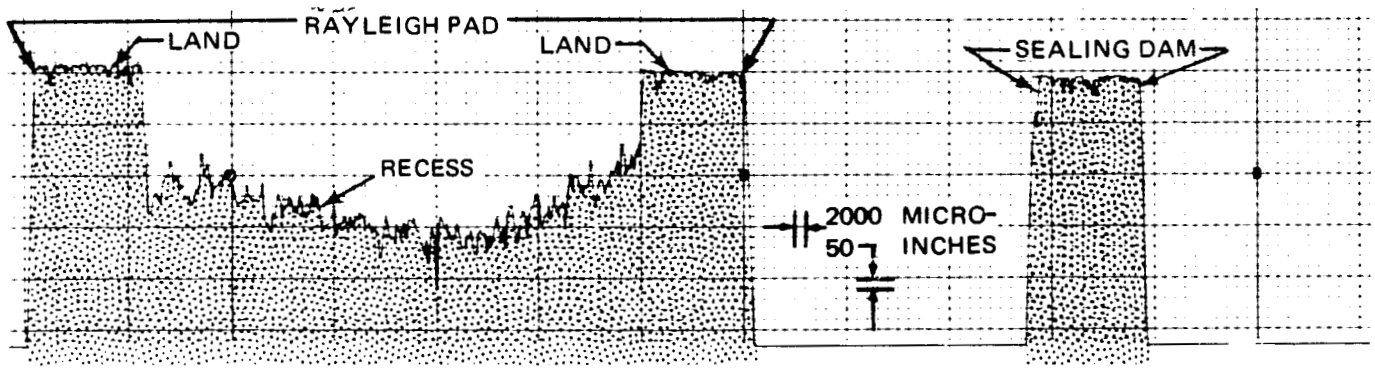

Figure 71 Representative Profile Trace Taken Radially Across the Face of the Carbon Nosepiece from the Narrow-Pad Seal after First 5.0 Hours of Build 3-1 Endurance Testing. Total Time on Nosepiece 29.9 Hours

After the 20-hour endurance test at 750°F, operation was attempted at temperatures above 800°F, but rapid increases in seal air leakage indicated unstable operation. The seal assembly was then removed from the test rig to determine the reasons for the instability. Visual inspection of the seal nosepiece and seal revealed that both were in good condition. A close-up of the carbon nosepiece is shown in Figure 72.

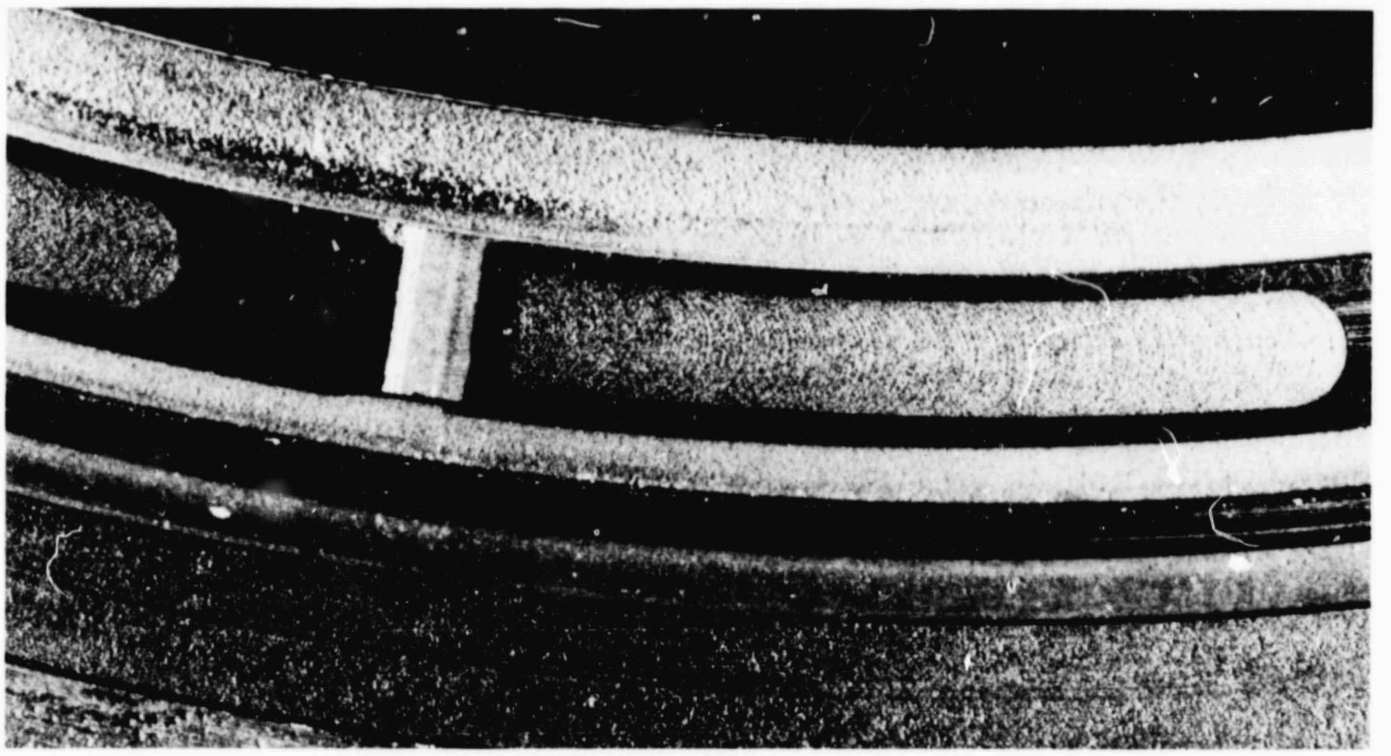

Figure 72 Close-Up View of the Carbon Nosepiece from Build 3-1 of the Narrow-Pad Seal. Total Time on Nosepiece 70.2 Hours

Profile traces across the nosepiece again indicated tapered wear, with an average Rayleigh pad wear of 0.14 mil at the inner edge, 0.25 mil at the outer edge, and a seal dam wear of 0.30 mil for the 70.2 hours of testing. A profile trace from the same location as Figures 60, 67, and 71 is shown in Figure 73. The tapered wear is also revealed in Figure 74, which is a profile trace taken across the land surface of a Rayleigh pad and the seal dam.

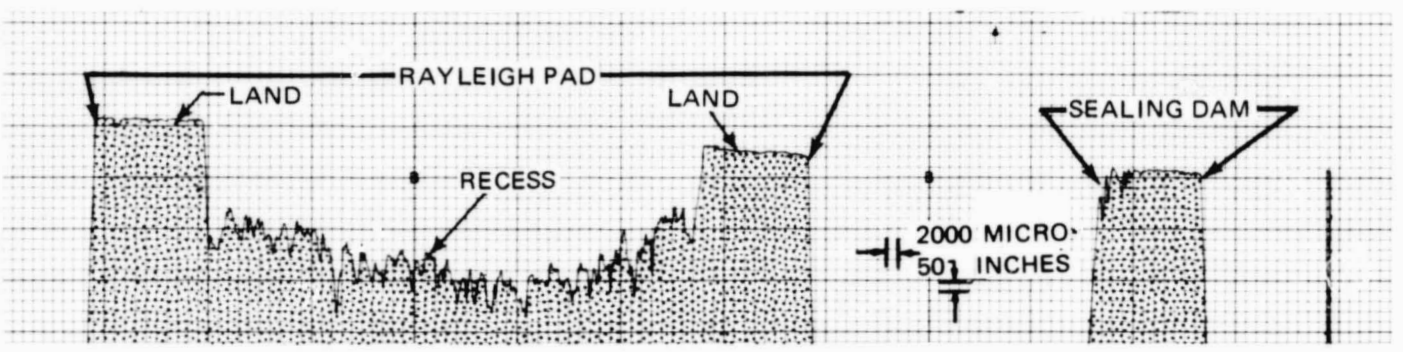

Figure 73 Representative Profile Trace Taken Radially Across the Face of the Carbon Nosepiece from the Narrow-Pad Seal After 55.7 Hours of Build 3-1 Testing. Total Time on Nosepiece 70.2 Hours

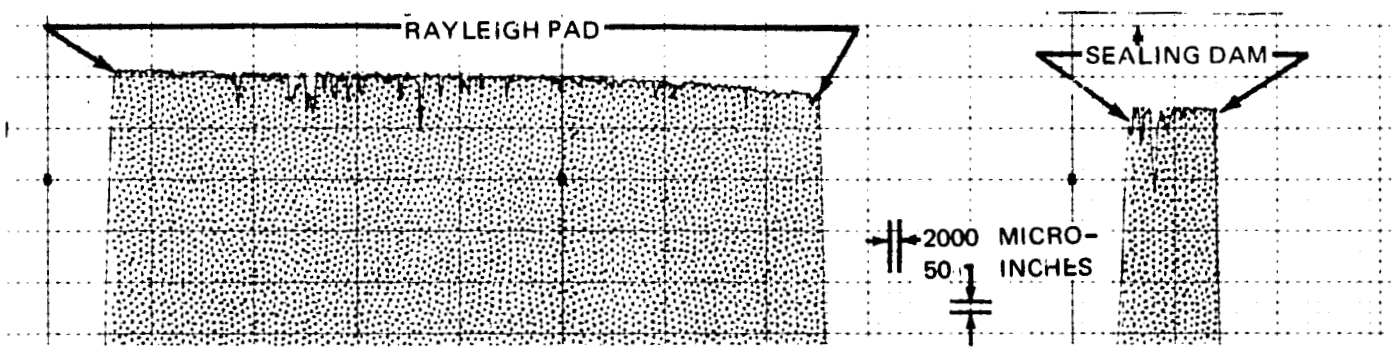

Figure 74 Profile Trace Taken Radially Across the Face of the Carbon Nosepiece from the Narrow-Pad Seal at a Rayleigh Pad Land After 55.7 Hours of Build 3-1 Testing. Total Time on Nosepiece 70.2 Hours

Inspection also revealed that the inner surface (diameter) of the seal dam was uneven. In one area, which was approximately 10 percent of the circumference, the width of the dam was 16 mils instead of the required nominal size of 25 mils. The reduced width of the sealing dam decreased the local closing force on the seal, raising the local equilibrium film thickness to the point where the film stiffness was insufficient to allow proper tracking at some conditions.

SECTION VI
EXPERIMENTAL EVALUATION OF THE WIDE-PAD SEAL

The wide-pad seal tested under Phase III of this contract is identical to the Type A gas-film seal evaluated under Phase II (Reference 3). It is described in Section III of this report, and a layout of the seal is shown in Figure 6. The wide-pad seal was substituted as a "rework" for the ceramic seal because tests on the ceramic seal had indicated that its fracture failure mode would not be satisfactory. Because Phase II testing of the seal had demonstrated its feasibility, the Phase III testing was intended to explore its operational limits. During Phase II the seal was operated at maximum conditions of 450 ft/sec sliding speed, 250 psi pressure, differential, and 1200°F air temperature.

Under Phase III, the wide-pad seal successfully completed 305.9 hours of testing at sliding speeds from 345 to 500 ft/sec, pressure differentials from 100 to 300 psi, and air temperatures from room temperature to 1200°F. Testing on Builds 1 and 3 was terminated because of excessive leakage past the secondary seal, and testing on Builds 2 and 4 was terminated because of rig problems. The test programs for Builds 5 through 9 were successfully completed. In general, the actual leakage during the elevated-temperature tests was somewhat higher than the predicted leakage, but the overall operation of the seal was quite satisfactory. A summary of the tests conducted on the wide-pad seal is presented in Table V.

A. PRELIMINARY DYNAMIC TESTING - BUILD 1

Since the wide-pad seal had been previously tested under Phase II of this contract, the preliminary dynamic checkout was kept to the minimum necessary to ensure that the rig and seal were operating properly. The results of the preliminary dynamic checkout are plotted in Figure 75. Total leakage is the sum of leakage past the primary and secondary seals.

B. ELEVATED TEMPERATURE TESTING - BUILD 1

Thirty hours of steady-state elevated-temperature testing were completed on Build 1 of the wide-pad seal. The test conditions and leakages are summarized below:

Time (hrs)	Sliding Speed (ft/sec)	Seal Pressure (psi)	Air Temperature (°F)	Actual Total Air Leakage (scfm)
5	345	50	400	5.7
5	395	100	600	18.5
5	350	150	600	11.0
1	425	200	600	30.0
4	400	200	600	26.5
5	400	250	600	31.5
Testing interrupted to reduce rig vibration				
5	350	150	800	12.5

An oil-in temperature of 250°F was used for all of the above tests.

TABLE V
WIDE-PAD SEAL TEST SUMMARY

Build No.	Nosepiece	Seal Seat	Piston Ring	Carrier	Spring Load (lbs)	Other Special Features	Type of Test	Reason for Test Termination	Condition After Test: Nosepiece Face	Condition After Test: Seal Seat Face	Total Bld End Hours	Total Bld Hours
1	Repaired Nosepiece From Phase II	Re-lapped Seal Seat Phase II	New	New	15.5	Coatings: Piston Ring - Chrome Flash Seal Seat - Chrome Carbide Carrier - Chrome Carbide	PC* & ET**	Excessive Air Leakage at Elevated Air Temperatures Due to Secondary Seal	Pad Wear Less Than 0.05 Mil	Good	30.0	53.0
2	Used From Bld 1	Used From Bld 1	New	Re-paired Carrier From Bld 1	15.5	Carrier Bore Coating Changed to Aluminum Oxide Piston Ring Material Changed to Carbon (Configuration No. 1) (See Fig. 76)	ET	Excessive Test Rig Vibration	Pad Wear Less Than 0.05 Mil	Good	22.0	54.0
3	Used From Bld 2	Used From Bld 2	Used From Bld 2	Used From Bld 2	25.0		ET	Excessive Secondary Seal Air Leakage	Tapered Face Wear: Average Rayleigh Pad Wear 0.06 Mil, Seal Dam Wear 0.14 Mil	Good	2.5	6.0
4	Used From Bld 3	Used From Bld 3	New	Used From Bld 3	25.0	Changed Support to Eliminate Effects of Thermal Coning New Carbon Piston Ring Same Configuration As That Used in Bld 2	ET	Air Line Burst Causing Damage To Seal	Tapered Face Wear: Average Rayleigh Pad Wear 0.10 Mil, Seal Dam Wear 0.35 Mil	Good	13.7	26.3
5	Repaired Nosepiece From Phase II	Used From Bld 4	Used From Bld 4	Used From Bld 4	25.0		ET	Completed Program	Face Wear Less Than 0.05 Mil, Dam Scratched Some Scratches 0.50 Mil Deep	Good	40.0	49.0
6	Used From Bld 5	Used From Bld 5	Used From Bld 5	Used From Bld 5	25.0		ET	Completed Program	Rayleigh Pad Wear Less Dam Slightly Tapered: Outer Edge 0.05 Mil Lower Than Inner Edge. Scratches As Deep As 0.8 Mil	Good	13.8	21.3

TABLE V (Cont'd)

Build No.	Nosepiece	Seal Seat	Piston Ring	Carrier	Spring Load (lbs)	Other Special Features	Type of Test	Reason for Test Termination	Condition After Test: Nosepiece Face	Condition After Test: Seal Seat Face	Total Bld. End Hours	Total Bld. Hours
7	Used From Bld 6	Used From Bld 6	New	Used From Bld 6	25.0	New Carbon Piston Ring Used Configuration No. 2 (See Pg. 76 & Fig. 85)	ET	Completed Program	Rayleigh Pad Wear Less Than 0.05 Mil, Seal Dam Wear 0.10 Mil	Good	23.3	33.5
8	Used From Bld 7	Used From Bld 7	New	Used From Bld 7	25.0	New Carbon Material Same Configuration As Original Carbon Ring Used (See Fig. 76)	ET	Completed Program	Visual Inspection Revealed Face To Be In Good Condition	Good	20.0	26.9
9	Used From Bld 8	Used From Bld 8	New	Used From Bld 8	25.0	TZM Piston Ring Used Same As Ring Used In Bld 1 With No Coating	ET	Completed Program	Rayleigh Pad Wear Less Than 0.05 Mil, Seal Dam Wear 0.30 Mil	Good	24.3	35.9
								Total Wide-Pad Carbon Nosepiece Type Seal Test Time			189.6	305.9

* PC = Preliminary Dynamic Checkout Testing
** ET = Elevated Temperature Testing

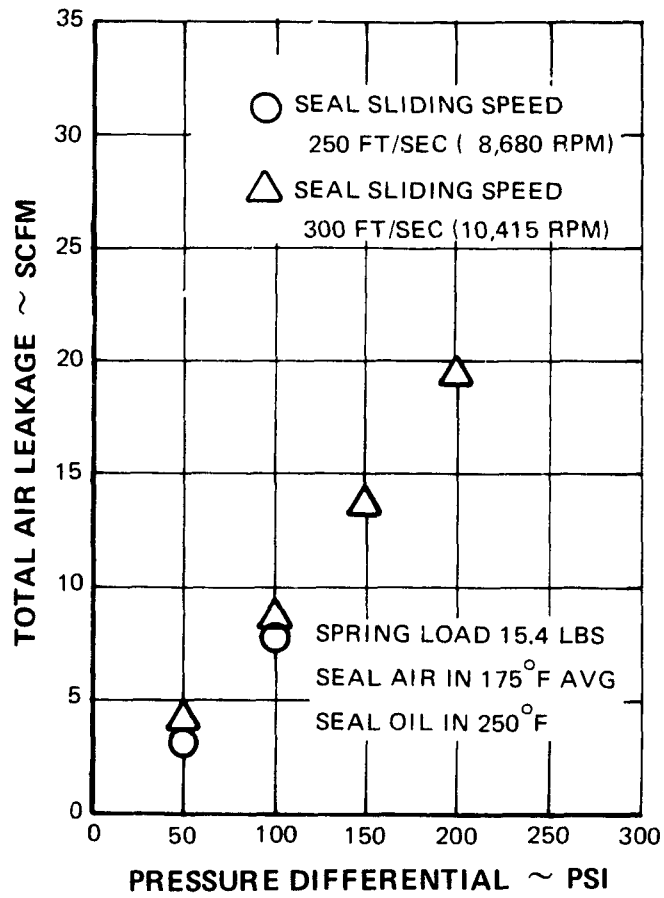

Figure 75 Air Leakage Past Build 1 of the Wide-Pad Seal

The testing at 345, 395, and 350 ft/sec sliding speeds was completed without difficulty. However, after one hour of testing at 425 ft/sec the rig vibration increased suddenly, and the sliding speed was reduced to 400 ft/sec to reduce the vibration. After the test at 400 ft/sec and a seal pressure differential of 250 psi it was decided to interrupt testing and inspect the rig to determine the cause of the vibration.

Rig inspection showed that the quill shaft which drives the test rig was out of balance and that a bearing in the gearbox drive-shaft assembly had been damaged. The shaft was refurbished and the bearing replaced.

Inspection of the test seal showed that the Rayleigh pads on the carbon nosepiece had worn less than 0.05 mil (the minimum amount detectable) and that the sealing dam on the carbon nosepiece had worn 0.08 mil. The carrier piston ring bore surface (coated with flame-sprayed chromium carbide) had worn about 0.5 mil in the piston-ring land wear track and less than 0.3 mil in the piston-ring seal-dam wear track. The land area on the TZM piston ring (flash coated with chromium) looked slightly rough, but the seal dam was in good condition.

Build 1 testing was resumed at a sliding speed of 350 ft/sec, a seal pressure differential of 150 psi, and an initial air temperature of 70°F. The sliding velocity and pressure differential were kept constant and the air temperature was raised to 950°F at a rate about 100°F per hour. At a temperature of 950°F the air leakage past the seal became erratic, so the temperature was dropped to 800°F and five hours of testing were completed at that condition.

Inspection after the final Build 1 test revealed the nosepiece and seal seat to be in good condition; the only signs of distress were in the secondary seal area. In that area the piston ring showed new signs of scuffing where it had rubbed against the seal support. The wear observed in this location after 49.8 hours of running was greater than the wear observed on the Type A seal run during Phase II of this contract. In the Phase II (Reference 3) seal a chromium-flashed TZM piston ring was run against a chromium-plated TZM carrier; only 0.1 mil of wear was observed on the carrier after 570 hours of running.

C. ELEVATED TEMPERATURE TESTING - BUILD 2

For Build 2 of the wide-pad seal the chrome carbide coating on the TZM carrier was machined off and replaced with PWA 53-10, an aluminum oxide material. In addition, the chrome flashed TZM piston ring was replaced by a carbon piston ring supplied by NASA. The carbon ring had been machined to the same dimensions as the previous ring (see Figure 76).

Endurance testing on the Build 2 seal was completed at the following conditions:

Time (hrs)	Sliding Speed (ft/sec)	Seal Pressure (psi)	Air Temperature (°F)	Actual Total Air Leakage (scfm)
5	400	200	800	22.4
5	350	150	900	15.7
5	400	200	1000	26.2
5	400	250	800	26.0

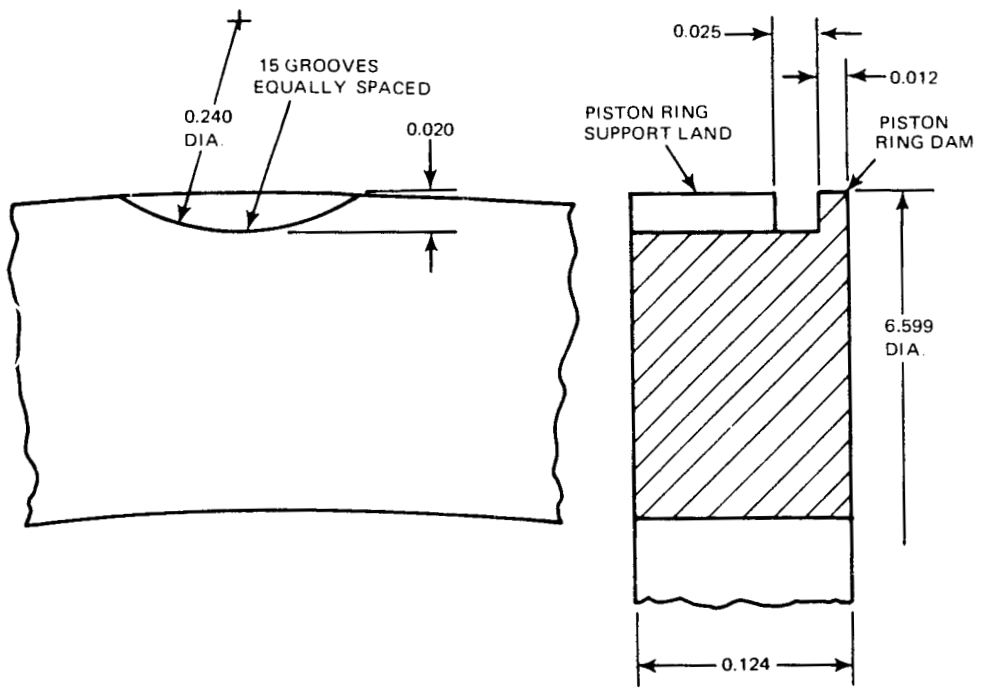

Figure 76 Dimensions of the Carbon Piston Ring Used in Build 2 of the Wide-Pad Seal

Measurements made on the piston ring after the first five hours of endurance testing indicated approximately 0.1 mil wear at the support land surface. In general, the outside surface of the piston ring (which runs in contact with the carrier bore) appeared smoother than it did before the test. Although they were not measured at that time, the seal nosepiece, seal seat, and the carrier bore appeared to be in good condition.

Inspection after the first five hours of endurance testing showed that the heat shield on the inner surface of the piston ring support had collapsed in the center and was contacting the support. Such contact would significantly reduce the effectiveness of the heat shield. The heat shield was removed and repaired. Asbestos insulation was placed between the heat shield and the support to prevent contact, as shown in Figure 77. In addition, two thermocouples were installed on the piston-ring support. They were used to provide additional data on the secondary seal behavior.

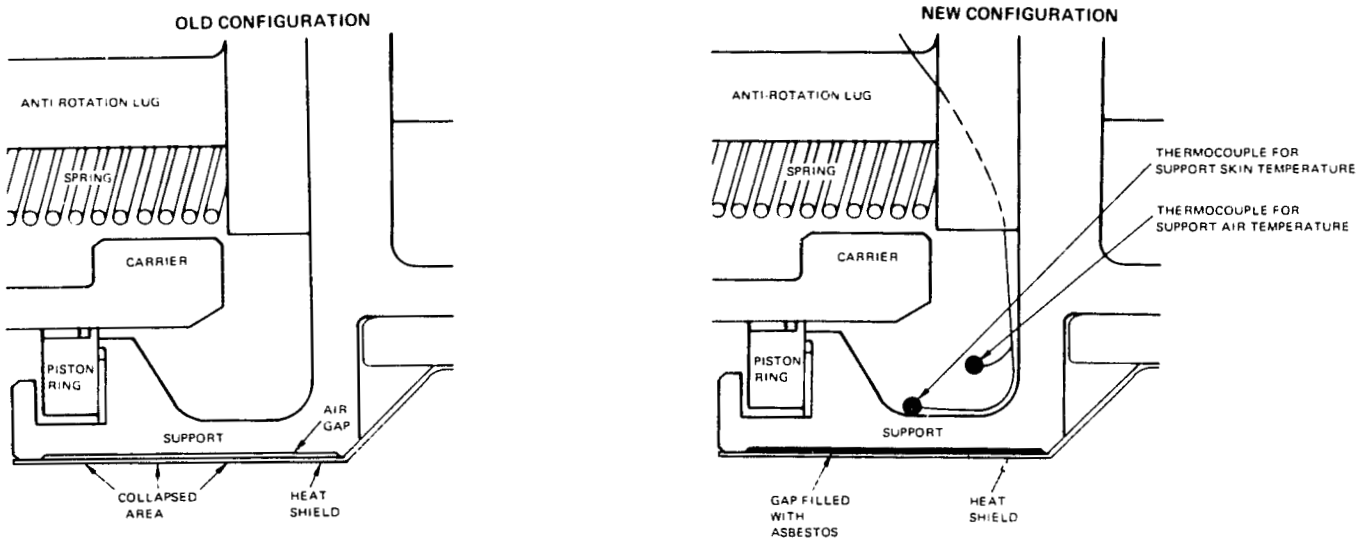

Figure 77 Asbestos Insulation and Thermocouples Added Near the Piston Ring in the Wide-Pad Seal

The air leakage during each of the four five-hour endurance tests decreased with time. Tabulated below are the average leakages and final leakages from each test run:

Time (hrs)	Average Air Leakage (scfm)	Final Air Leakage (scfm)
5	22.4	20.5
5	15.7	14.5
5	26.2	24.5
5	26.0	23.7

The air leakage results from the final five-hour test are presented in Figure 78, along with air temperature, skin temperature of the piston-ring support, and air temperature at the low-pressure side of the piston ring. The decrease in air leakage was judged to be due in part to a decrease in piston-ring leakage, evidenced by the temperature decrease in the secondary-seal area. Apparently the piston ring seal was wearing in at each endurance test condition, although the amount of wear in each case was extremely small.

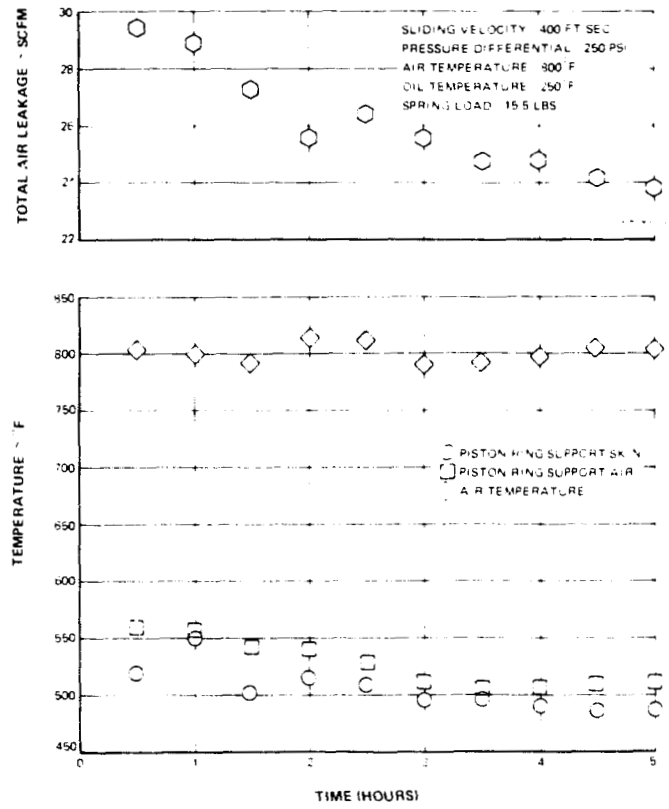

Figure 78 Air Leakage and Temperature Data from Build 2 of the Wide-Pad Seal

One further test run was attempted with the Build 2 seal, but it was found that vibration had increased significantly at all speeds since the previous run. Testing was discontinued after 2.4 hours, making a total accumulated time for Builds 1 and 2 of 94.8 hours.

After the rig was removed from the test stand, visual inspection showed that the nosepiece, carrier, and piston ring were in good condition. However, the seal seat axial runout had increased from a pretest value of 0.8 mil to a post-test value of 1.5 mils, and the rotor was found to be unbalanced by 1.5 oz-in. Previous experience with the test rig had indicated that this would be enough to cause severe vibration problems.

D. ELEVATED TEMPERATURE TESTING - BUILD 3

The most likely reason for the increase in imbalance experienced during Build 2 testing was that the hub components had shifted with respect to the rotor, and that the most likely component to have a major effect on the imbalance was the 8-pound seal seat. For Build 3 the seat was relapped and reinstalled on the rotor, and the rotor was dynamically balanced with-

in 0.2 oz-in. After the rotor was reinstalled on the test rig the axial runout on the seal seat was found to be 0.8 mil. Brief room temperature testing indicated that the rig vibration level was considerably lower than had been encountered in the last Build 2 test.

In order to reduce the leakage past the primary seal and to increase the gas-film stiffness the spring load on the test seal was increased from 15 to 25 pounds. Endurance testing was completed at the following conditions:

Time (hrs)	Sliding Speed (ft/sec)	Seal Pressure (psi)	Air Temperature (°F)	Actual Total Air Leakage (scfm)	Air Leakage Calculated From Design Curves (scfm) Primary + Secondary = Total
1	350	300	800	43.5	8.5 + 6.4 = 14.9
0.5	400	300	800	43.5	10.2 + 6.4 = 16.6
1	500	300	800	44.1	14.1 + 6.4 = 20.5

Operation at all conditions was stable, but the observed air leakage was considerably higher than either the calculated values or the earlier observed air leakages at similar sliding speeds and pressure differentials. Subsequent inspection of the seal indicated that thermal coning of the seal support structure had rolled the carbon piston ring, causing excessive leakage past the secondary seal. The uneven wear caused by rolling the ring can be clearly seen by comparing a pretest profile trace of the ring (Figure 79) with a post-test tract (Figure 80). To keep the support from rolling the piston ring, 0.005 inch of material was removed from the support as shown in Figure 81.

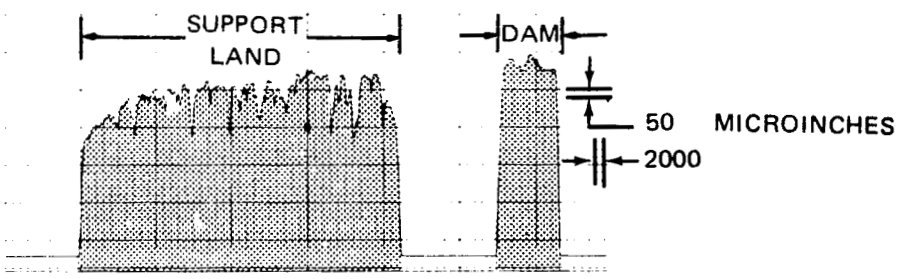

Figure 79 Representative Profile Trace Across the Carbon Piston Ring from Build 3 of the Wide-Pad Seal Before Testing

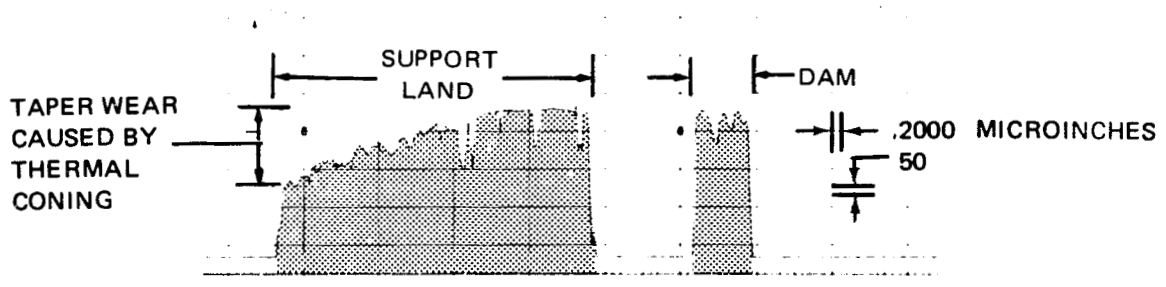

Figure 80 Representative Profile Trace Across the Carbon Piston Ring from Build 3 of the Wide-Pad Seal After 2.5 Hours of Testing

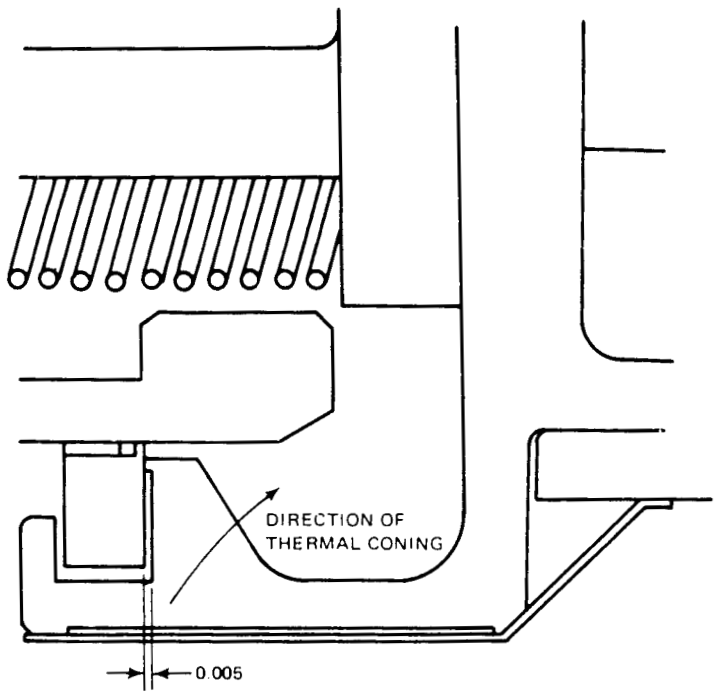

Figure 81 Revised Piston-Ring Support to Prevent Thermal Coning

E. ELEVATED TEMPERATURE TESTING - BUILD 4

A new carbon piston ring was installed for Build 4 and testing was completed at the following conditions:

Time (hrs)	Sliding Speed (ft/sec)	Seal Pressure (psi)	Air Temperature (°F)	Actual Total Air Leakage (scfm)	Air Leakage Calculated From Design Curves (scfm) Primary + Secondary = Total
5	400	200	800	18.0	4.8 + 4.3 = 9.1
5	400	200	1000	13.0	4.8 + 4.0 = 8.8
1	450	200	1000	18.0	6.0 + 4.0 = 10.0
1	500	200	1000	19.0	7.2 + 4.0 = 11.1
Testing interrupted for inspection of seal					
1.7	500	300	1200	25.5	13.3 + 5.7 = 19.0

All tests were conducted with an oil-in temperature of 250°F.

The actual leakages observed in Build 4 were much closer to the predicted values than was the case in Build 3, indicating that the relief cut in the piston-ring support was preventing the support from rolling the piston ring. The inspection after the 12th hour of testing showed that the seal nosepiece, seal seat, and piston ring were in good condition.

The Build 4 seal was reinstalled in the rig and the last Build 4 test took place at the maximum contract conditions. Testing was terminated after 1.7 hours when the air supply line burst at the electric air heater. Post-test inspection of the seal revealed that the seal dam on the nosepiece had worn about 0.3 mil and the Rayleigh pads had worn about 0.08 mil. As shown in Figure 82, wear on the carbon piston ring was much more uniform than it had been in Build 3. The severe wear on the seal dam was attributed to the rapid loss of air pressure and subsequent rapid shutdown when the air line broke.

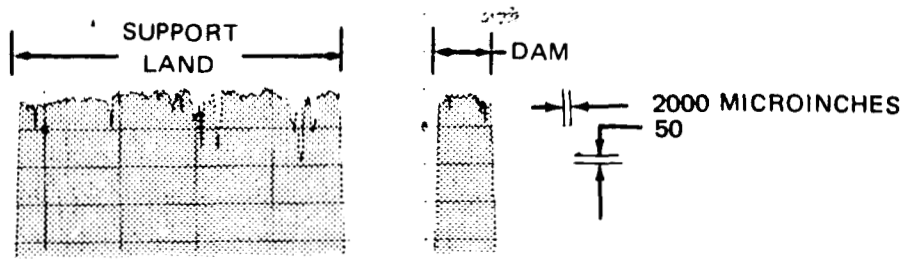

Figure 82 Representative Profile Trace Across the Carbon Piston Ring from Build 4 of the Wide-Pad Seal After 14.7 Hours of Testing

F. ELEVATED TEMPERATURE TESTING - BUILD 5

Before testing the Build 5 seal, the test rig was checked for possible damage from the rapid shutdown at the end of the Build 4 testing. Operation at the maximum sliding speed of 500 ft/sec requires a shaft speed of 17,300 rpm, and the maximum pressure differential of 300 psi results in a thrust load of 10,300 pounds on the thrust bearings. When the air line broke loss of pressure resulted in complete loss of the thrust load on the thrust bearing. The checkout revealed no damage to the rig.

A spare carbon nosepiece was used for Build 5, and testing was completed at the following conditions:

Time (hrs)	Sliding Speed (ft/sec)	Seal Pressure (psi)	Air Temperature (°F)	Actual Total Air Leakage (scfm)	Air Leakage Calculated From Design Curves (scfm) Primary + Secondary = Total
20	425	110	800	4.8	1.8 + 2.4 = 4.2
15	425	200	800	14.5	5.6 + 4.3 = 9.9
5	425	250	800	19.1	8.0 + 5.3 = 13.3

After the 49 hours of Build 5 testing the seal assembly was removed from the test rig for inspection. Profile traces were taken across the surface of the carbon nosepiece and the carbon piston ring. By comparing Figures 83 and 84, it can be seen that the nosepiece had worn less than 0.05 mil. The sealing dam on the nosepiece was slightly scored, with some scratches as deep as 0.5 mil.

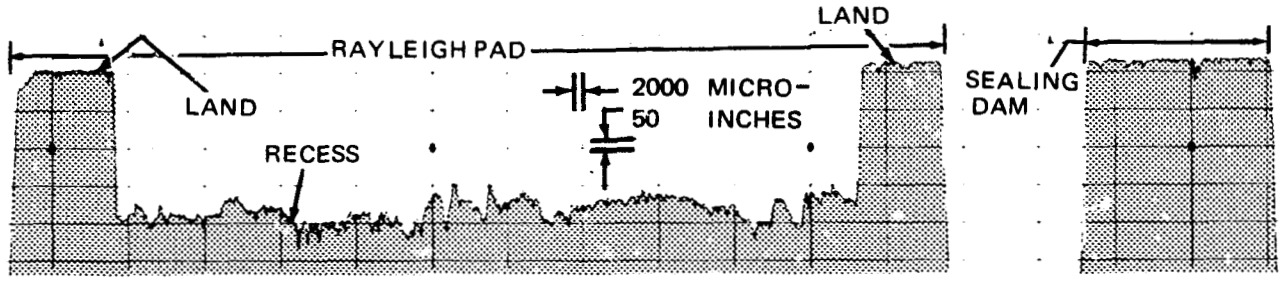

Figure 83 Representative Profile Trace Taken Radially Across the Nosepiece of the Build 5 Wide-Pad Seal Before Testing

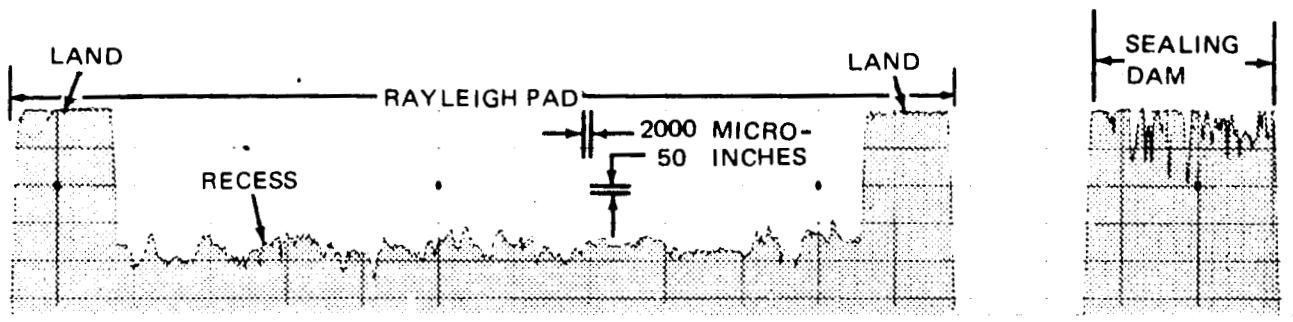

Figure 84 Representative Profile Trace Taken Radially Across the Nosepiece of the Build 5 Wide-Pad Seal After 49.0 Hours of Testing. Same Location as Figure 83.

The piston ring had been previously used in Build 4, and had accumulated a total test time of 75.3 hours. Its support lands showed uneven wear, with tapers up to 0.25 mil across the support lands. A profile trace of the piston ring is shown in Figure 85. The dam on the piston ring had localized wear areas every 12°, corresponding to the locations of the 15 vent grooves and the centers of the 15 support lands. At some of these locations the height of the dam was reduced as much as 0.25 mil, while the width of the dam (12 to 15 mils) was reduced by 7 to 10 mils.

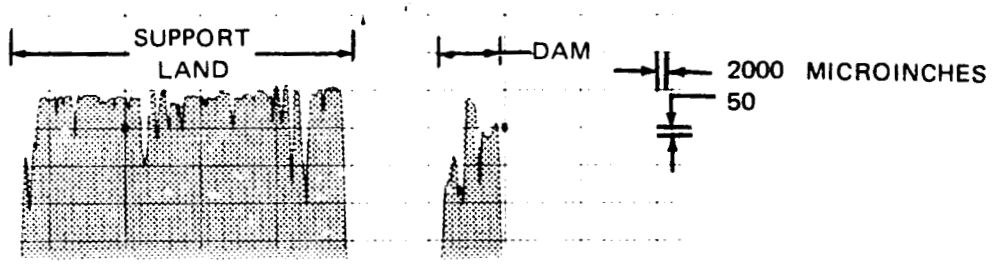

Figure 85 Representative Profile Trace Across the Carbon Piston Ring from Build 5 of the Wide-Pad Seal. Total Time on Piston Ring: 75.3 Hours

Axial profile traces of the carrier bore in the area contacted by the carbon piston ring did not reveal any wear. The carrier is made of TZM and coated with Al_2O_3. However, a circumferential trace of the carrier bore revealed that the surface had four lobes. The difference between maximum and minimum diameters was 1.4 mils. The out-of-roundness was from the manufacturing process and not from test operation. The carrier bore surface was reground and the difference between the maximum and minimum diameters was reduced to 1.1 mils.

G. ELEVATED TEMPERATURE TESTING - BUILD 6

The test seal for Build 6 was the same as that used in Build 5 except for the carbon piston ring. The ring from Build 3 was used in Build 6, since it was in better condition than the ring used in Builds 4 and 5. The Build 6 seal was tested at the following conditions:

Time (hrs)	Sliding Speed (ft/sec)	Seal Pressure (psi)	Air Temperature (°F)	Actual Total Air Leakage (scfm)	Air Leakage Calculated From Design Curves (scfm) Primary + Secondary = Total
1.0	500	300	1000	25.6	13.8 + 6.0 = 19.8
2.0	475	300	1000	24.0	13.1 + 6.0 = 19.1
2.0	450	300	1000	23.7	12.4 + 6.0 = 18.4
2.0	425	300	1000	21.2	11.0 + 6.0 = 17.0
4.0	400	300	1000	22.0	10.1 + 6.0 = 16.1
0.5	500	250	1000	24.9	10.4 + 4.9 = 15.3
0.5	500	300	1000	30.2	13.8 + 6.0 = 19.8
1.75	450	250	1000	32.8	8.8 + 4.9 = 13.7

Testing was abruptly terminated at the last condition when a fitting on the air supply line split. The leakage at the last three conditions, which was higher than anticipated was probably caused by leakage at the fitting before it broke completely.

Inspection after the tests revealed that the Rayleigh pad lands on the nosepiece had worn less than 0.05 mil, while the primary seal dam was slightly tapered, with the outer edge 0.05 mil lower than the inner edge (see Figure 86). The sealing dam on the nosepiece was slightly more scratched than it had been at the end of Build 5 testing: the depth of some scratches had increased to 0.8 mil from 0.5 mil.

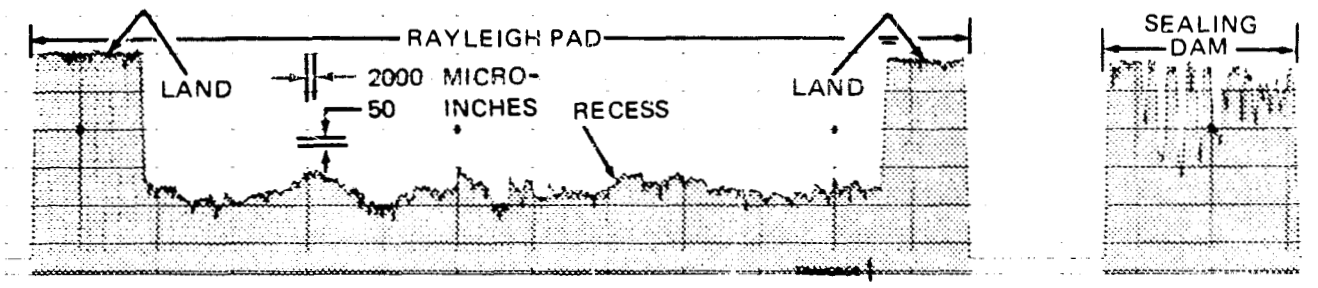

Figure 86 Representative Profile Trace Taken Radially Across the Nosepiece of the Build 6 Wide-Pad Seal. Total Time on Nosepiece: 70.3 Hours

The wear pattern on the carbon piston ring was similar to the wear observed in Build 5, but more severe. Localized wear on the piston-ring dam was as deep as 0.75 mil, while the taper on the support lands was as much as 0.4 mil. A profile trace taken at a point of maximum dam wear is shown in Figure 87. The total time on the piston ring at the time the trace was taken was 27.3 hours, 6.0 hours from Build 3 and 21.3 hours from Build 6.

H. ELEVATED TEMPERATURE TESTING - BUILD 7

The Build 7 seal was reassembled with a new carbon piston ring supplied by NASA. This ring was similar to that shown in Figure 76 except the support land was only 1/3 as wide. Endurance testing on Build 7 was completed at the following conditions:

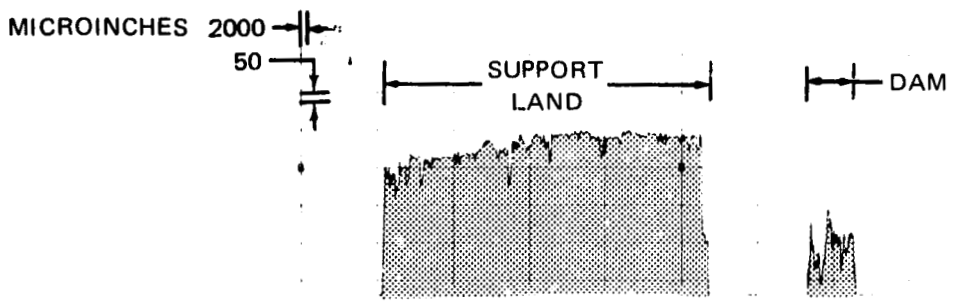

Figure 87 Profile Trace Across a Point of Maximum Wear on the Carbon Piston Ring from Build 6 of the Wide-Pad Seal. Total Time on Piston Ring (Build 3 and Build 6): 27.3 Hours

Time (hrs)	Sliding Speed (ft/sec)	Seal Pressure (psi)	Air Temperature (°F)	Actual Total Air Leakage (scfm)	Air Leakage Calculated From Design Curves (scfm) Primary + Secondary = Total
1.0	350	150	1000	9.3	2.4 + 2.9 = 5.3
1.0	400	200	1000	16.0	4.8 + 4.0 = 8.8
1.0	500	300	1200	23.8	13.3 + 5.7 = 19.0
1.25	400	200	1000	14.4	4.8 + 4.0 = 8.8
2.0	400	200	600	18.7	4.9 + 4.7 = 9.6
17.0	400	200	800	17.4	4.8 + 4.3 = 9.1

The oil-in temperature for all of these tests was kept at 250°F.

Post-test inspection revealed that the seal seat and nosepiece were in good condition. Profile traces of the carbon nosepiece showed that wear was less than 0.1 mil for the 103.8 hours of testing it had endured. A typical profile trace is shown in Figure 88. The scratches on the seal dam of the nosepiece had deepened to about 1.0 mil from the 0.8 mil-deep scratches found after Build 6 testing. The carbon piston ring had a 40-mil long piece missing from the 12-mil wide seal dam. Examination indicated that the piece had chipped out during either assembly or testing. A typical profile trace of the piston ring (not at the chip location) is shown in Figure 89. A photograph of the seal assembly is shown in Figure 90. Note the excellent appearance of all the Rayleigh pads. A close-up of the pads is shown in Figure 91.

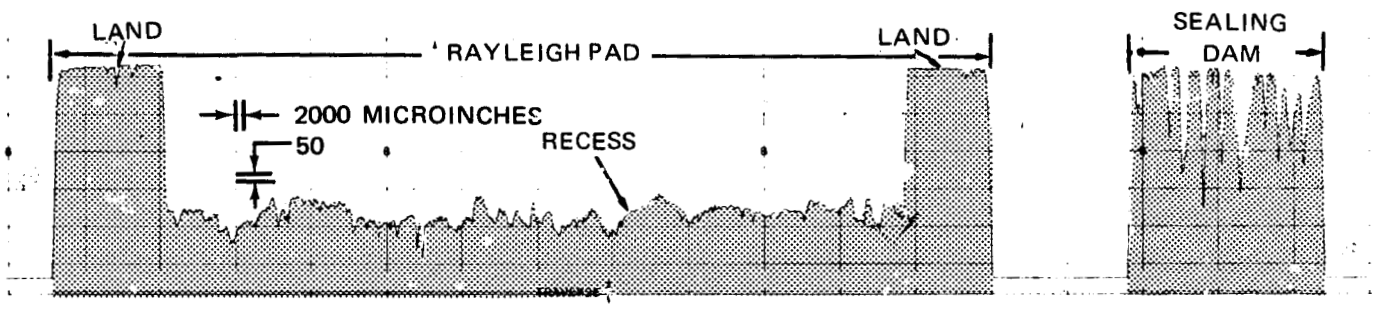

Figure 88 Representative Profile Trace Taken Radially Across the Nosepiece of the Build 7 Wide-Pad Seal. Total Time on Nosepiece: 103.8 Hours

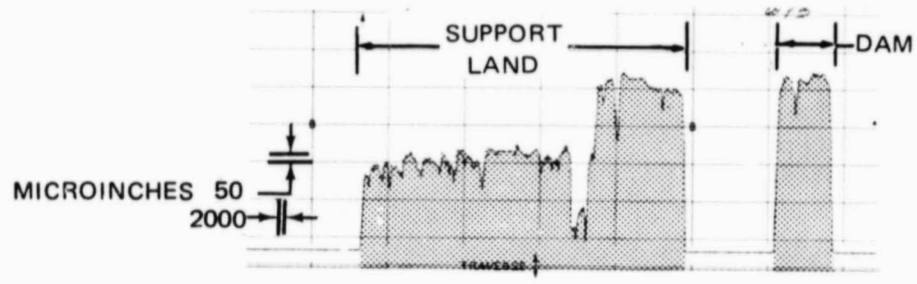

Figure 89 Representative Profile Trace Across the Carbon Piston Ring from Build 7 of the Wide-Pad Seal. Total Time on Piston Ring: 23.25 Hours

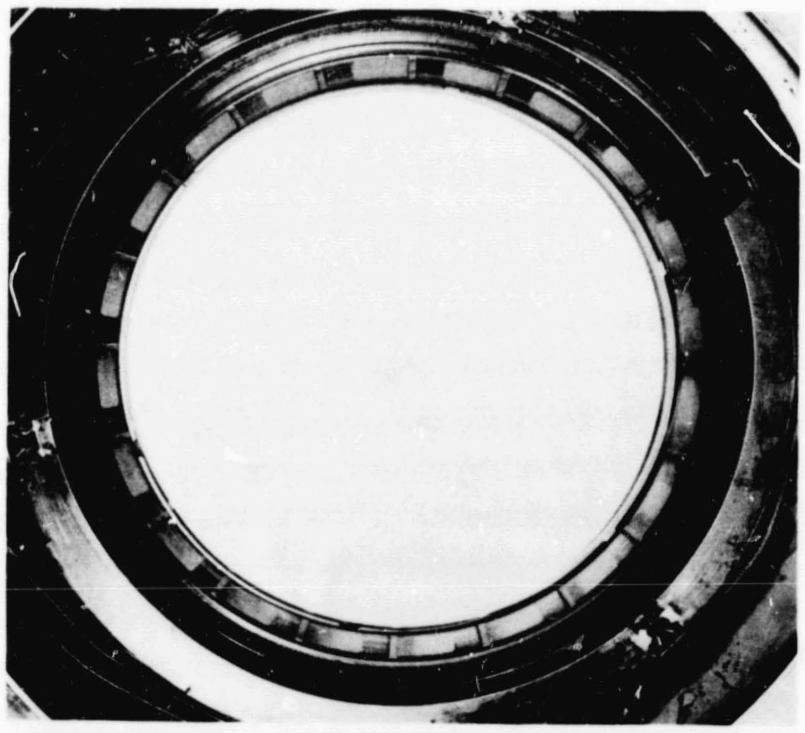

Figure 90 Nosepiece from the Wide-Pad Seal After Build 7 Testing (CN-30942)

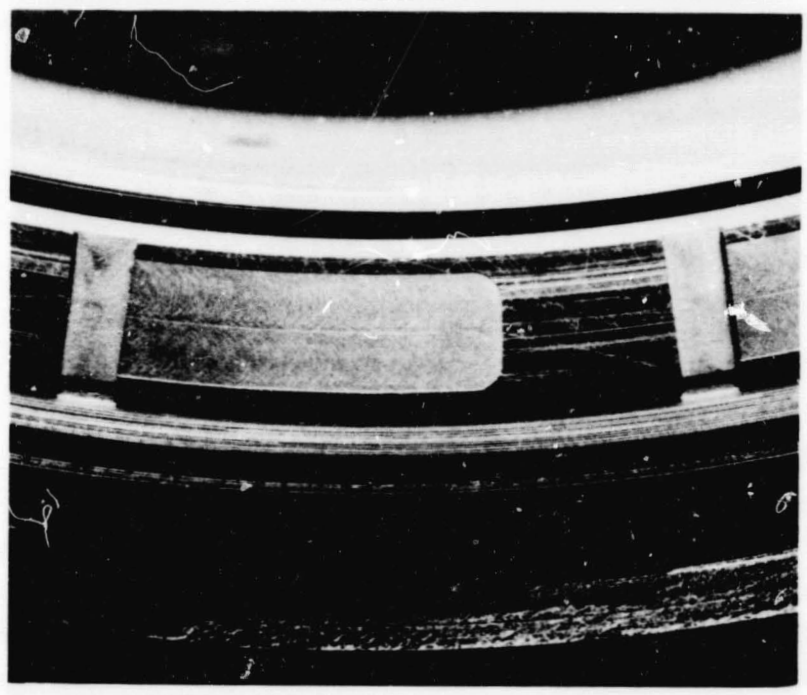

Figure 91 Close-Up of the Nosepiece from the Wide-Pad Seal After Build 7 Testing. Note Original Lapping Marks on Pad Surface.

(CN-30944)

I. ELEVATED TEMPERATURE TESTING - BUILD 8

Build 8 of the wide-pad seal was reassembled with a new piston ring made of a new high-temperature carbon. Build 8 testing was completed at the following conditions:

Time (hrs)	Sliding Speed (ft/sec)	Seal Pressure (psi)	Air Temperature (°F)	Actual Total Air Leakage (scfm)	Calculated Air Leakage (scfm) Primary + Secondary = Total
5	500	200	1000	25.4	7.2 + 4.0 = 11.2
5	400	200	1000	19.1	4.8 + 4.0 = 8.8
5	500	300	1000	38.4	13.8 + 6.0 = 19.8
5	400	300	1000	31.5	10.1 + 6.0 = 16.1

Inspection of the seal assembly after the test revealed that the sealing dam on the piston ring was undersize, causing additional leakage past the secondary seal. As shown in Figure 92, the sealing dam height was 0.5 mil less than the support land height, causing a 0.5-mil hole around the circumference. As a result of the additional leakage path, the seal support temperatures during the Build 8 testing were 65°F hotter than the Build 7 temperatures for similar test conditions. It should be noted, however, that the high-temperature carbon used in this piston ring appeared to be in much better condition after the Build 8 test than the other piston rings did after comparable amounts of testing. A photograph of the piston ring after the 20 hours of steady-state elevated-temperature testing is shown in Figure 93.

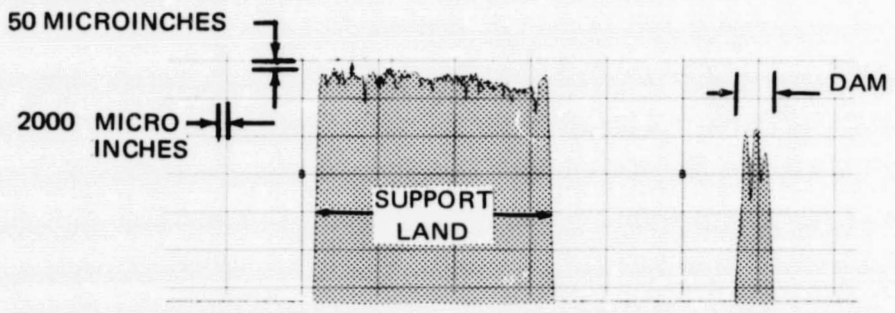

Figure 92 Representative Profile Trace Across the High-Temperature Carbon Piston Ring from Build 8 of the Wide-Pad Seal After 20 Hours of Testing

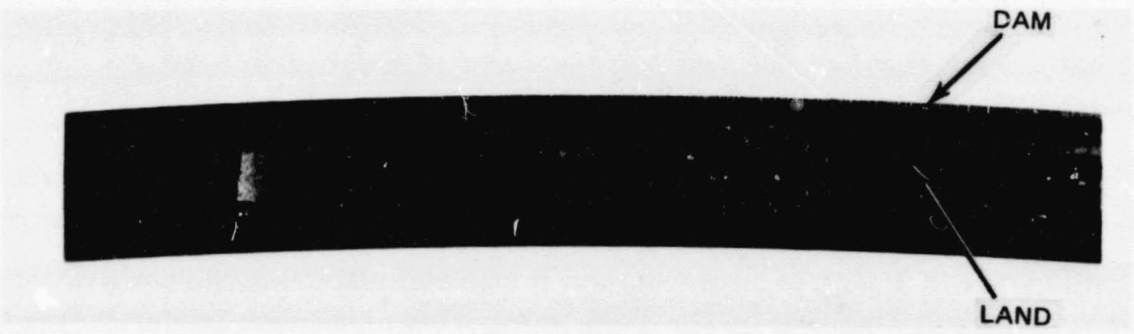

Figure 93 Close-Up of the High-Temperature Carbon Piston Ring from Build 8 of the Wide-Pad Seal After 20 Hours of Testing (CN-31175)

J. ELEVATED TEMPERATURE TESTING - BUILD 9

The wide-pad seal was reassembled with a TZM piston ring for Build 9. The chrome coating which had been flashed on the ring was etched off, leaving the base material exposed. The aluminum oxide coating was left on the carrier bore. Build 9 was tested at the following conditions:

Time (hrs)	Sliding Speed (ft/sec)	Seal Pressure (psi)	Air Temperature (°F)	Actual Total Air Leakage (scfm)	Calculated Air Leakage (scfm) Primary + Secondary = Total
17.25	400	200	1000	25.5	4.8 + 4.0 = 8.8
7.00	400	200	1200	20	4.9 + 3.8 = 8.7

The leakage remained about 19.1 scfm for the first 5.5 hours of testing at the last condition. At that time an electrical power failure caused the air supply to be shut off, so the rig was shut down. The test was continued after power had been restored, but the air leakage had increased to 25.5 scfm. The increased leakage during the last 1.5 hours was probably caused by wear on the seal dam (see Figure 94). This uneven seal dam wear was similar to that observed in Build 4, where a rapid loss of air pressure had similar, but more severe, results. Experience in Phase II (Reference 3) indicated that rapid rig shutdowns where pressure was maintained on the seal cause no seal damage. However, in both this build and Build 4 of the wide-pad seal, the rapid speed drop was accompanied by a rapid pressure drop and tapered wear was observed in both cases. Evidently the combined drops in pressure, speed, and temperature result in an axial seal seat runout due to the sudden drop in load on the rig thrust bearings as well as distortions due to the thermal gradients in the seal seat and nosepiece. The runout and distortions are apparently greater than that which can be accommodated by the seal design and result in contact between the nosepiece sealing dam and the seal seat.

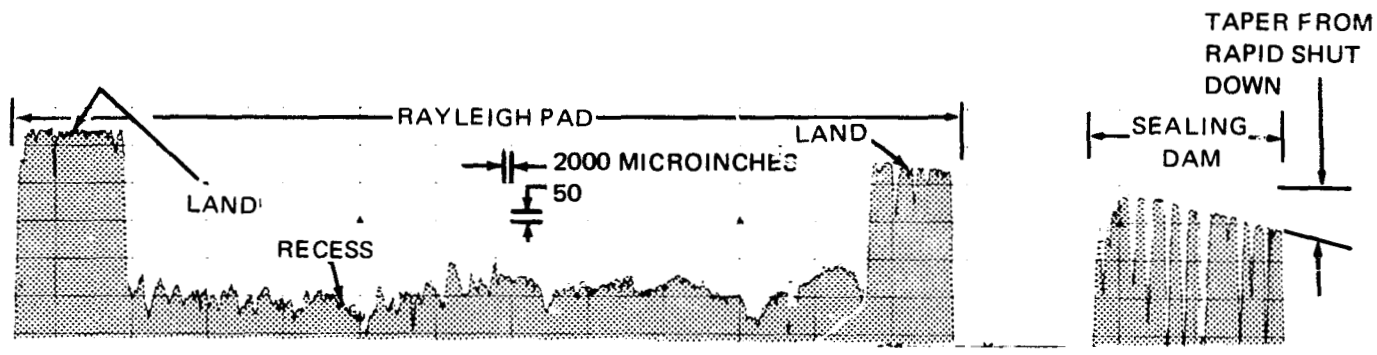

Figure 94 Representative Profile Trace Taken Radially Across the Nosepiece of the Build 9 Wide-Pad Seal. Total Time on Nosepiece: 128 Hours

Visual inspection of the nosepiece, seal seat, and piston ring after testing revealed that all were in good condition. The wear on the TZM piston ring can be seen by comparing the profile traces shown in Figures 94 and 95. Both of these traces were taken at the same location. A profile trace across the nosepiece is shown in Figure 96.

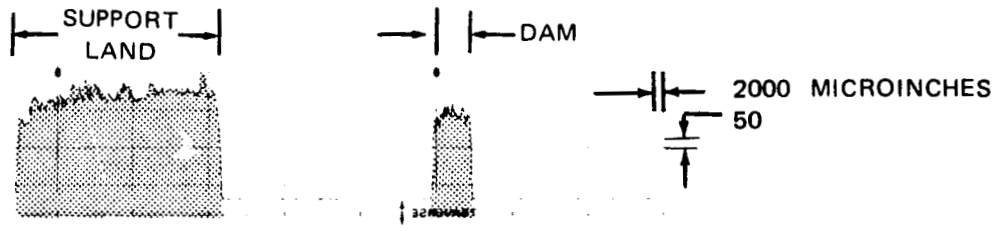

Figure 95 Representative Profile Trace Across the TZM Piston Ring from Build 9 of the Wide-Pad Seal Before Testing

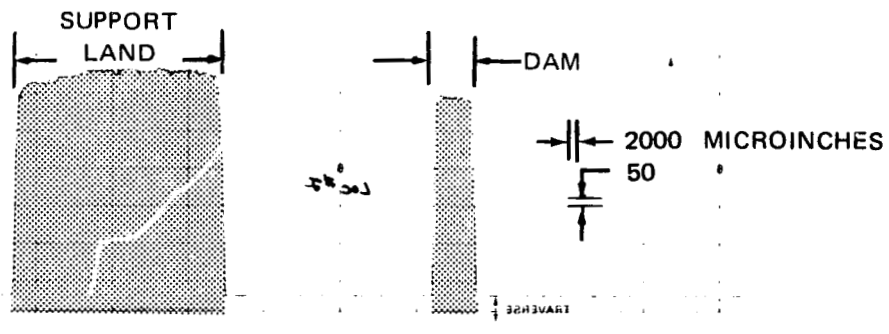

Figure 96 Representative Profile Trace Across the TZM Piston Ring from Build 9 of the Wide-Pad Seal After 24.25 Hours of Testing

Although the piston ring appeared to be in good condition, the support temperatures during Build 9 testing were approximately 115°F higher than those experienced during Build 7 testing at similar conditions. The temperature increase indicated that much of the increased leakage observed during Build 9 was coming through the piston ring secondary seal.

SECTION VII
EXPERIMENTAL EVALUATION OF THE REVISED NARROW-PAD SEAL

The revised narrow-pad seal is described in Section III of this report, and a layout of the seal is shown in Figure 7. Briefly, the revised narrow-pad seal was created by modifying the narrow-pad seal; the revisions were confined to increasing the width of the Rayleigh pads from 0.125 inch to 0.188 inch, increasing the width of the seal dam from 0.025 inch to 0.050 inch, and increasing the width of the piston ring seal dam from 12 mils to 27 mils. A photograph of the nosepiece before testing is shown in Figure 97.

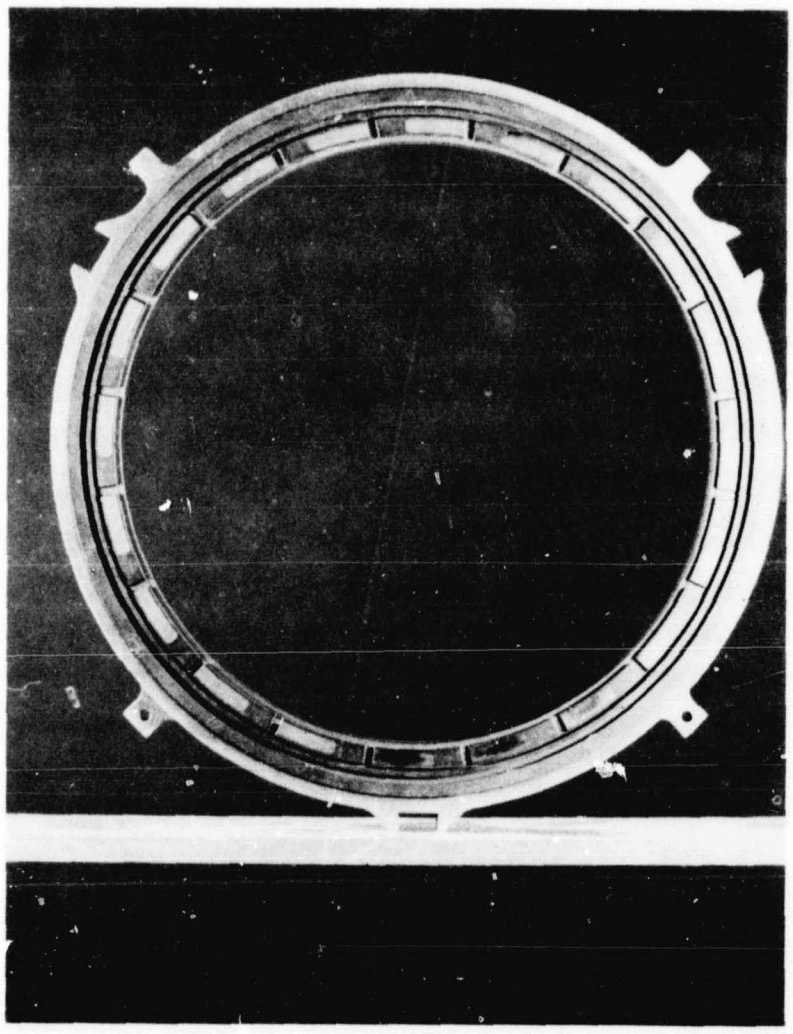

Figure 97 Carbon Nosepiece of the Revised Narrow-Pad Seal Before Testing (CN-31173)

The increase in pad width provided the seal with load capacity and stiffness levels which were midway between those of the narrow-pad and the wide-pad seals. The increased load capacity reduced the seal's sensitivity to force balance variations (particularly at elevated pressures) while the increased stiffness reduced the seal's sensitivity to seal seat runout at high speeds. Other geometric features of the pads were unchanged, since similar optimization principles apply to all three designs.

The width of the seal dam was increased to 0.050 inch because experience indicated that seal performance was too sensitive to edge chipping and deterioration of the seal dam surface when a narrow dam was used. The new width was the same as that used in the wide-pad and ceramic seals.

The width of the piston-ring dam was increased to 27 mils in order to reduce secondary seal leakage. A wider dam was expected to reduce leakage past the piston-ring secondary seal by decreasing the film thickness of the leakage path as well as increasing its length. The reduced film thickness resulted from the increased seating loads produced by the wider seal dam. The increased piston-ring conformity available from the use of graphite carbon (which has a low elastic modulus) was also a factor in designing for lower secondary-seal leakage. Carbon also has a lower coefficient of friction, which made it possible to increase seating loads without increasing piston-ring friction to the extent that it would degrade seal performance.

Just one build of the revised narrow-pad seal was required for the entire test program, which included a preliminary dynamic checkout and extensive endurance testing. The endurance tests were generally quite successful, but there was some performance deterioration after the test points at high speeds and high air temperatures were run. A total of 119.8 test hours were accumulated on this seal.

A. PRELIMINARY DYNAMIC TESTING – BUILD 1

The seal was assembled with a spring load of 15.4 pounds and subjected to 6.8 hours of preliminary dynamic testing with unheated air. These tests were performed at sliding speeds up to 450 ft/sec (15,630 rpm) and pressure differentials up to 300 psi, and demonstrated a distinct performance improvement over the narrow-pad seal. Air leakage data from the preliminary dynamic checkout is shown in Figure 98. Total air leakage is the sum of air leakage past the primary and secondary seals. The static leakage can be assumed to represent piston-ring leakage, and indicates that significant leakage improvement was brought about by the increased piston-ring dam width (compare Figure 98 with Figures 61, 63, 65, and 68). The dynamic air leakage indicates that leakage past the primary seal was also improved. The primary leakage was quite low, except for the test points at 450 ft/sec and pressure differentials of 150 psi or less. This speed level was considerably higher than the 360 ft/sec speed limit of the narrow-pad seal. Visual inspection of the nosepiece and seal seat showed that they were in good conditions after the preliminary dynamic checkout.

The extent to which the primary seal leakage deviated from theoretical values is shown for each of the speeds tested in Figures 99 through 102. The dynamic data on these figures indicate that the primary film stiffness increased at high pressures, since seal leakage deviations at 450 ft/sec were controlled by increasing the pressure differential across the seal. Such an increase in film stiffness would be possible only with a uniform decrease in film thickness, probably caused by a seal opening force slightly lower than the nominal design value. At a pressure differential of 300 psi, only an 8-pound reduction in the seal opening force would be sufficient to explain the difference between the calculated and measured air leakages. Much of this reduction might be accounted for by the fact that the seal dam was found to be slightly oval, with its minor diameter 3 mils smaller than its major diameter. The major diameter was equal to the nominal design dimension.

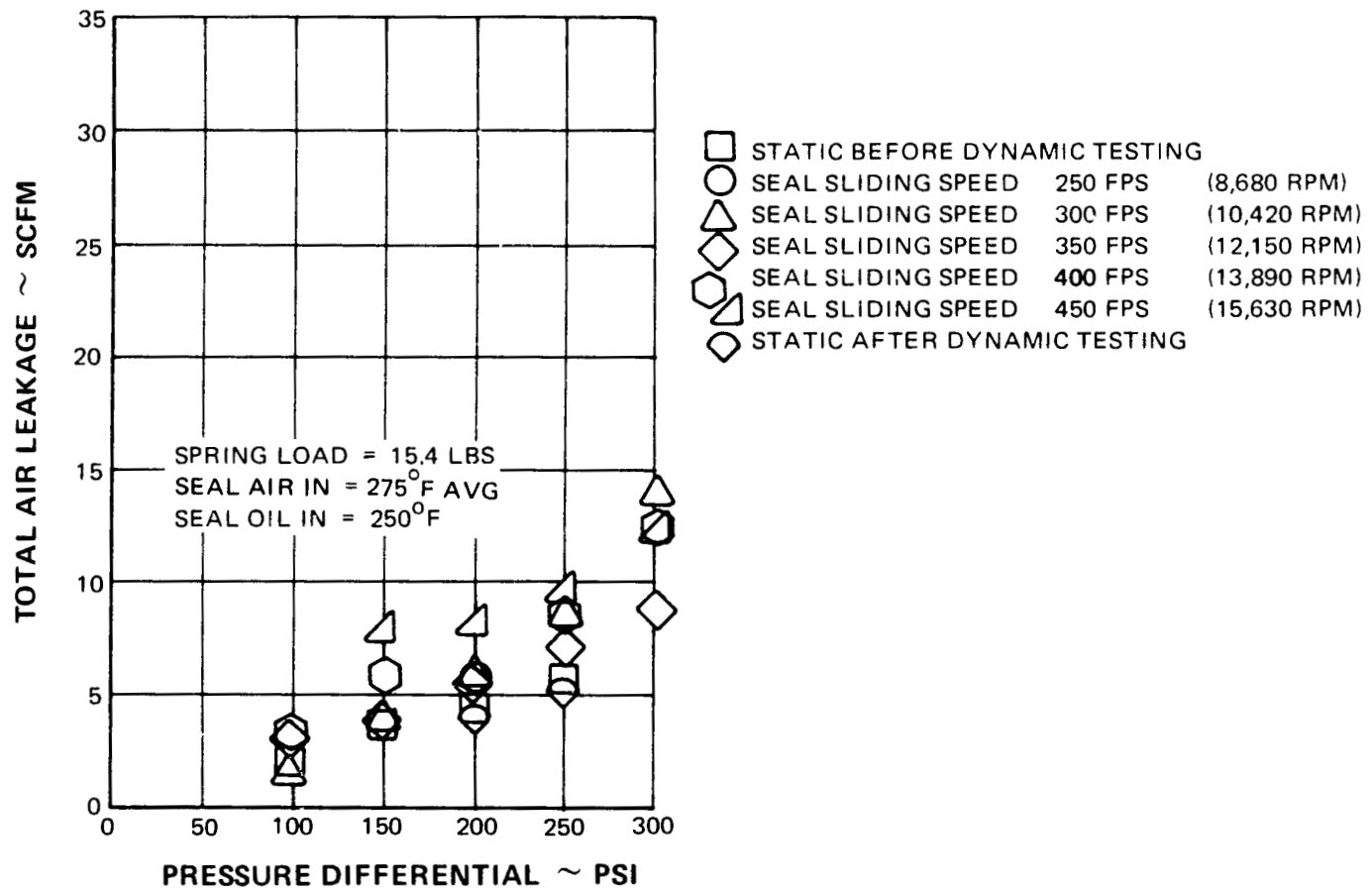

Figure 98 Air Leakage Past Build 1 of the Revised Narrow-Pad Seal

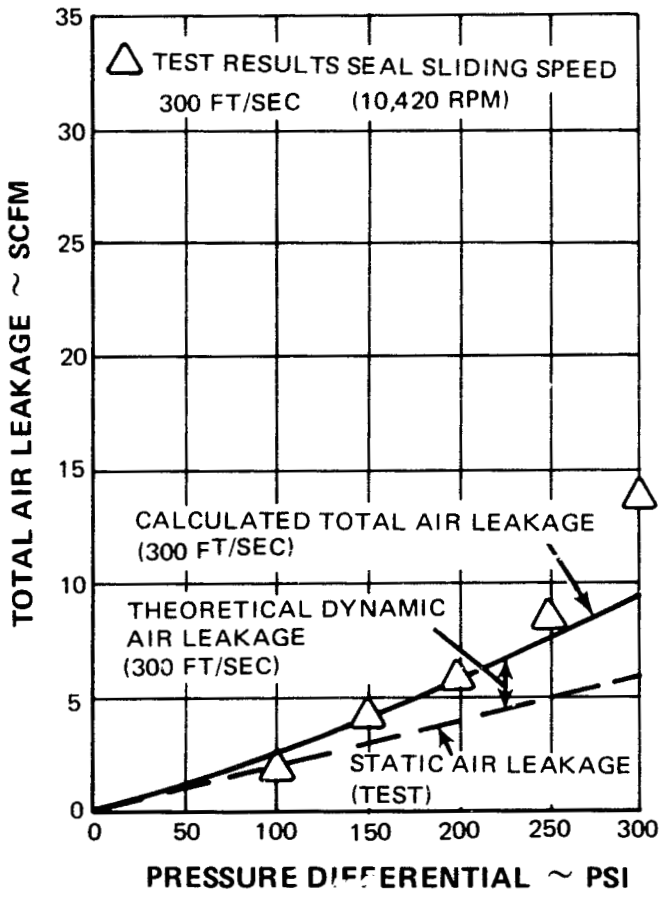

Figure 99 Calculated and Actual Air Leakage Past Build 1 of the Revised Narrow-Pad Seal at a Sliding Speed of 300 ft/sec with Ambient Air

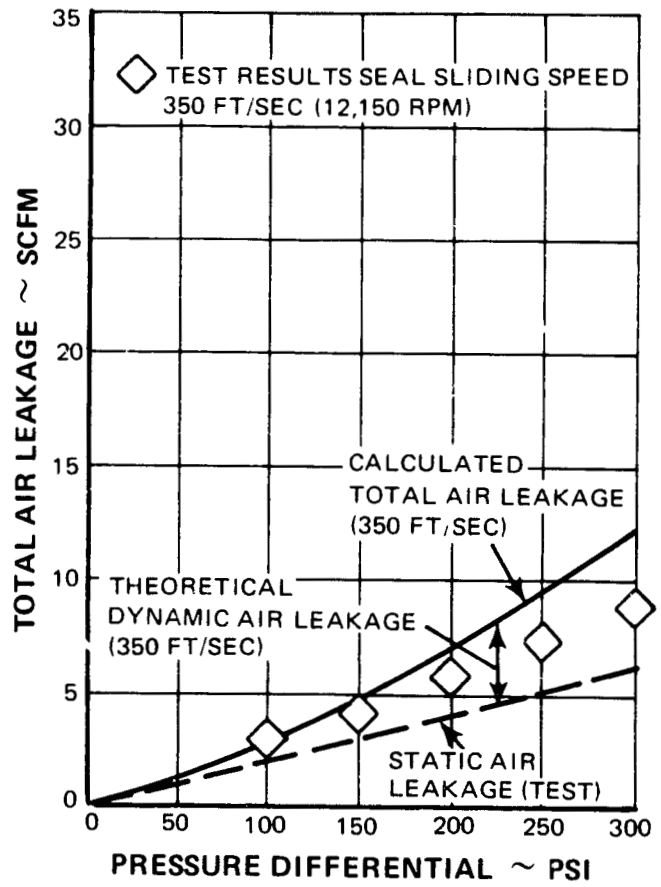

Figure 100 Calculated and Actual Air Leakage Past Build 1 of the Revised Narrow-Pad Seal at a Sliding Speed of 350 ft/sec with Ambient Air

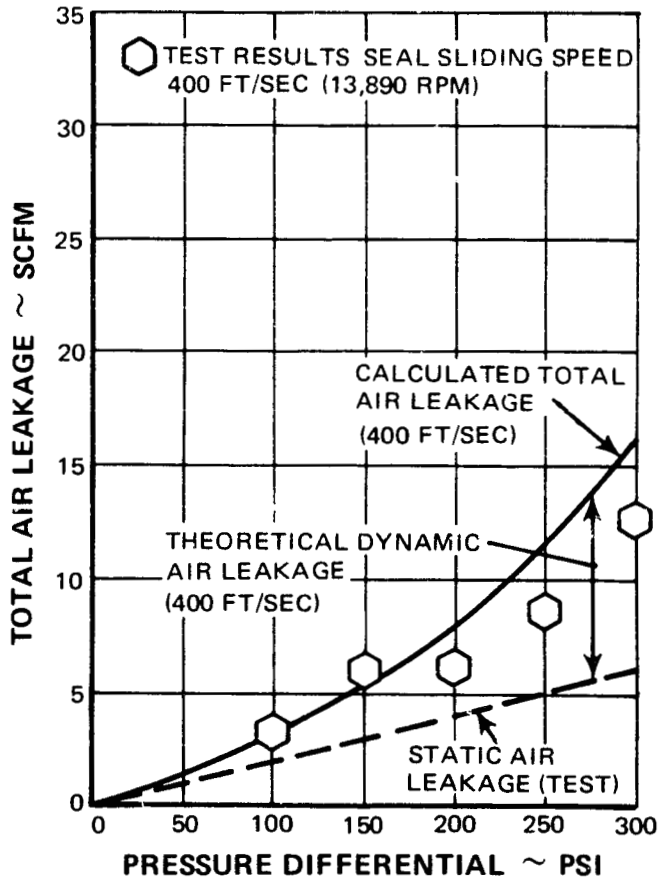

Figure 101 Calculated and Actual Air Leakage Past Build 1 of the Revised Narrow-Pad Seal at a Sliding Speed of 400 ft/sec with Ambient Air

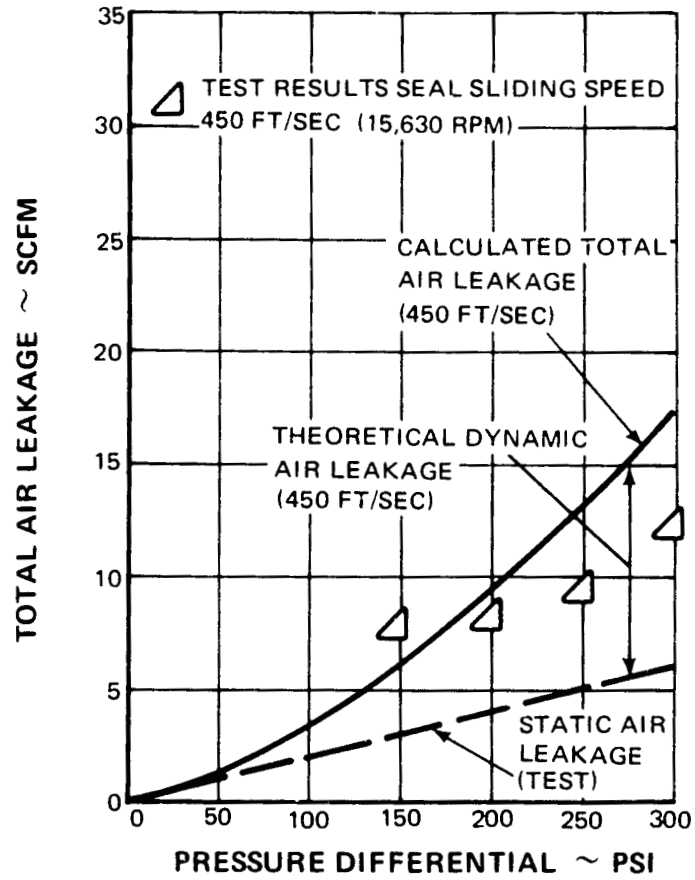

Figure 102 Calculated and Actual Air Leakage Past Build 1 of the Reivsed Narrow-Pad Seal at a Sliding Speed of 450 ft/sec with Ambient Air

B. ENDURANCE TESTING – BUILD 1

After inspection, the revised narrow-pad seal was reinstalled in the test rig for elevated-temperature testing. Endurance tests were completed at the following conditions:

Time (hrs)	Sliding Speed (ft/sec)	Seal Pressure (psi)	Air Temperature (°F)	Actual Total Air Leakage (scfm)	Air Leakage Calculated From Design Curves (scfm) Primary + Secondary = Total
7.5	400	200	600	7.5	3.8 + 3.1 = 6.9
21.5	350	100	600	2.9	0.8 + 1.6 = 2.4
5.0	400	100	600	3.6	1.1 + 1.6 = 2.7
5.0	350	50	600	2.0	0.4 + 0.8 = 1.2
5.0	350	100	400	3.3	0.8 + 1.7 = 2.5
1.0	350	100	250	4.1	0.8 + 1.8 = 2.6
5.0	400	200	1000	9.7	3.8 + 2.8 = 6.6
1.0	350	100	400	4.1	0.8 + 1.7 = 2.5
8.0	400	300	1000	13.0	9.0 + 4.2 = 13.2
7.0	450	200	1200	10.9	4.8 + 2.7 = 7.5
4.3	400	300	1200	14.6	8.8 + 4.0 = 12.8
1.0	500	300	1200	21.7	12.0 + 4.0 = 16.0
3.5	450	200	1200	11.2	4.8 + 2.7 = 7.5
0.7	500	300	1200	24.3	12.0 + 4.0 = 16.0
1.3	400	200	1200	13.8	3.8 + 2.7 = 6.5
7.0	450	200	1200	15.4	4.8 + 2.7 = 7.5

The oil-in temperature for all 83.8 hours of endurance testing was 250°F.

Performance deterioration was observed during the endurance testing at 1200°F. During the second run at 500 ft/sec and 300 psi (the maximum contract conditions), operation was erratic and the test was terminated after 0.7 hours. Leakage during this run ranged from 22.3 to 29.8 scfm. During further testing at other conditions the leakage stabilized, but it was significantly higher than in earlier tests as evidenced by the increased leakage at 450 ft/sec, 200 psi and 1200°F.

After the elevated-temperature testing summarized above, some of the preliminary dynamic check points were rerun to determine the extent of the performance deterioration. The data from these selected check points is presented in Figure 103. The static leakage had increased to approximately three times the initial leakage shown in Figure 98.

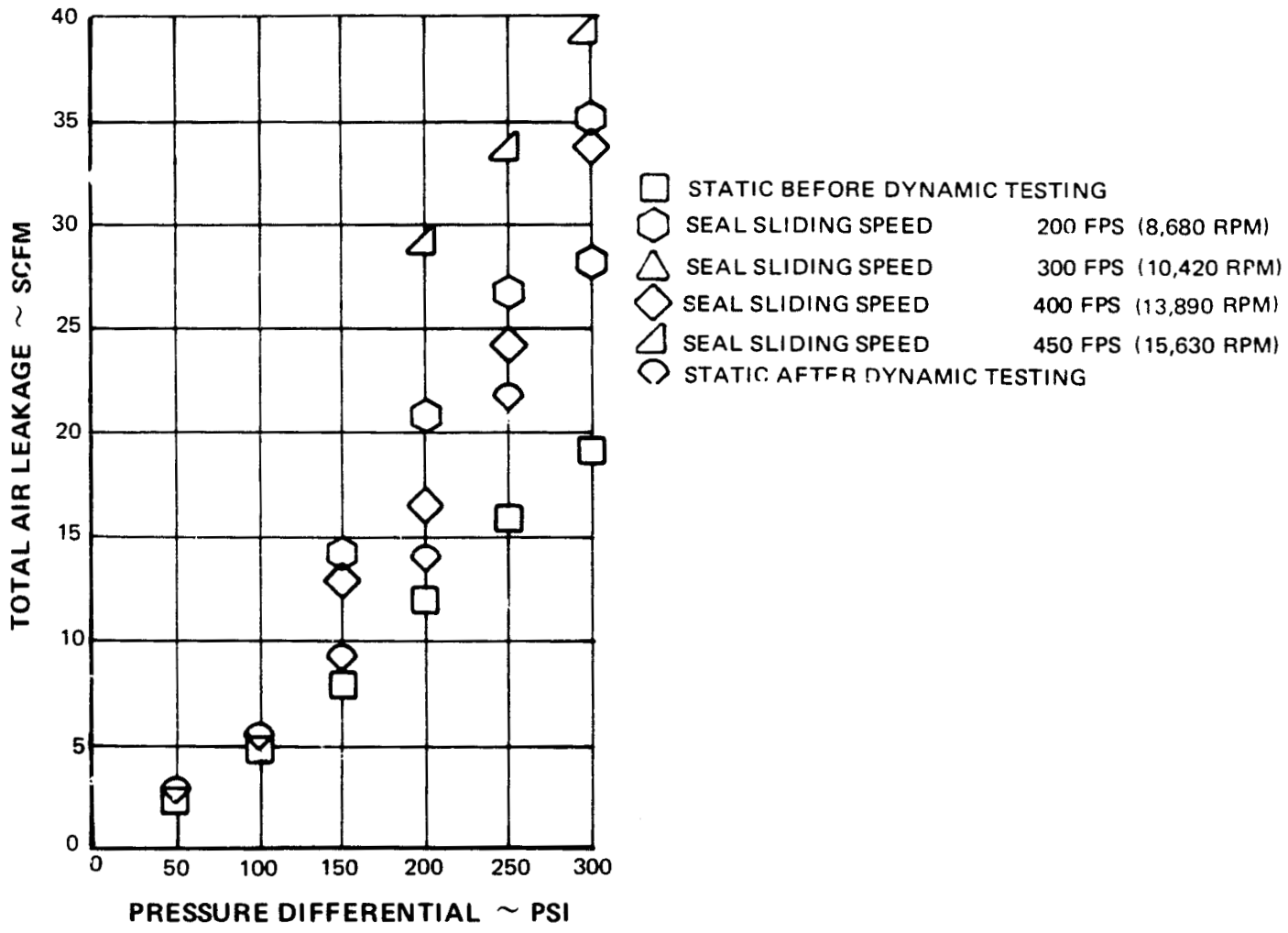

Figure 103 Air Leakage Past Build 1 of the Revised Narrow-Pad Seal with Ambient Air. These Measurements Made After Elevated-Temperature Testing

Following the completion of dynamic testing the seal was removed from the rig for inspection. A comparison of pretest and posttest profile traces (Figures 104 and 105) showed that the Rayleigh pad wear was less than 0.05 mil for the total test time of 119.8 hours. However, the seal dam showed heavy circumferential scratches about 2 mils deep. The seal dam width and height changed very little, with an average wear of only 0.05 mil. Photographs of the seal after testing are shown in Figures 106 and 107.

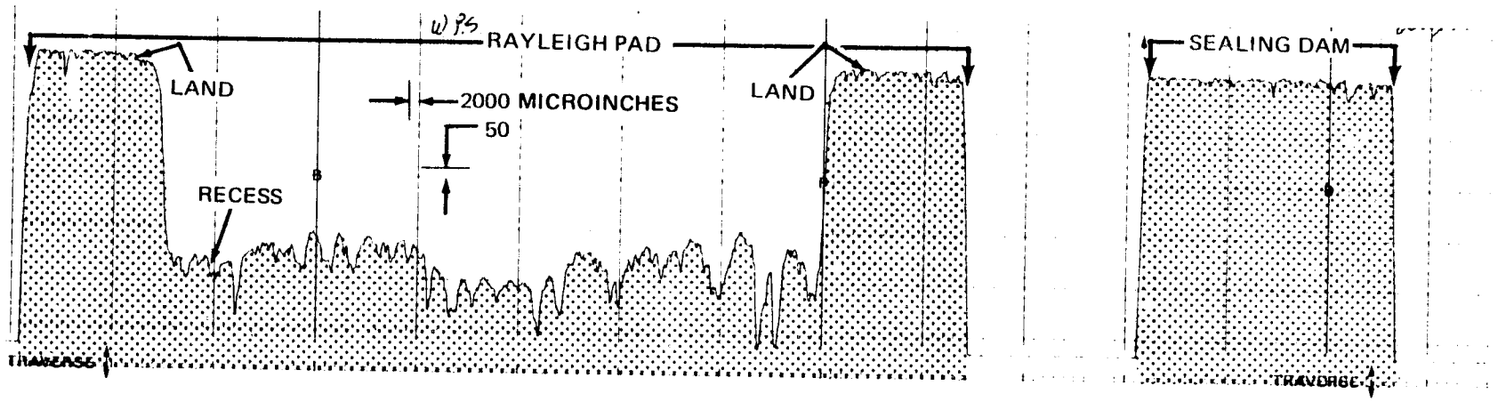

Figure 104 Representative Profile Trace Taken Radially Across the Nosepiece of the Revised Narrow-Pad Seal Before Testing

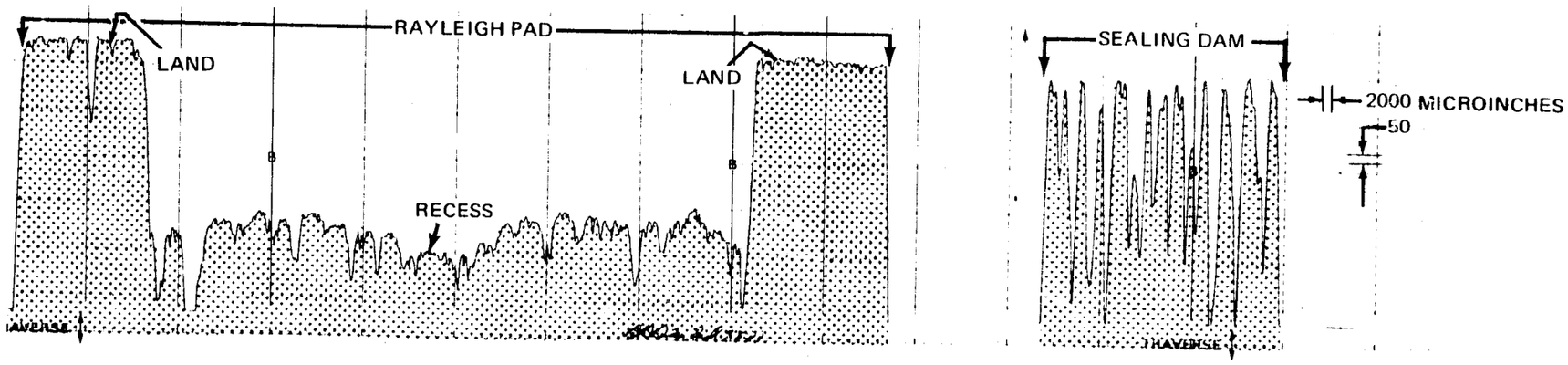

Figure 105 Representative Profile Trace Taken Radially Across the Nosepiece of the Revised Narrow-Pad Seal After Testing

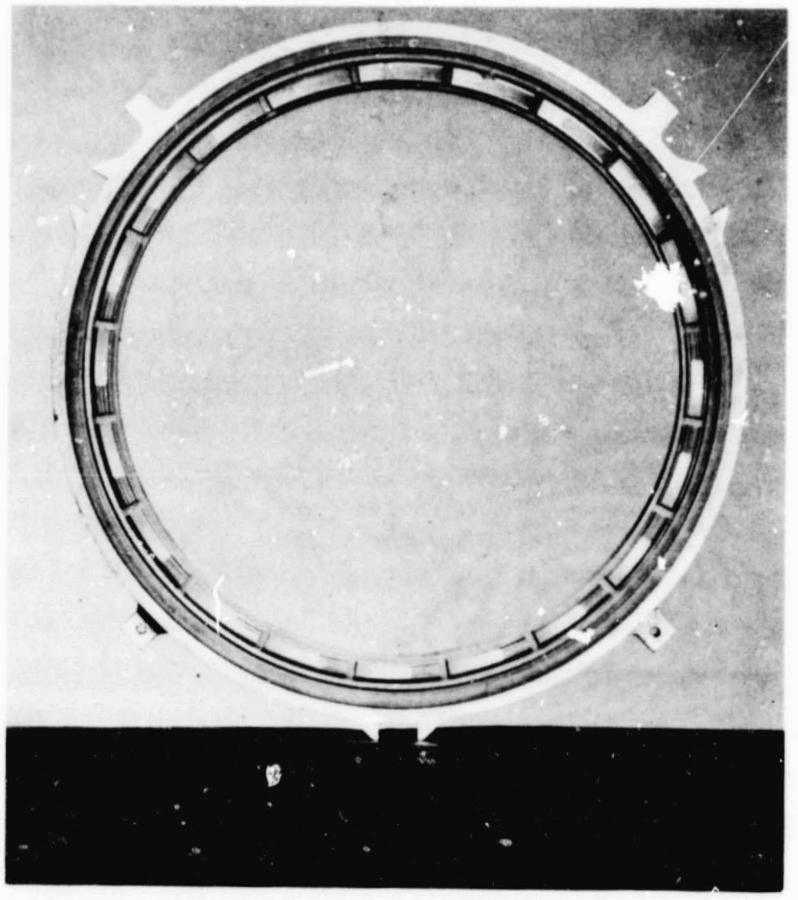

Figure 106 Carbon Nosepiece of the Revised Narrow-Pad Seal After Testing (CN-31506)

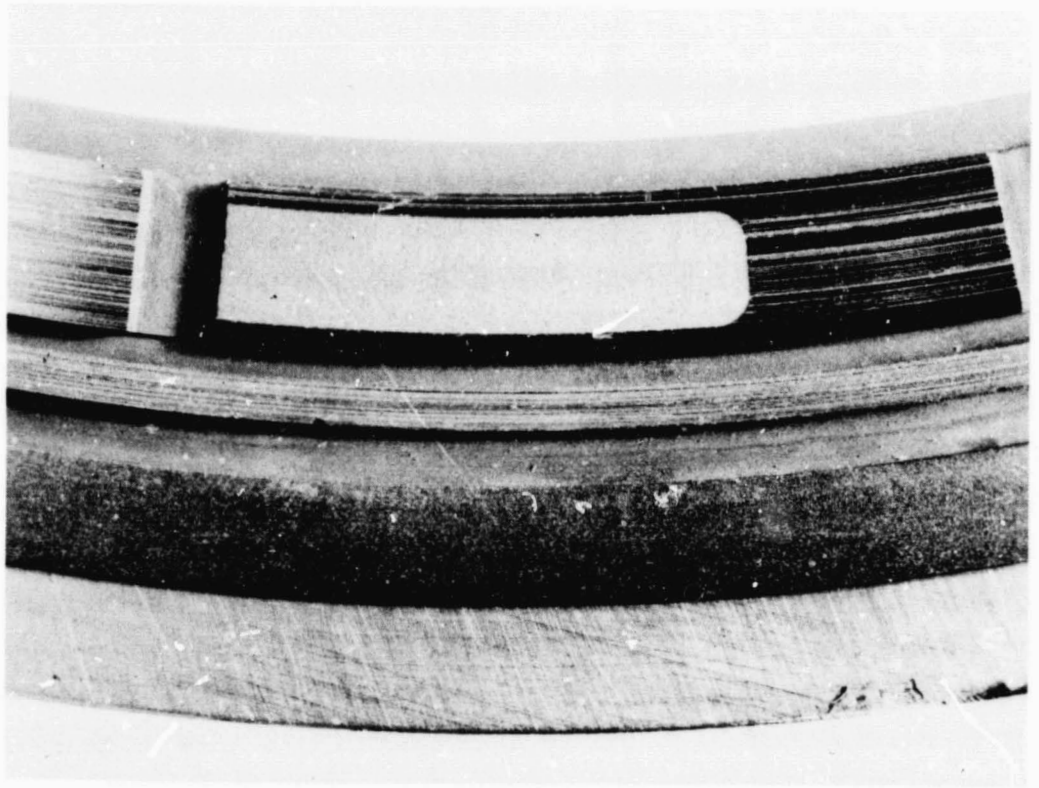

Figure 107 Close-Up of the Carbon Nosepiece from the Revised Narrow-Pad Seal After Testing (CN-31505)

Examination of the piston ring showed that the sealing face had made proper contact. There were some axial grooves worn on the outer surface of the dam; these were probably the sources of some of the increased leakage noted in the last few endurance tests. The carrier bore showed some light coking on the low-pressure side of the piston-ring contact area, but the coking was not uniform, which indicated that there had been a lack of complete contact between the piston-ring and the bore in some areas. A seal-support thermocouple in the area of the worst piston-ring damage showed a 30°F rise in temperature during testing at the last endurance point run. Air leakage at that point was 15.4 scfm, as compared to 11.2 scfm recorded for the same conditions on an earlier run. It is clear from these observations that at least part of the increase in leakage was caused by piston-ring degeneration. The condition of the seal dam caused the remainder of the increased air leakage observed.

PRECEDING PAGE BLANK NOT FILMED

SECTION VIII
TEST EQUIPMENT

A. TEST RIG

The seals evaluated in Phase III of this contract were tested in a full-scale test rig developed in Phase I. The rig was mounted on a bed plate and driven by a Ford industrial engine through a five-speed truck transmission and a 12:1 ratio gearbox. Facilities for heating the oil required for testing were located in the test cell, and the air was heated by an electrical heater. A schematic diagram of the test facility is shown in Figure 108 and a photograph is shown in Figure 109.

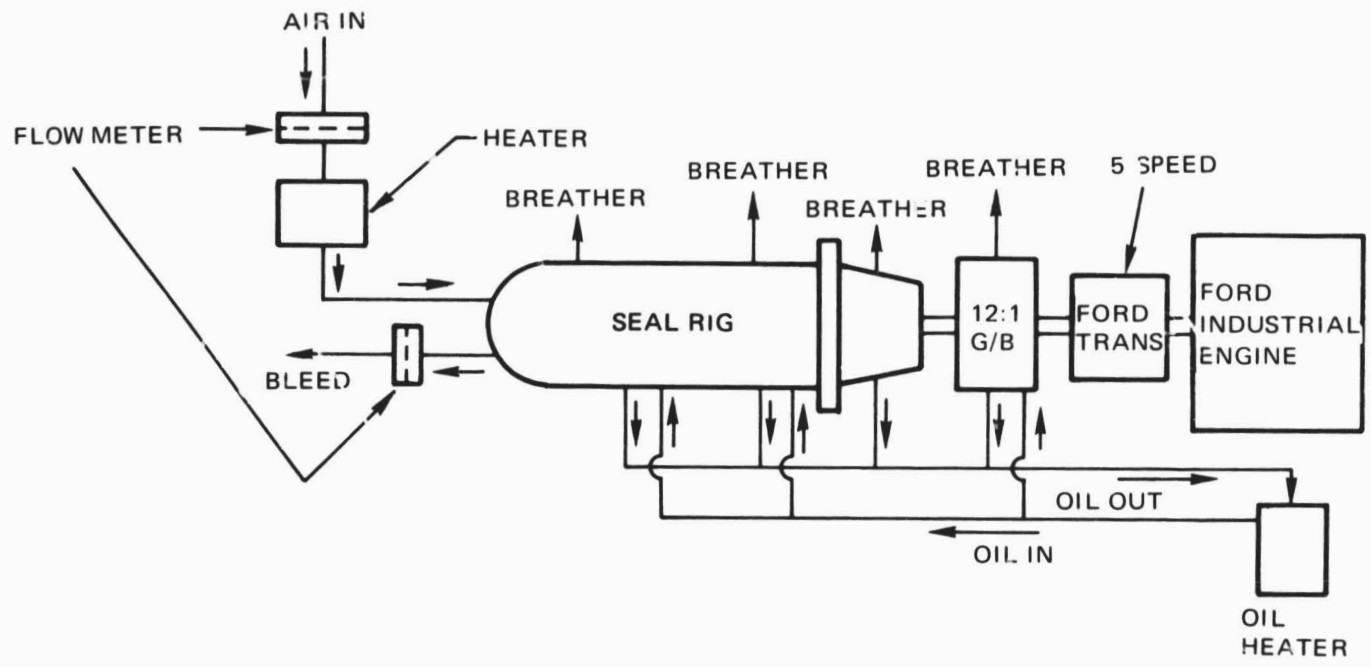

Figure 108 Schematic Diagram of Seal Test Facility

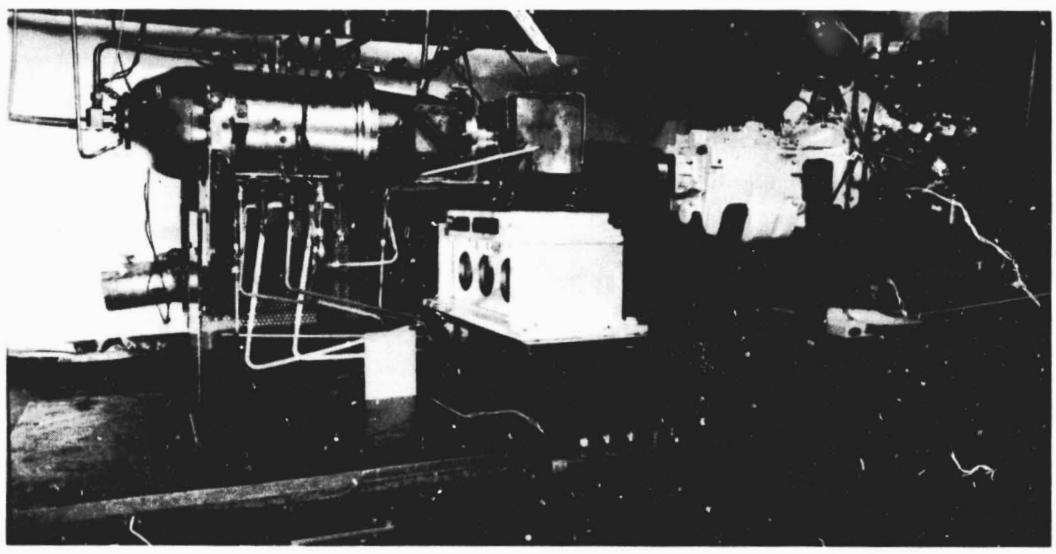

Figure 109 Overall View of the Test Stand Showing Mainshaft Seal Rig, Gearbox, and Drive Engine (CN-6928)

The test rig was designed and fabricated for evaluating mainshaft seals at sliding speeds of 500 ft/sec (17,300 rpm), pressure differentials across the seal of 300 psi and s' ated gas temperatures up to 1200°F. The test rig simulates the roller bearing sump at the turbine location in an advanced gas-turbine engine. The test seal provides the separation between the high-pressure-hot gas (turbine side) and the low-pressure mixture of oil and air (sump side). The seals evaluated in the rig have had a maximum face diameter of approximately 7 inches.

A layout of the test rig is shown in Figure 110. Pressurized and heated air entered the test compartment via the conical manifold attached to the inside of the pressure dome. The pressure dome was insulated to cut heat losses during testing. Air temperatures at the seal were continually monitored and adjusted by means of a bleed valve. Oil was brought to the thrust bearings by means of a calibrated jet and scoop arrangement. Oil was brought to the test seal from a jet via a scoop and passageways which allowed under-race cooling of the roller bearing. This oil was then centrifugally thrown out of the seal seat through radially drilled holes, thus providing cooling for the seal seat. The roller bearing was lubricated with mist and spray in the bearing compartment. The flight-weight parts used in the rig were:

- Duplex ball thrust bearings
- Inner and outer thrust bearing supports
- Thrust bearing support mount
- Roller bearing
- Roller bearing support mount
- Test seal seat
- Test seal assembly

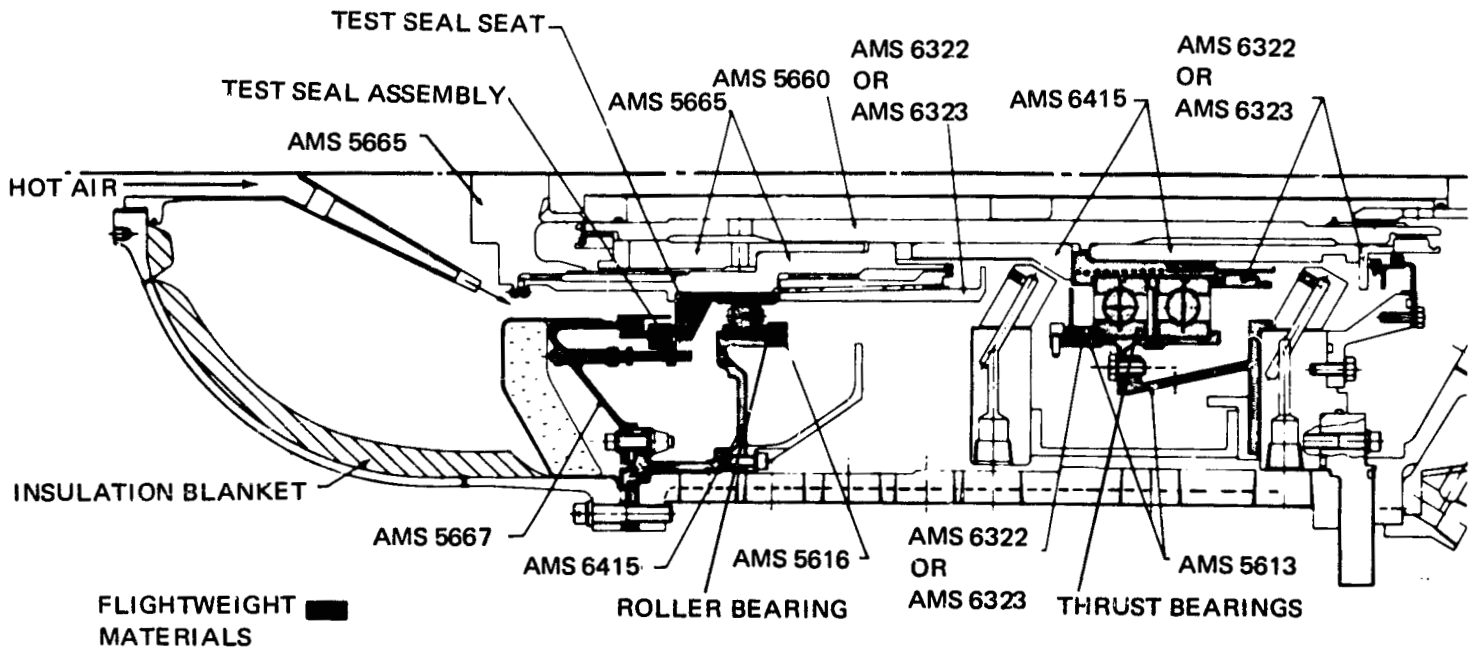

Figure 110 Rig Layout Showing Test Seal Location and Materials Used

B. PRESSURE CHECK FIXTURES

Two pressure check fixtures were designed and fabricated in Phase II of this contract to permit thorough checks of both the test seals and the test rig. The seal fixture is shown in Figure 111. It consisted of a pressure vessel which positioned the seal assembly against a simulated seat. The seal was pressurized through the bore and the air leakage into the low-pressure compartment was collected and measured. Additionally, removal of the fixture's cover allowed observation of the air leakage paths. This feature of the fixture was of great assistance during Phase III in determining whether excessive leakage during some of the tests was coming past the primary seal or past the secondary-seal piston ring.

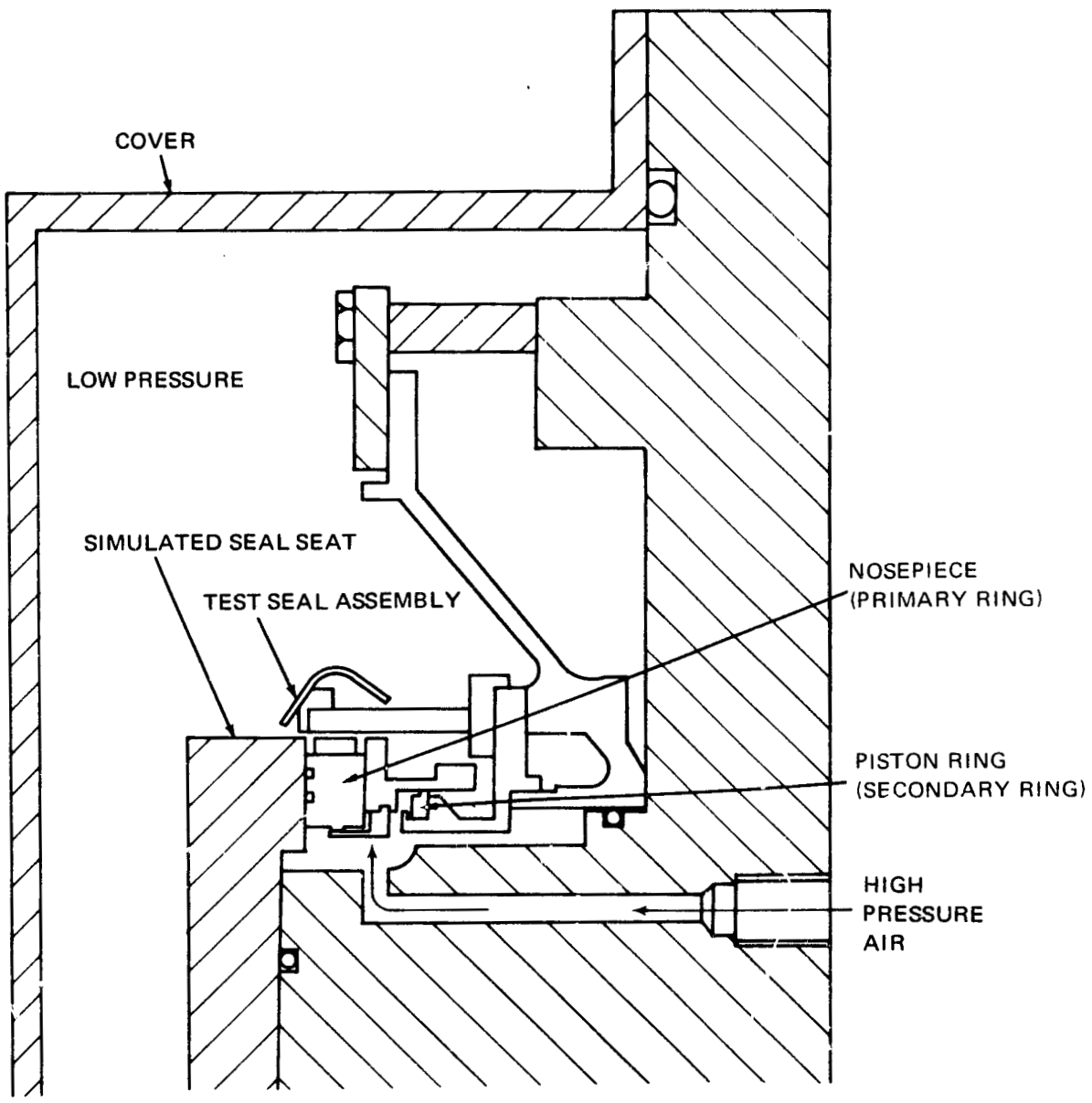

Figure 111 Schematic Diagram of Pressure Check Fixture for the Seal

The test rig fixture shown in Figure 112 replaced the entire seal assembly in the test rig, and allowed a systematic check of possible leakage paths in the rig and rotor assembly. With the rubber gasket and both O-rings in place, it was possible to pressurize the static rig gaskets. Removal of the inner O-ring allowed pressurization of the bellows spacer. When excessive leakage occurred during the course of the Phase III tests, this fixture was used to make sure that the leakage was actually going past the test seal and not through some other possible leakage path in the test rig.

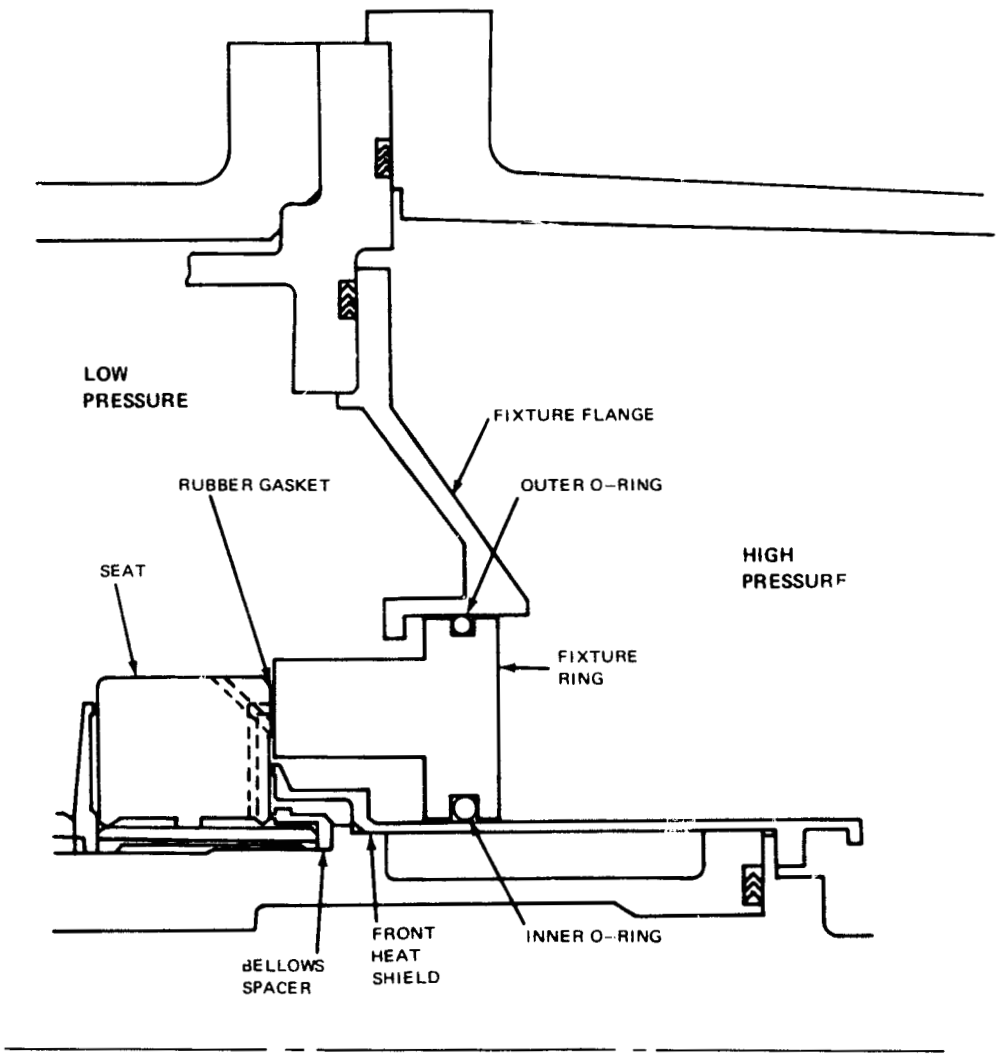

Figure 112 Schematic Diagram of Pressure Check Fixture for the Rig

REFERENCES

1. Semiannual Report No. 1, "Development of Compressor End Seals, Stator Inter-stage Seals, and Stator Pivot Seals in Advanced Air-Breathing Engines"; PWA-2752, NASA CR-54625; R.M. Hawkins et al; Pratt & Whitney Aircraft, East Hartford, Connecticut; January 1966.

2. Semianual Report No. 2, "Development of Compressor End Seals, Stator Inter-stage Seals, and Stator Pivot Seals in Advanced Air-Breathing Engines"; PWA-2875; R.M. Hawkins et al; Pratt & Whitney Aircraft, East Hartford, Connecticut; July 1966.

3. "Development of Mainshaft Seals for Advanced Air Breathing Propulsion Systems - Phase II"; PWA-3933, NASA CR-72737; V.P. Povinelli and A.H. McKibbin; Pratt & Whitney Aircraft, East Hartford, Connecticut; June 1970.

4. "Compressible Flow Across Shaft Face Seals"; NASA TM X-52959; John Zuk, Lawrence P. Ludwig, and Robert L. Johnson; Lewis Research Center, Cleveland, Ohio.

5. Part 1, "Advanced Turbine Engine Mainshaft Lubrication System Investigation, Phase II"; NASA CR-72854, SKF AL69T016; W.L. Rhoads and L.A. Peacock; SKF Industries, Inc., King of Prussia, Pennsylvania; January 1971.

6. Part 2, "Advanced Turbine Engine Mainshaft Lubrication System Investigation, Phase II"; NASA CR-72873, SKF AL69T016; W.L. Rhoads and L.A. Peacock; SKF Industries, Inc., King of Prussia, Pennsylvania; January 1971.

7. "Development of Main Shaft Seals for Advanced Air Breathing Propulsion Systems"; PWA-3161, NASA CR-72338; A. J. Parks, A. H. McKibbin, and C. C. W. Ng; Pratt & Whitney Aircraft, East Hartford, Connecticut; August 1967.